Title

Jekyll/UDP-glucose dehydrogenase is required for cardiac valve, semicircular canal, and cartilage development in zebrafish

Author

Walsh, Emily Cecile

Publication Date

2001

Peer reviewed|Thesis/dissertation

Jekyll/UDP-glucose dehydrogenase is required for cardiac valve, semicircular canal, and cartilage development in zebrafish.

by

Emily Cecile Walsh

DISSERTATION

Submitted in partial satisfaction of the requirements for the degree of

DOCTOR OF PHILOSOPHY

in

Genetics

in the

GRADUATE DIVISION

of the

UNIVERSITY OF CALIFORNIA, SAN FRANCISCO

Acknowledgements:

This work is dedicated to the memory of Betty Louise Atkins who instilled in me the two most important qualities for a graduate student: perseverance and curiosity. This work is also dedicated to Martha, Dennis and Kate Walsh, my family. Without your support, my success in life would be much reduced and much less gratifying. I love you very much. I must also thank Ashkan Javaherian, your insight and help were critical to my success. Man ashegetam.

Furthermore, without the generous support intellectual and otherwise of my advisor, Didier Y. R. Stainier, I could never have made it to this point. Didier pushed me to succeed by broadening my horizons. Under his tutelage, I not only increased my insight into the realm of scientific inquiry and technique, but as well learned a great deal about the art of participating in a scientific community. Didier achieved these feats in three ways: 1) by providing me with many opportunities to participate in scientific courses and meetings, 2) by creating a lab environment of curiosity and fellowship, and 3) belgian chocolate.

This work could not have been completed without the training, support and facilities available to students of UCSF's Program in Biological Sciences (PIBS). I thank the PIBS program for providing me with the fantastic opportunity to work and learn here. I thank my Thesis Committee for their guidance and the Howard Hughes Medical Institute for their generous predoctoral support.

Of course, this work could not have been done without all of the members of the Stainier Lab past and present. In particular, I'd like to thank Erik Kupperman, Wayne

Liao, Leon Parker, and Debbie Yelon for teaching me molecular biology, stress management, and organization.

However, this graduate work was not completed in a bubble at UCSF. I had numerous collaborators from other universities. First and foremost, I must thank those collaborators who helped with the *jekyll* project. Mark Fishman provided me with the *jekyll* allele described herewith. Bernard and Christine Thisse (Strausbourg), Michael Lardelli (Adelaide), and Masazumi Tada (NIMR) each provided important in situ probes critical to the understanding of the molecular defects in *jekyll* mutant embryos. Tony Capehart at Eastern Carolina University, graciously provided the TC2 antibody. Genomic efforts by the Max Planck Institute in Tubingen, Germany; the Zon and Fishman labs in Boston, MA; and the Talbot lab at Stanford University were critical to the cloning of the *jekyll* locus. Also critical was the zebrafish EST sequencing effort from the Johnson lab at the Washington University. I must also thank Andrew Pitsillides at the Royal Veterinary College in London for his work on Ugdh activity analysis. Lila Solnica-Krezel at Vanderbilt University kindly provided information about *knypek* and *pipetail* mutations prior to publication. John McDonald and Todd Camenisch at the Mayo Clinic in Scottsdale, Arizona, and Ray Runyan at the University of Arizona, were incredibly helpful colleagues to have along my path toward a further understanding of valve development.

During my tenure in the Stainier lab, there were of course non-*jekyll* projects and other collaborations. I must acknowledge Frank Reifers, Michael Brand, Phillip Crossley, and Gail Martin who were all collaborators with the work I did on the *acerebellar* mutation. Nico Scheer and Jose Campos-Ortega were great collaborators and

kind hosts during my initial attempts at a binary misexpression system. Reinhard Koester and Scott Fraser graciously provided their unpublished GalVP16 constructs prior to publication, making possible our ongoing attempts to understand the role of Neuregulin in valve formation. Fabrizio Serluca and Mark Fishman also helped in that regard by providing a clone of the zebrafish *neuregulin* gene.

Finally, I need to thank Scott Fraser and Marianne Bronner-Fraser who allowed my to take the embryology course and subsequently teach the zebrafish module at the Marine Biological Laboratory in Woods Hole, MA. I also need to thank other MBL persons: Richard Harland, Lee Niswander, and the "Frog, Fish, and Chick Chicks" (Elke Ober, Francesca Mariani, Karen Liu, John Wallingford, Elena Casey, Mary Ellen Lane, Julie Kuhlman and Josh Gamse). During the past 5 summers I've been lucky enough to be surrounded by these people. All of the folks at the Marine Biological Laboratory helped me to grow professionally and scientifically in ways I'll never be able to quantify.

Abstract

Jekyll/UDP-glucose dehydrogenase is required for cardiac valve, semicircular canal, and cartilage development in zebrafish.

Emily Cecile Walsh

Cardiac valve formation is a complex process that involves cell signaling events between the myocardial and endocardial layers of the heart across an elaborate extracellular matrix. These signals lead to dramatic morphogenetic movements and transdifferentiation of the endocardial cells at chamber boundaries. In this thesis, I analyze the most severe valve mutation identified to date in zebrafish, *jekyll*. I show, through examination of an endothelially-restricted GFP transgene, that heart valve initiation is deficient in *jekyll* mutants. Through positional cloning, I demonstrate that the *jekyll* mutation disrupts a vertebrate homologue of *Drosophila* Sugarless, an enzyme required for heparan sulfate, chondroitin sulfate and hyaluronic acid production. In *Drosophila*, Sugarless function has been shown to be important for both Wg and Fgf signal transduction. I show that atrioventricular border cells never differentiate from their neighbors in *jekyll* mutants, suggesting that Jekyll is required in a cell signaling event that establishes a boundary between the atrium and ventricle.

jekyll mutants also exhibit defects in semicircular canal formation and in alcian staining for sulfated proteoglycans in the developing arches and fins. Despite these defects in alcian staining, many molecular aspects of chondrocyte differentiation occur normally. However, proper morphogenesis of the arches fails to occur and the

morphogenetic defects present greatly resemble those found in *knypek/glypican* and *pipetail/wnt5a* mutants. This suggests that in the branchial arches, Jekyll may function in the Wnt5a pathway and act to modify the heparan sulfate proteoglycan, Glypican.

In the case of the heart, Jekyll activity does not seem to be required for Fgf or Wnt signalling but rather may function in the Neuregulin signalling pathway. I have begun experiments to address this possibility and those are detailed herewith.

Table of Contents

Acknowledgements iii

Abstract.....vi

Table of contents.....viii

List of symbols and abbreviations.....x

List of Figures.....xii

Chapter 1: Introduction 1

Chapter 2: *jekyll*: a vertebrate *sugarless* homologue is required for cardiac valve formation.....28

Chapter 3:Jekyll is required for a signalling event which specifies the atrioventricular boundary as a valve forming region.....46

Chapter 4: Jekyll is required for morphological differentiation of the branchial arches and may act to facilitate Pipetail/Wnt5a signalling through Knypek in that tissue.. 69

Appendix 1: *jekyll* genomic organization.....75

Appendix 2: Analysis of *cardiofunk* valve defects.....77

Appendix 3: *has2* morpholino and β-xyloside treatment of zebrafish embryos.....80

Appendix 4: Acerebellar/Fgf8 is required for zebrafish heart induction 82

Appendix 5: Analysis of BMP pathway mutant heart phenotypes: *lost-a-fin* and *snailhouse* mutations.....110

Appendix 6: RNA *in situ* analysis of zebrafish heart differentiation.....113

Appendix 7: Analysis of TC2 antibody staining of *jekyll* and *cardiofunk* mutant embryos.....117

Appendix 8: Attempts to establish a binary system in zebrafish.....119

Appendix 9: Role of *jekyll* in neural development.....121

Appendix 10: Future directions.....123

Reagents and Methods.....127

Curriculum Vitae.....138

Works cited.....140

List of Symbols and Abbreviations

A	atrium
ace	*acerebellar (fgf8.1)*
AV boundary	atrioventricular boundary
BMP	Bone morphogenetic protein
cfk	*cardiofunk*
clo	*cloche*
cmlc	*cardiac myosin light chain*
ctnt	*cardiac troponin T*
dCAPs	methodology to create primer-based RFLP
DNA	deoxyribonucleic acid
dpf	days post-fertilization
EGF	Epidermal growth factor
EST	expressed sequence tag
FGF	Fibroblast growth factor
GAG	glycosaminoglycan
Gal VP16	*gal4* DNA binding domain fused to *vp16* transactivator domain
gata	"GATA" binding transcription factor
GFP	green fluorescent protein
HA	hyaluronic acid
has2	*hyaluronic acid synthase 2* (also called *dg42*)
hdf	*heart defect* mutation
hpf	hours post-fertilization
Ig	immunoglobin
jek	*jekyll (ugdh)*
lacZ	beta-galactosidase
laf	*lost-a-fin (alk8)*
MF20	myosin heavy chain whole heart antibody
μ	micro
MO	morpholino
Nkx	"NK" homedomain protein

PAC	phage artifical chromosome
PCR	polymerase chain reaction
PG	proteoglycan
RFLP	restriction fragment length polymorphism
RH	radiation hybrid panel
RNA	ribonucleic acid
S46	myosin heavy chain atrial specific antibody
snh	*snailhouse (bmp7)*
SNP	single nucleotide polymorphism
SSCP	single stranded conformation polymorphism
TC2	anti-chondroitin sulfate GAG antibody
TGF-β	Transforming growth factor beta
tie2	*tie2, angiopoietin receptor*
UAS	upstream activating sequence, Gal4 binding site
UDP	uridine diphosphate
ugdh	*udp-glucose dehydrogenase*
UTR	untranslated region
V	ventricle

List of Figures/Illustrations

1 Glycosaminoglycan enzymatic pathway

2 Heart induction

3 Secondary convergence

4 Valve formation

5 Cardiac septation

6 Trabeculation

7 Hyaluronic acid and semicircular canal formation

8 Mapping of the *jekyll* mutation

9 Sequence analysis of zebrafish *ugdh*

10 Protein sequence of Ugdh and *jekyll* missense mutation

11 *In situ* analysis of *ugdh* RNA expression

12 Morpholino antisense targeting *ugdh*

13 Common single nucleotide polymorphisms in human *ugdh*

14 *jekyll* heart phenotype

15 Atrioventricular boundary formation in *jekyll* mutants

16 Chamber specification in *jekyll* mutants

17 Atrioventricular boundary formation in *cloche* mutants

18 Model of *jekyll*'s role in atrioventricular boundary formation

19 Expression of the zebrafish *neuregulin* gene

20 Gal VP16 binary system constructs to test Neuregulin's role

21 Molecular analysis of the *jekyll* branchial arch defect

22 Similarity of *pipetail* and *jekyll* mutant phenotypes

23 Appendix 1: Genomic organization of the *jekyll* locus and PAC rescue of phenotype

24 Appendix 2: Atrioventricular boundary formation in *cardiofunk*

25 Appendix 3: Comparison of the requirement of HA and PG's for valve formation

26 Appendix 4: Role of *acerebellar* in valve formation

27 Appendix 5: Role of *lost-a-fin* in heart development

28 Appendix 5: Role of *snailhouse* in valve formation

29 Appendix 6: *In situ* analysis of valve development

30 Appendix 6: *notch1b in situ* hybridization time course

31 Appendix 7: Comparison of wildtype and mutant TC2 Immunofluorescence

32 Appendix 9: Comparison of wildtype and *jekyll notch1b* neural expression

Introduction

The vertebrate heart is initially composed of two cell layers, an outer muscular myocardium and an inner endocardium that connects the heart to the vasculature. Much attention has been focused toward understanding not only the initial induction of these two cell types, but also the ensuing morphogenesis that results in the formation of a multi-chambered, beating organ. As the construction of the vertebrate heart is an intricate process, genetic analysis has been particularly effective in its study. In fact, some of the most illuminating work in the field of heart development has employed genetic techniques including forward screens for heart defects in zebrafish and targeted gene disruption in mouse.

One of the most powerful approaches to understanding any biological problem is a genetic screen. For this reason, the zebrafish is an excellent system for studying heart development. This is largely due to its relatively short generation time, external fertilization, and transparent early embryonic development. Not only can one isolate novel players in cardiac development through forward genetic screens in zebrafish, but one can also delineate entire signalling pathways through modification or suppression screening. Two large scale morphological screens[1,2] and one small scale molecular screen[3] in zebrafish have isolated 136 mutations that perturb heart development and provided a genetic framework for the morphogenetic pathway leading to the formation of a functional adult heart.

This thesis will discuss the molecular characterization and cloning of one of these mutations, *jekyll*. *jekyll* mutant embryos lack atrioventricular (AV) valve formation, as

well as exhibiting defects in semicircular canal and cartilage formation. As I will describe herewith, a synteny cloning approach allowed the isolation of the *jekyll* gene which encodes a homologue of the UDP-glucose dehydrogenase/Sugarless enzyme. UDP-glucose dehydrogenase is required to convert UDP-glucose into UDP-glucuronate, a basic building block of hyaluronic acid and heparan and chondroitin sulfate glycosaminoglycans (Fig. 1). However, even before *jekyll's* genetic identity was known, the defects present in mutant embryos led us to hypothesize that Jekyll might be required for the production of glycosaminoglycans. In this introduction, I will first describe the steps of wildtype heart development in zebrafish, making comparisons, where appropriate, with similar steps in mouse and chick development. Next, I will detail what is currently known about the roles of glycosaminoglycans in the development of cardiac valves, semicircular canals and branchial arches.

Heart Formation

Gastrulation

Fate mapping studies in several model organisms have defined the heart precursors at early stages in development[4-6] (Fig. 2). At the onset of gastrulation in zebrafish, the bilateral domains of cardiac precursors are located 90 degrees from the future dorsal side [6]. The heart precursors involute early during gastrulation and join with the rest of the mesoderm in its convergence toward the developing axis (Fig. 2). At the end of gastrulation, the myocardial anlagen are located in the anterior lateral plate mesoderm where they begin to show signs of differentiation. The myocardial-specific homeodomain protein, Nkx 2.5, is expressed in these cells at this time, along with its

more widely expressed orthologue, Nkx 2.7 [4]. Also at this time, *gata* genes (4-6) are even more broadly expressed throughout much of the anteroposterior extent of the lateral plate.[5]

The murine equivalents of these precardiac cells are located distal and lateral to the primitive streak as gastrulation begins at E6.5. The heart precursors also ingress with other mesodermal derivatives into the primitive streak.[6] They then leave the streak anterolaterally and at the end of gastrulation can be found in the anterior lateral plate, like their zebrafish counterparts (Fig. 2). At around E7.5, one sees *nkx2.5* expression in the heart primordia.[7] Murine *gata* genes are expressed slightly earlier (E 7.0) throughout the headfold mesoderm that contains the cardiac progenitors.[8,9]

Secondary convergence and heart tube assembly

The heart progenitors are now set to undergo a second convergence from the lateral plate mesoderm toward the midline where they will join to form a single tube. Some of the most interesting mutations that perturb heart development affect this convergence and result in the formation of two physically separate cardiac structures, commonly referred to as cardia bifida. What makes these cardia bifida mutations so striking is that many seem to affect the process in a cell non-autonomous fashion. That is to say, these genes are not required in the cardiac mesoderm but rather in another tissue that presumably interacts with the heart precursors. Study of these mutations has revealed a critical role for endodermal derivatives in heart fusion.

The movements that elaborate a definitive heart tube have been documented in zebrafish using both molecular and genetic analysis (Fig. 3).[10] At 19 hours post-fertilization (hpf), the two fields of myocardial precursors merge posteriorly to form a horseshoe-shaped structure. The horseshoe transforms into a ring as anterior cells migrate to close the circle. Next, the cardiac ring telescopes to form a tube. The ventricular end of the heart tube assembles first in a medial location, followed by the atrial end, which assumes a left-sided position. This leftward bias of heart assembly is the embryo's first morphological break in bilateral symmetry.

At around 19 hpf, the endocardial cells also converge at the midline of the developing zebrafish embryo. There they form a sheet that underlies the myocardial precursors.[11] As the myocardium telescopes, the endocardium follows, lining the inside of the developing tube. Subsequently, the endocardium connects seamlessly with the endothelium lining the dorsal aorta. Intriguingly, the endocardium is not required during early cardiac development. Work on the zebrafish *cloche* mutation, which perturbs endocardial induction, revealed that early myocardial differentiation, as well as the fusion event itself, proceed without consequence.[12] However, myocardial function and, as I will discuss later, AV boundary formation are defective in *cloche* mutants.

Murine myocardial movements are mainly similar. Cardiac fusion begins between embryonic day 7.5 and 8 (E7.5-E8). As the left and right endoderm sheets undergo ventral folding at the midline, they bring the bilateral myocardial and endocardial precursors into proximity.[13] Once near the midline, the bilateral heart precursors fuse to form the definitive heart tube. Several studies have addressed the exact

manner by which the myocardial precursors form a single tube around the endocardium.[14,15] As in zebrafish, the ventricular end of the murine heart tube assembles first, followed by the atrial end (Fig. 3). Also as in zebrafish, mouse embryos lacking endocardium have apparently normal myocardial cells.[16]

Looping morphogenesis

During the process of dextral looping, the heart tube undergoes a dramatic three-dimensional reorganization. This looping event is conserved among all vertebrate organisms studied to date.[17] In vertebrates with lungs, this rearrangement helps to align the outflow tract over the left and right ventricles such that unoxygenated blood is sent to the lungs and oxygenated blood is returned to the body. However, this cannot be the only reason for the conservation of looping among vertebrates as some (e.g. zebrafish) do not have lungs or four-chambered hearts. Nonetheless, these less complex hearts undergo the same rightward bending. This fact leads to the hypothesis that looping is a prerequisite for some other yet unidentified aspect of heart function.

At the end of tube assembly, the vertebrate heart is asymmetrically aligned, with the atrium to the left of the midline (as seen in Fig. 3). At 33 hpf in zebrafish, the heart bends back to the right, bringing the ventricle into a position ventral to the atrium, thus completing looping morphogenesis in the zebrafish embryo. Murine looping is similar. Around E9.5 the heart begins a sweeping dextral motion that positions the future right and left ventricles side by side and ventral to the atria.

Valve formation

Valves form at three sites along the anteroposterior axis of the developing heart: the outflow tract, AV boundary, and sinus venosus. Once formed, these largely acellular structures serve to prevent retrograde blood flow through the heart. However, at early stages these valve development sites are hotbeds of cell signalling, migration, and proliferation.

At the three sites of valve initiation, a conversation occurs between the myocardium and endocardium (Fig. 4). *In vitro* tissue recombination experiments in the chick show that a subset of endocardial cells at the AV boundary are competent to respond to a signal provided by the overlying myocardium (reviewed in 18). In response to this signal, the endocardial cells undergo an endothelial-to-mesenchymal transition. They then migrate into the extracellular matrix between the endocardium and myocardium (also called the cardiac jelly). Once there, these cells form an endocardial cushion that is later remodeled into a valve.

Zebrafish valve induction is initiated at around 36 hpf. At this time, the first molecular indication of AV boundary differentiation is present, restricted expression of the TGF-β family member, *bmp4*.[18] As I will discuss below and in Chapter 3, *jekyll* mutants can be identified molecularly at this very early stage as they lack this heightened *bmp4* expression in the AV boundary. At 43 hpf, using transgenic embryos that express GFP under the *tie2* endocardial promoter, one sees that endocardial cells have clustered at the site of valve formation. It is at about this time that *notch1b* expression is restricted to the endocardium of the valve.[19] At 48 hpf, other signs of molecular differentiation are

apparent including the myocardial AV boundary-restricted expression of the *fibulin-1* (encoding an extracellular matrix protein)[20] and *br146* (*versican*).[20] It is at this time that the embryo becomes dependent on its valves to prevent retrograde blood flow.

In the mouse, valve formation is initiated around E9.5. Similar to the case in zebrafish, *bmp4* expression (as well as *bmp2* and *bmp7*) is restricted to the myocardium overlying the developing valve. However, in the mouse and chick much work has focused on the role of other TGF-β class signalling molecules in valve formation.

tgfβ1, *tgfβ2*, and *tgfβ3* are expressed dynamically in the valve forming region (reviewed in 22). In mouse, *tgfβ1* is initially expressed throughout the endocardium, becoming restricted to the valve forming region at the time of cushion formation, while *tgfβ2* is expressed in the overlying myocardium. *tgfβ3* is not expressed until after the establishment of a cushion. In the chick, however, *tgfβ2*, and *tgfβ3* are expressed in both layers, and *tgfβ3* is also expressed in the migrating endothelial cells. *tgfβ1* has not been analysed as yet. Like their expression patterns, the role of these genes in valve formation is complex at best. Loss of function studies in the mouse[21-23] suggest that there may be some functional overlap between the various TGF-βs. Single knockouts of *tgfβ1*, *tgfβ2*, or *tgfβ3* do not result in the same drastic defects as seen in antibody-based ligand/receptor inhibition experiments in chick.[24-26]

Results from an *in vitro* assay seem to suggest two different roles for TGF-β in valve development: endocardial cell separation in the epithelium and endocardial cell

invasion of the cushion. However, just which TGF-β does what is still contested. For instance, one group finds that TGF-β3 appears to function as an autocrine cell separation signal in the endocardium.[27] While another group finds that TGF-β2 plays that role.[28] One difference may be in the timing of explant, as some results indicate that stage 14+ chick hearts have already induced the transformation event.[27] However, most evidence is consistent with the assertion that TGF -βs are not the complete myocardial-to-endocardial signal.

Morphogenetically speaking, valvulogenesis is much more complex in the mouse and chick as it will lead to the formation of a four-chambered structure, rather than a simple two-chambered one. The process that divides the heart in this manner is known as septation (Fig. 5). Septation morphogenesis involves not only mesenchymal endocardial cells but also migrating neural crest cells. However the relative contribution of each of these cell types is still being analyzed and is well reviewed.[29] As such I will limit my discussion to the general morphogenetic movements.

Beginning at E9.5, endocardial cushions grow in from opposing sides of the AV boundary, thereby bisecting this structure. This central AV cushion then experiences a second phase of growth to partially bisect the atrium. Meanwhile, the outflow tract cushions are undergoing growth to contribute to the ventricular septum. However, the bulk of the atrial and ventricular septa are fashioned from fenestrated myocardial outgrowths between the future left and right chambers.[17] At E13.5, this complex process is complete.

Trabeculation

Around E9.5 in mouse and 4 dpf in zebrafish myocardial cells in the ventricle begin to make muscular outgrowths into the cardiac jelly (Fig. 6). These trabeculae are thought to be important for the optimal performance of the ventricle. Interestingly, a number of mutations in the mouse that perturb septation and/or valve formation also affect the process of ventricular trabeculation. The *jekyll* mutation also falls into this class as mutants exhibit dramatic defects in ventricular muscularization which will be discussed in Chapter 3.

Glycosaminoglycans and development

Valve formation

One aspect of the *jekyll* mutant phenotype that seemed entirely consistent with a Jekyll role in glycosaminoglycan production was the heart phenotype. At the time of our initial mapping of *jekyll*, four mutations were known to perturb this process in mouse. Three of these mutations affected genes which, in retrospect, relied on Jekyll for their proper production, *hdf*; function, *has2*; or expression, *bmp4*.

The *hdf* (*heart defect*) mutation was identified as a recessive lethal insertion of a *lacZ* containing transgene.[30] Later cloning efforts showed that the *hdf* locus encoded the chondroitin sulfate proteoglycan, Versican (Cspg2).[31] As mentioned in the introduction, chondroitin sulfate glycosaminoglycans include a UDP-glucuronate subunit, which *jekyll* is required to produce.

Mice homozygous for the insertion die around day E10.5. This timing is comparable to that of other AV valve mutants. Since the transgene that caused the

mutation contained the *lacZ* gene, expression analysis of the locus was possible prior to cloning. Staining for beta-galactosidase activity was found throughout the anteroposterior axis of the heart, with heaviest staining in the ventricles and outflow tract. This expression is consistent with findings of outflow tract valve defects and reduced right ventricular development in *hdf* mutants. However, this reported expression is somewhat different from the *br146 versican* homologue in zebrafish, which is initially expressed throughout the heart and then becomes restricted to the AV boundary (figure 15 and appendix 6). However, there is an EST in zebrafish, fc73b01, with sequence similarity to *versican* that is not identical to *br146*. The expression of this clone has not been well examined. It is possible that like other duplicated genes in zebrafish, these two *versican* genes have split the original expression domain during their divergence. It is also possible that the appropriate stages of expression have not been directly compared as expression of *br146* is highly dynamic in the zebrafish.

In addition to the failed ventricular differentiation, *hdf* mutants lack proliferation of matrix and cellular invasion at the AV boundary. Surprisingly, *hdf*-mutant AV endocardial cells were competent to invade in an *in vitro* system.[30] This result suggests that some component of the collagen gel matrix in the *in vitro* system was able to complement the loss of *versican*. This result is in stark contrast to the results of the *hyaluronic acid synthase 2* (*has2*) knockout.

Hyaluronic acid (HA) is a high molecular weight glucosaminoglycan polymer synthesized by a family of plasma membrane-integral proteins. As a component of the extracellular matrix, HA binds water and creates a voluminous, highly structured gel. In

addition to this architectural role, HA is also implicated in cell adhesion and migration.[32] Has2 is the earliest expressed of the three mammalian HA synthases (Has1-3), all three of which appear to have similar activities.[32] Loss of the *has2* gene results in severe defects in cardiac development that closely resemble those of the hdf mice discussed above.[32] *has2*-null mice lack cardiac jelly production, ventricular trabeculation, and endocardial cushion formation. *has2*-negative hearts also have severe reductions in outflow tract and right ventricular tissue.

However, unlike the *hdf* phenotype, *has2* mutant AV boundary explants cannot invade a collagen matrix *in vitro*.[32] This defect is rescued by transfection of the wildtype gene into the explants or by the addition of exogenous HA to the culture medium/collagen gel matrix. This observation suggests that the *has2*-negative endocardial cells at the AV boundary are competent to invade the cardiac jelly, but require Has2 activity for migration to occur. Interestingly, *has2* antisense morpholino injections into zebrafish embryos appear to affect heart formation at an earlier stage as is discussed in appendix 3.

The *bmp4* knockout is of interest as, based on its expression pattern, it could act as the proposed myocardial signal initiating endocardial migration [33,34]. As mentioned above, *bmp4* is initially expressed throughout the myocardium, then its expression becomes restricted to the myocardium overlying sites of valve formation before the initiation of the endocardial clustering event in zebrafish and cushion formation in the mouse. Jekyll activity is required for this heightened, restricted expression of *bmp4* at the valve.

Depending on genetic background, very few *bmp4*-mutant embryos survive to day E10.5.[35] Many homozygous mutant embryos show drastic retardation starting at the egg cylinder stage, and most seem to be resorbed sometime between days E9.5 and E11.5. Those few that do progress past egg cylinder stage have severe defects in endocardial cushion formation. While matrix seems to be deposited at normal levels, the cushions remain acellular. However, this observation warrants further investigation. As the authors suggest, it is unclear whether these heart defects result from a direct requirement of Bmp4 in the heart, or whether these embryos are simply delayed and unhealthy. Unquestionably a tissue-specific knockout of the *bmp4* gene is called for here, as the authors suggest. This will be critical for ascertaining whether Bmp4 is the myocardial signal for endocardial-to-mesenchymal transition, or whether it behaves in a more complicated fashion at the valve.

Semicircular canal formation

Another of the striking features of the *jekyll* phenotype is the absence of semicircular canal formation in the developing otic vesicle[36] (Fig. 7). Semicircular canals form as protrusions from the anterior, posterior and medial aspects of the vesicle wall meet and fuse in the center. In *jekyll* mutants, these protrusions occur but never meet to fuse and form the semicircular canal. This phenotype is also seen upon injection of hyaluronidase, an enzyme that degrades HA, into the developing otic vesicle in Xenopus. These injection experiments in Xenopus have lead to the hypothesis that HA functions as a propellant of the elongation of the semicircular canals as high concentrations of HA have been localized to the tip of the protrusion.[37] Additional

corroborating evidence for the role of HA in semicircular canal formation comes from mouse and zebrafish experiments. *has2* -/- mouse embryos lack semicircular canal formation (J. Mc Donald, personal communication), as do *has2* antisense morpholino injected zebrafish embryos (Feng Liu, Woods Hole Embryology Course 2001).

Cartilage formation

The defects seen in the *jekyll* mutant cartilage resemble those seen in several mutations affecting the production of sulfated glycosaminoglycans or the proteoglycans they decorate. The most striking similarities are found when comparing *jekyll* and *knypek* mutant phenotypes (chapter 4). *knypek* encodes a heparan sulfate proteoglycan core protein, Glypican. Another class of mutations that resemble the loss of Jekyll function are found in the *diastrophic dysplasia sulfate transporter* gene. Mutations in this gene in mice and humans lead to dwarfism and a lack of alcian staining in the developing cartilage. In human these mutations are causal for many different syndromes including Diastrophic Dysplasia and Achondrodysplasia Type 1B (OMIM 222600, 600972).

Figure 1. Glycosaminoglycan enzymatic pathway. (A) UDP-glucose dehydrogenase is required for the production of glycosaminoglycan chains which are used in two ways by cells. 1) The chains are directly secreted into the extracellular matrix in the form of Hyaluronic acid. 2) Chondroitin and heparan sulfate glycosaminoglycan chains are covalently attached to proteoglycan core proteins. (B) Diagram of the cellular localization of UDP-glucuronate usage. First, UDP-glucuronate is used by Hyaluronic acid synthase at the cell membrane. Second, UDP-glucuronate is incorporated into growing glycosaminoglycan chains on proteoglycans. This presumably takes place in the golgi although this process has been less well studied than that of glycoprotein modification.

Figure 1

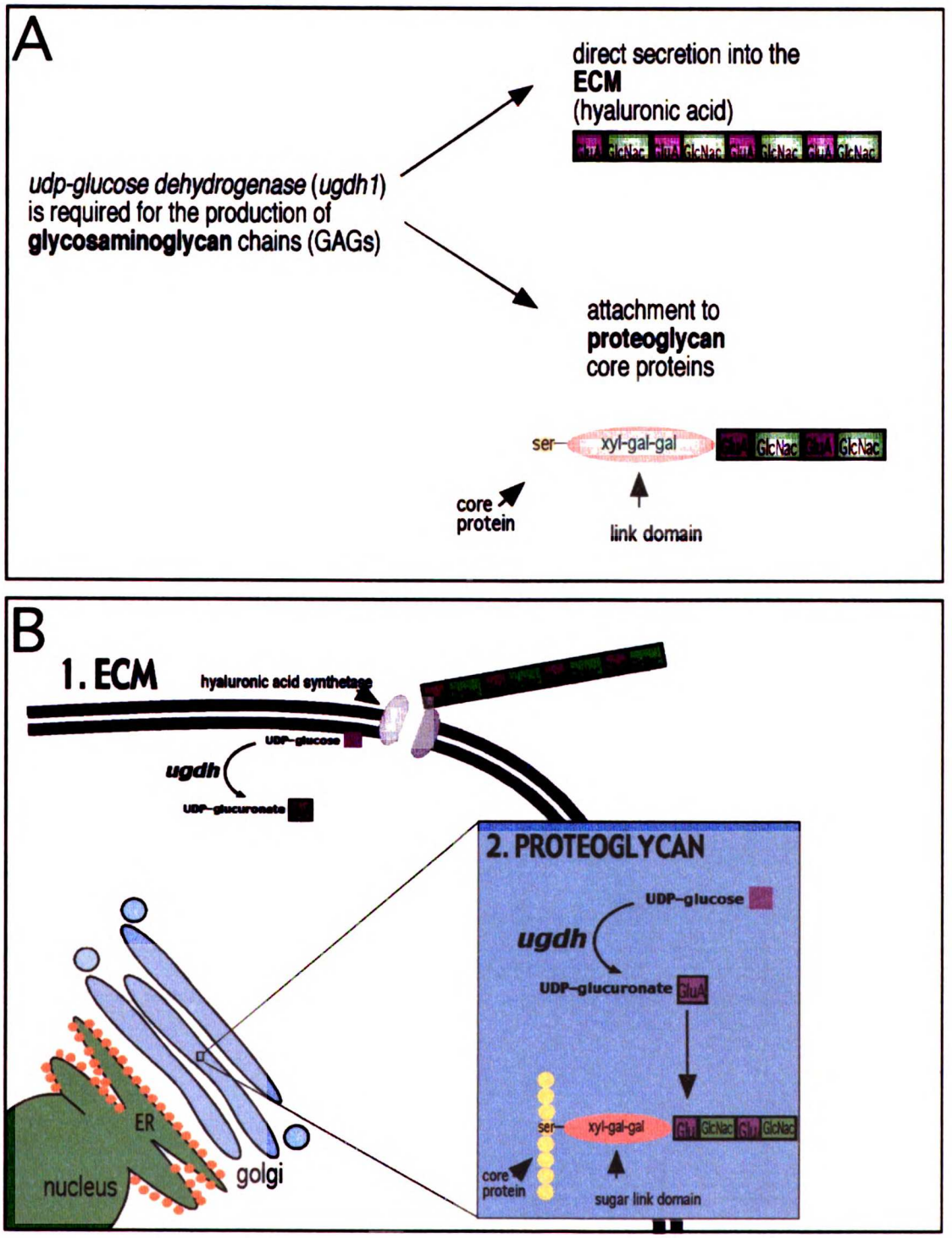
A
direct secretion into the
ECM
(hyaluronic acid)
udp-glucose dehydrogenase (ugdh1)
is required for the production of
glycosaminoglycan chains (GAGs)
attachment to
proteoglycan
core proteins
ser–
xyl-gal-gal
GlcNac
core
protein
link domain
B
1. ECM
hyaluronic acid synthetase
UDP–glucose
ugdh
UDP–glucuronate
2. PROTEOGLYCAN
UDP–glucose
ugdh
UDP–glucuronate
GluA
ser–
xyl-gal-gal
Glu
GlcNac
core
protein
sugar link domain
ER
nucleus
golgi

Figure 2. Heart induction. At the onset of gastrulation in zebrafish, the bilateral domains of cardiac precursors are located 90 degrees from the future dorsal side (top left). The murine equivalents of these cells are located distal and lateral to the node as gastrulation begins (top right). In both organisms, these cells involute early during gastrulation and join the rest of the mesoderm as it converges toward the developing axis. At the end of gastrulation, the bilateral myocardial anlagen are located in the anterior lateral plate mesoderm (bottom left and right).

Figure 2

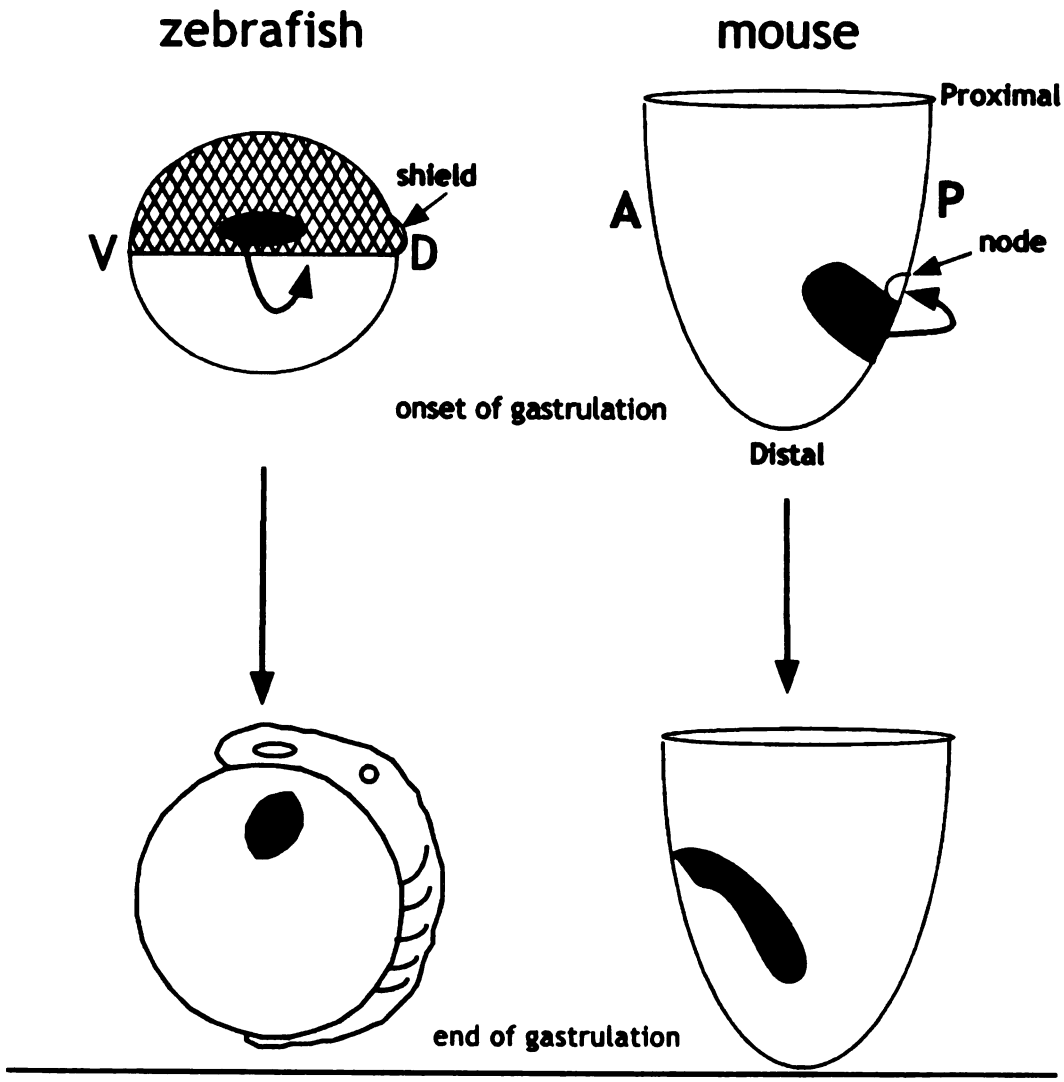
zebrafish
mouse
shield
V
D
Proximal
A
P
node
onset of gastrulation
Distal
end of gastrulation

Figure 3. Secondary convergence. In the zebrafish, secondary convergence begins at 19 hours post-fertilization (hpf) (left column, all views dorsal unless indicated otherwise). The two fields of myocardial precursors merge posteriorly to form a horseshoe-shaped structure. The horseshoe transforms into a ring as anterior cells migrate medially to close the circle. Next, the cardiac ring telescopes out to form a tube. The ventricular end of the heart tube assembles first, followed by the atrial end. Note the overt left-right asymmetry of the zebrafish heart at the end of fusion. By 19 hpf, the endocardial cells have converged at the midline. There they form a sheet that underlies the myocardial precursors. As the myocardium telescopes, the endocardium follows, lining the inside of the developing tube.

In the mouse, fusion begins around E7.5 (right column, ventral views, anterior to the top). At this time, ventral folding brings the bilateral myocardial and endocardial precursors into proximity. At the midline, these precursors fuse to form the definitive heart tube. As in zebrafish, the ventricular end of the murine heart tube assembles first, followed by the atrial end.

(Zebrafish panels adapted from Yelon et al., 1999, and unpublished data of Perens and Stainier, mouse panels adapted from DeRuiter et al., 1992)

Figure 3

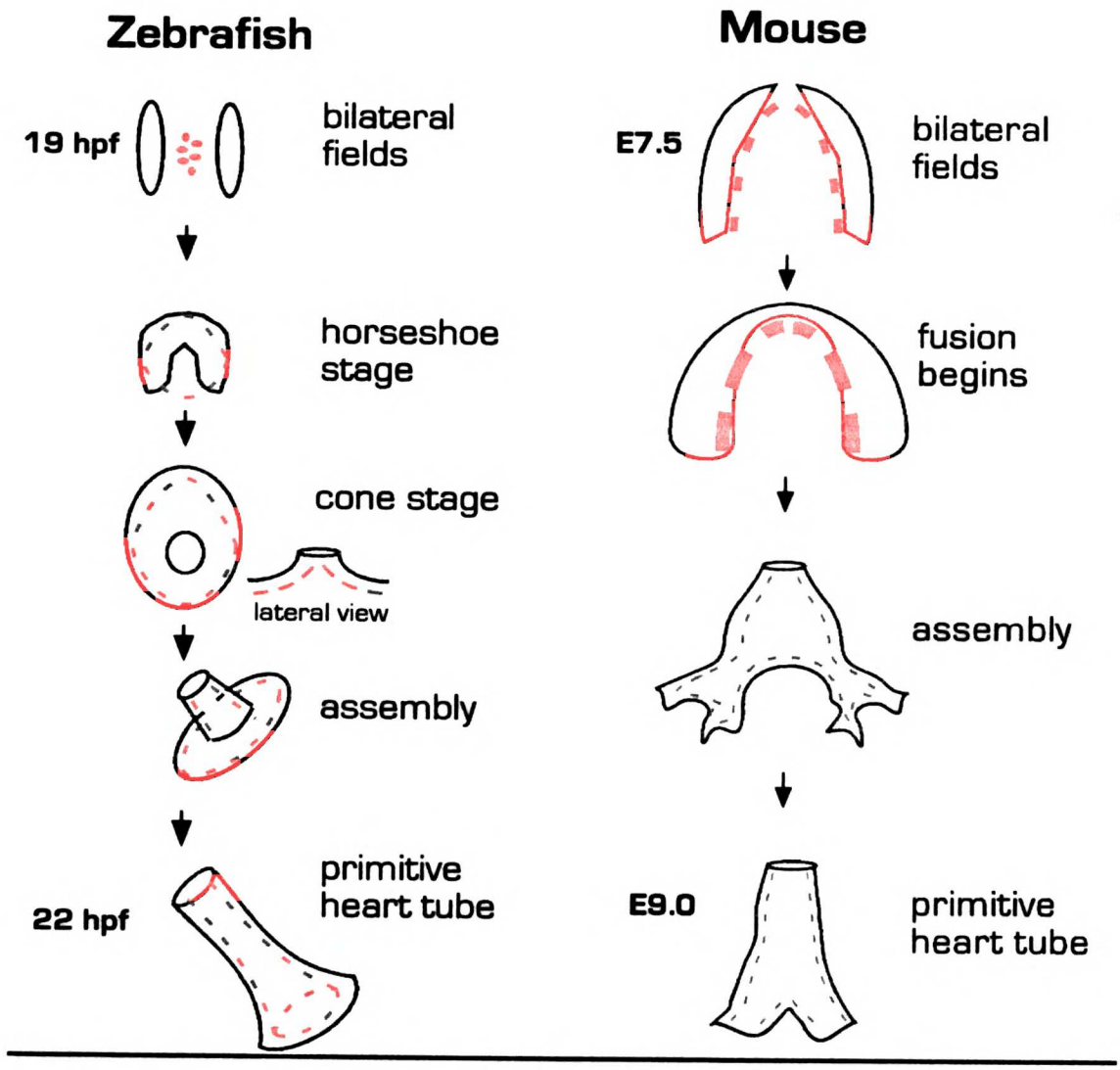
Zebrafish
Mouse
19 hpf
bilateral fields
horseshoe stage
cone stage
lateral view
assembly
22 hpf
primitive heart tube
E7.5
bilateral fields
fusion begins
assembly
E9.0
primitive heart tube

Figure 4. Valve formation. (A) Valves form at multiple locations along the anteroposterior axis of the developing heart (top panel illustrates two such positions, outflow tract and AV boundary). At these sites endocardial cells undergo an epithelial to mesenchymal transition and migrate into the extracellular matrix between the myocardium and endocardium (panels 1 and 2). There, the cells form "endocardial cushions" that are later remodelled to create flap-like structures (panel 3). The final products of this process are fibrous, largely acellular structures (not shown) that serve to prevent retrograde blood flow through the heart.

(B) *In vitro* recombination assays have elucidated some of the cellular interactions that occur during this process. Sections of endocardium and myocardium taken along the anteroposterior axis of the heart were recombined in a collagen gel matrix assay to test the requirements for epithelial to mesenchymal transition. These experminents suggest 3 steps to the process. First, there is an endocardial prepattern (step 1). Only endocardial cells taken from a valve forming region are competent to react *in vitro*. Second, there is a myocardial pattern and signal (step 2). Endocardial cells require juxtaposition with myocardium specifically from the valve forming region before epithelial to mesenchymal transition can occur.

Figure 4

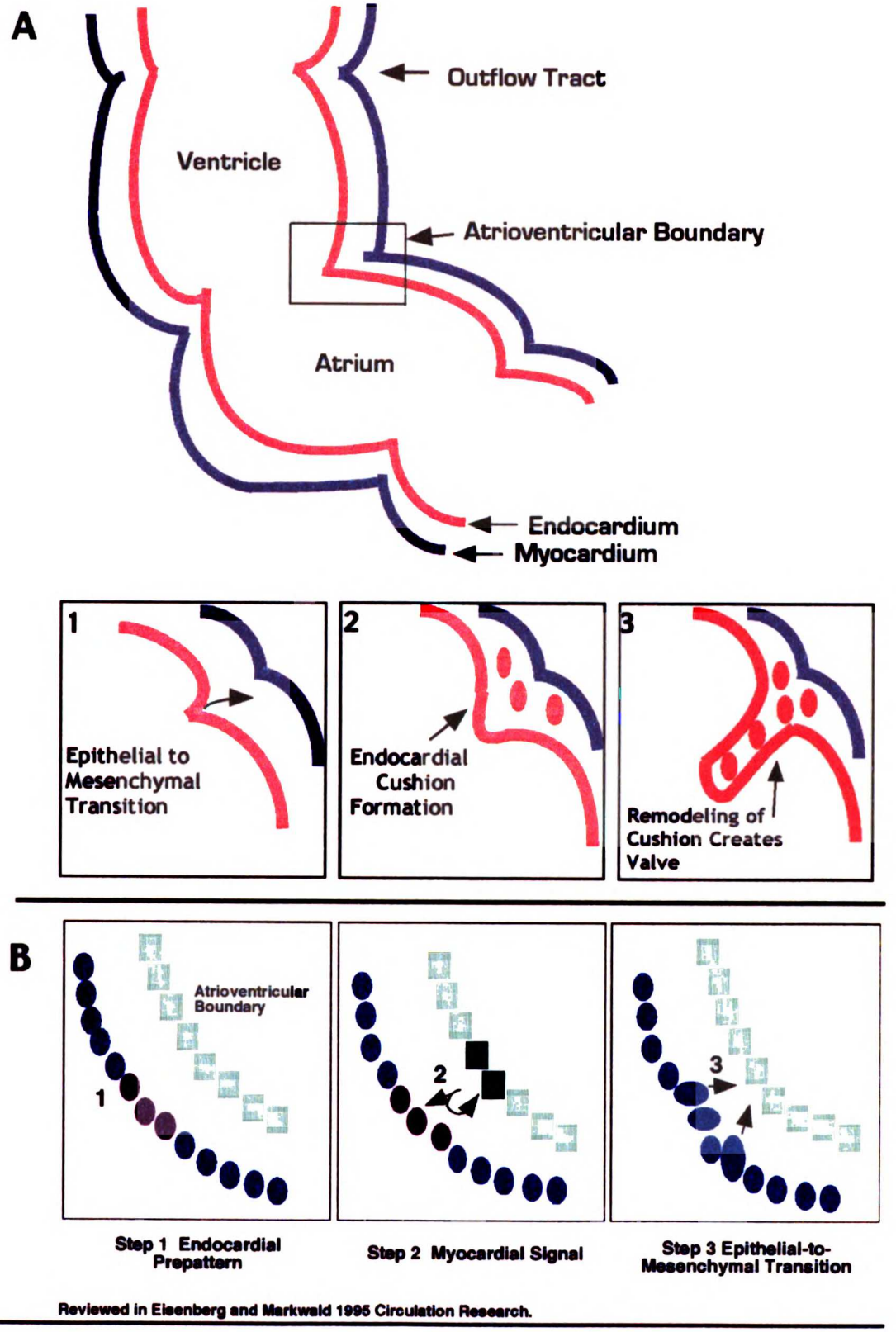

Reviewed in Eisenberg and Markwald 1995 Circulation Research.

Figure 5. Cardiac septation. The top row illustrates the process via a coronal section through the ventricle, viewed ventrally. The bottom row shows septation via an oblique cross section through the heart. At E9.5 in the mouse, endocardial cushions grow in from opposing sides of the AV boundary, thereby bisecting this structure (B and F). This central A-V cushion grows to partially bisect the atrium (G). Around the same time, the outflow tract cushions are undergoing growth to contribute to the ventricular septum (D). However, the bulk of the atrial and ventricular septa are fashioned from fenestrated myocardial outgrowths between the future left and right chambers (C, D and G, H).

Figure 5

Cardiac septation in mouse

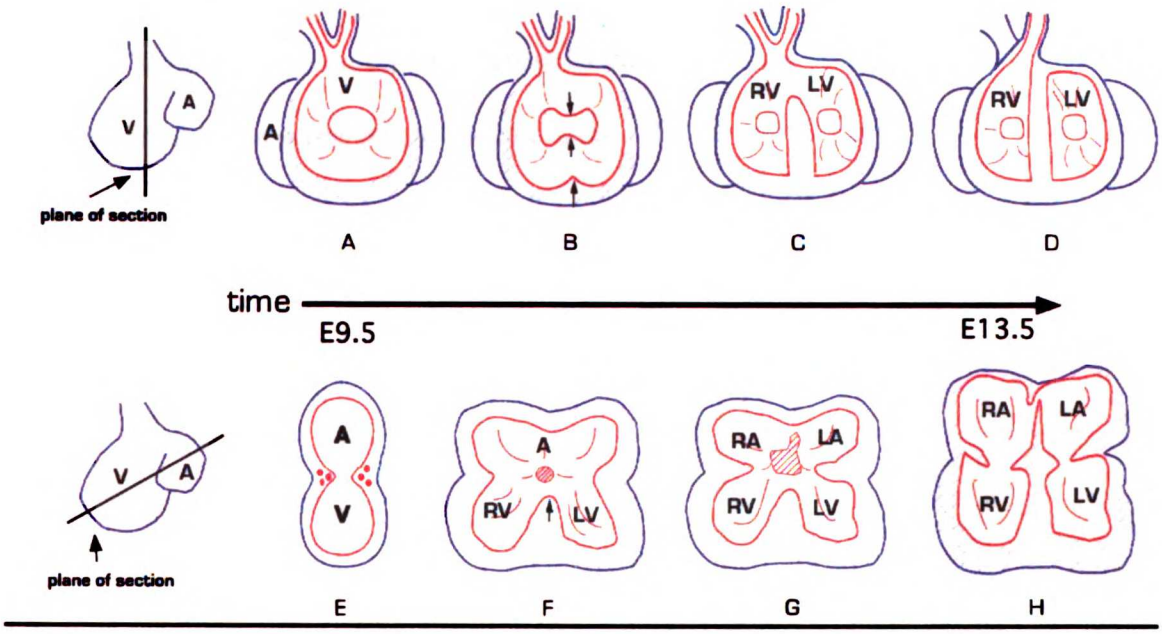

Figure 6. Trabeculation. (A) H&E stained section through the ventricle of an embryonic chick heart. Around E9.5 in mouse and 4 dpf in zebrafish myocardial cells in the ventricle begin to make muscular outgrowths into the cardiac jelly. These trabeculae are also indicated in the schematized section in (B). (Section kindly provided by Jim Bristow.)

Figure 6

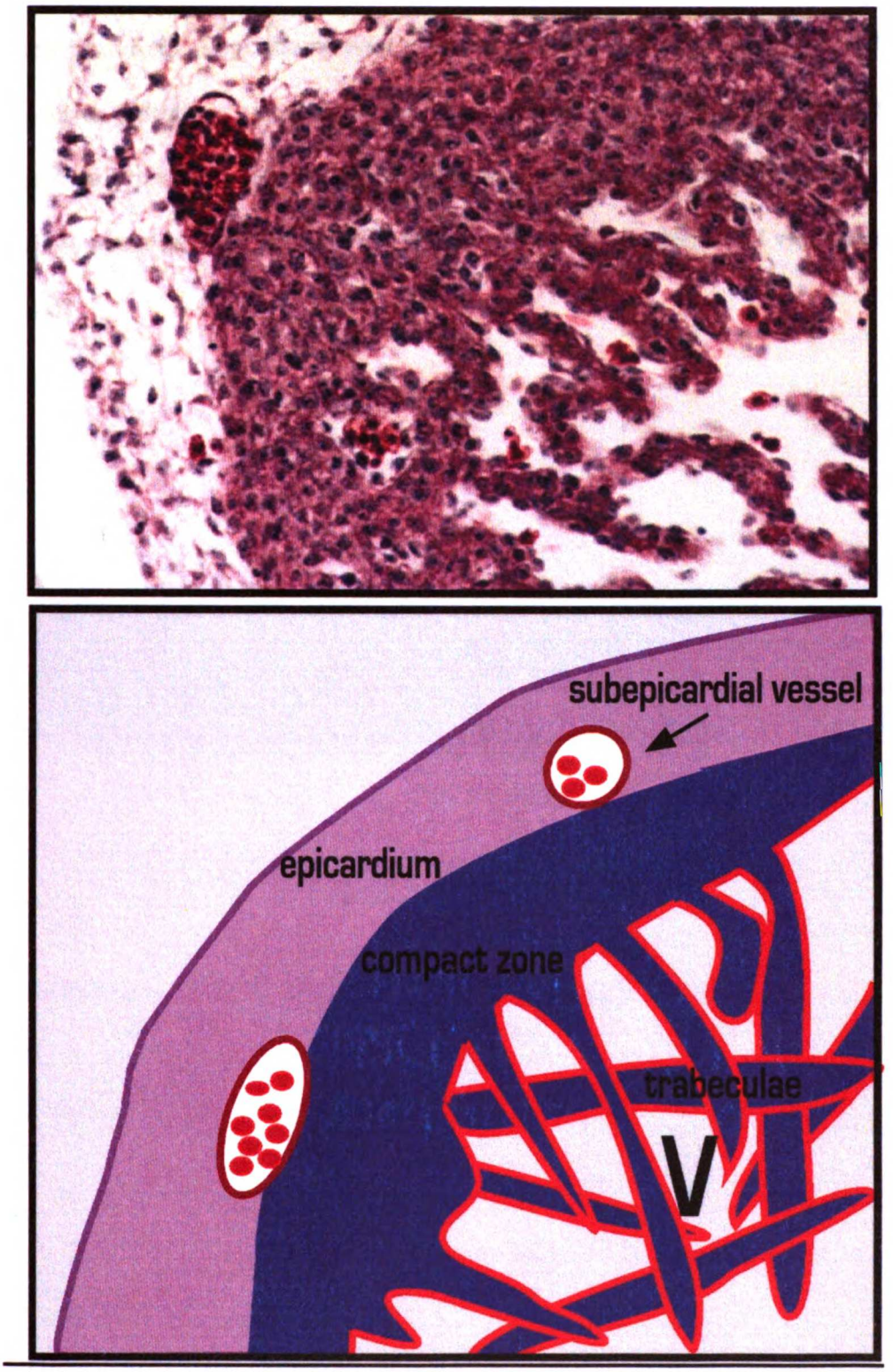
subepicardial vessel
epicardium
compact zone
trabeculae
V

Figure 7. Semicircular canal formation. (A-D) Semicircular canals form as protrusions from the anterior, posterior and medial aspect of the otic vesicle extend into the vesicle's center and fuse. First, the anterior protrusion fuses with the medial followed by the posterior protrusion's medial fusion. These schematic and bright field images show the initial anterior-medial fusion event which occurs normally in wildtype (A,C; arrow), but fails to occur in *jekyll* mutants (B, D). A, anterior; P, posterior; all views lateral, anterior to left.

Figure 7

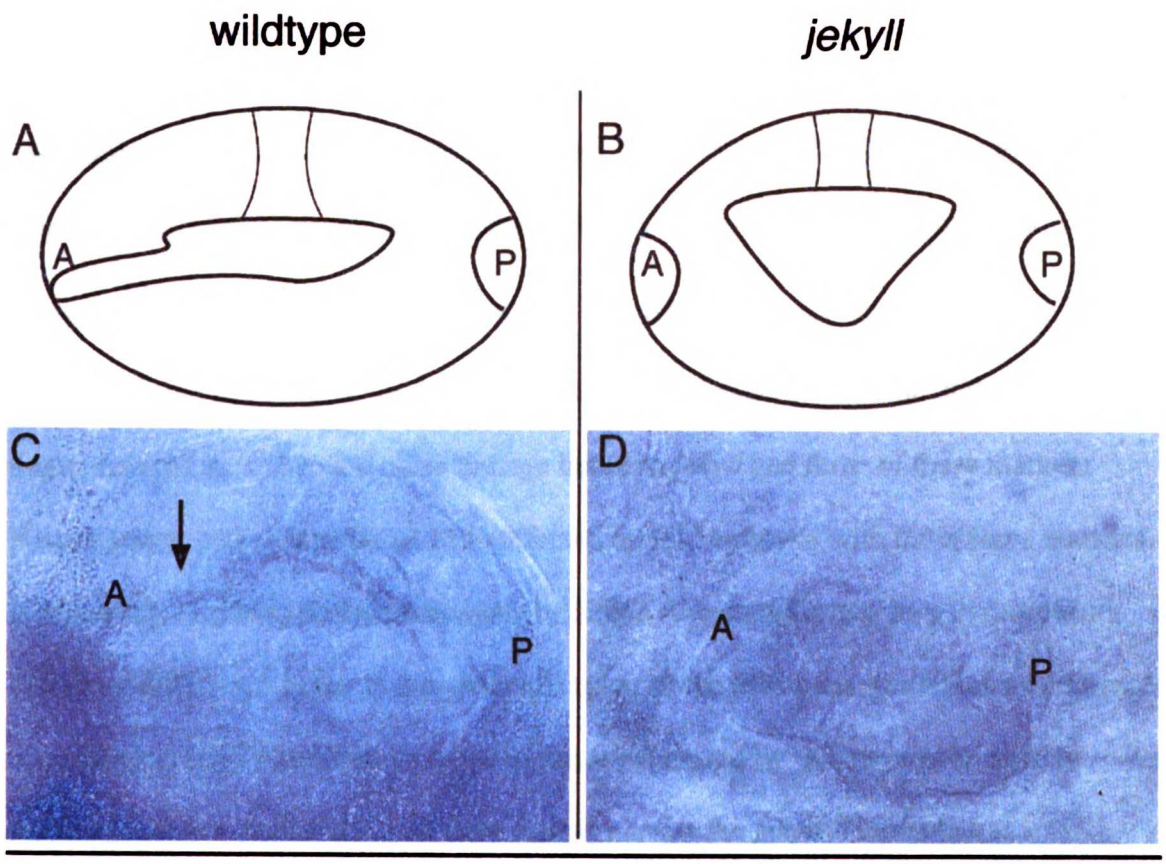

Chapter 2 jekyll cloning

Large-scale screens in zebrafish have identified several mutations that affect cardiac valve formation, the most severe of which is the recessive mutation *jekyll*.[2] To gain further insight into the *jekyll* valve defect, I isolated the disrupted gene by synteny cloning. I localized *jekyll* to a centromeric region of linkage group 1 using bulk segregant analysis[38] of embryos genotyped for polymorphic CA repeat markers. I then performed fine mapping of the region with 15 polymorphic markers on 200 wildtype haploid embryos, and found close linkage between *jekyll* and three of these markers. Next, I genotyped an additional 1150 affected diploid embryos with those three markers. Additionally, I genotyped recombinants by single strand conformation polymorphism (SSCP) a difference in the 3' untranslated region of the *ldb3* gene, for which an expressed sequence tag (EST) had been mapped to the *jekyll* region by radiation hybrid (RH) mapping. These studies allowed us to further narrow the *jekyll* interval to a 0.5 centimorgan region (Fig. 8).

Examination of the emerging map of the *jekyll* region revealed a remarkable conservation of synteny with a region of human chromosome 4p. Taking advantage of this conserved synteny, I mapped four zebrafish ESTs with homology to human genes in this 4p region. One of these ESTs, corresponding to a homologue of the *sugarless* gene (known as *UDP-glucose dehydrogenase* in humans and by convention, referred to as *ugdh* hereafter), was found by radiation hybrid mapping to lie between two markers closely flanking the *jekyll* locus. Sequence analysis of cDNA prepared from wildtype and mutant embryos revealed a T to A change at base pair 992 in the mutant allele (Fig. 10 A). Genotyping for this change revealed no recombination between *jekyll* and the

observed lesion in 2870 meioses.[39] The T to A change results in an isoleucine-to-asparagine substitution at residue 331 (Fig. 10 B). Isoleucine 331 is conserved in *Drosophila*, human, and zebrafish Ugdh and is situated in a pocket of nonpolar amino acids in the "hinge" of the omega loop "gate" that allows UDP-glucose access to the active site of the enzyme (Fig. 10 C).[40] This isoleucine-to-asparagine substitution is likely to affect enzyme activity.

To directly assess whether enzyme activity was lost or reduced as a result of the *jekyll* mutation, I began a collaboration with Dr. Andrew Pitsillides who had established an *in situ* colorimetric assay for Ugdh activity on cryostat sections. Preliminary results suggest that the *jekyll* mutation has severely reduced activity (data not shown). However these results are hard to interpret for a number of reasons: 1) as our collaborator had never worked with zebrafish, it was difficult to obtain similar sections from wildtype and mutant embryos (as level of activity does appear to vary from tissue to tissue, this was the major problem for comparison); 2) in at least one case our collaborator mistakenly identified a non-*jekyll* mutant as *jekyll*; this "mutant" appeared to have wildtype levels of activity (it was later shown to be wildtype by methylene blue staining). Further activity analysis is ongoing, but no results were available at the time of preparation of this thesis.

Ugdh enzymatic activity is required for the conversion of UDP-glucose into UDP-glucuronic acid, a critical component of hyaluronic acid, chondroitin sulfate, and heparan sulfate glycosaminoglycans.[41] Other mutations that affect the production of heparan sulfate proteoglycans in vertebrates result in defects during gastrulation. These include a targeted mouse mutation in the heparan sulfate glycosyltransferase, *EXT1*[42], and the

zebrafish *knypek* mutation, which disrupts a Glypican homologue.[43] The *jekyll* mutation, which should affect the production of heparan sulfate at the earliest step in the pathway, shows no obvious phenotype until organogenesis stages. One explanation for this incongruity is that zebrafish *ugdh* mRNA is provided maternally. Indeed, wholemount *in situ* hybridization analyses reveal the presence of *ugdh* mRNA at the 4-cell stage (Fig. 11 A), while zygotic transcription begins at the 1000-cell stage. Expression domains in the otic vesicle, heart, and branchial arches in older embryos (30, 37, and 48 hpf respectively) are consistent with the *jekyll* mutant phenotypes reported here and previously (Fig. 11 E-H).[36] Interestingly the maternal expression of *ugdh* may explain one of the anomalous findings of the *jekyll* phenotype. While the branchial arch phenotype which becomes apparent at 3.5 dpf is fully penetrant, the heart phenotype, apparent at 43 hpf, is not. This could represent only a partial requirement of *ugdh* for heart development, either due to functional overlap with another gene or from background/environmental differences between embryos. However, I favor the hypothesis that differences in loading of the maternal message are the cause of this reduced expressivity.

Morpholino antisense "knockdown"[44] of *ugdh* translation phenocopies the *jekyll* mutation (Fig. 12). Interestingly, this phenocopy can only be achieved by genetically sensitizing the injected embryos. Such sensitization can be attained in two ways: by halving the maternal product through the use of embryos generated from a cross between a *jekyll* heterozygote female and a wildtype male, in which case 90% of the antisense-injected embryos displayed the *jekyll* phenotype, or by halving the zygotic transcription, i.e., use of embryos from a *jekyll* heterozygote male and a wildtype female, in which case

35-50% of the antisense-injected embryos were affected. This sensitization is likely due to the decrease of early ubiquitous maternal and zygotic expression of the *jekyll* gene. Interestingly, the lack of an early phenotype in antisense-injected embryos suggests that in addition to *ugdh* mRNA, Ugdh protein is also provided maternally, or that another protein compensates for the lack of Ugdh, or even possibly that some maternal mRNA is protected from antisense-mediated translational inhibition.

Sulfated proteoglycans and enzymes required for their production have been implicated in human diseases that affect a variety of tissues and processes (*glypican3/4* in Simpson-Golabi-Behmel (OMIM 312870), *diastrophic dysplasia sulfate transporter* in Achondrodysplasia type IB (600972), *EXT1/2* in chondrosarcomas (215300), *xylosylprotein 4-beta-galactosyltransferase* in Ehler-Danlos (130070), *perlecan* in Schwartz-Jampel (255800), *nyctalopin* in congenital night blindness (310500), *CORNEAL n-acetylglucosamine-6-sulfotransferase* in macular corneal dystrophy (217800), *proteoglycan 4* in CAP syndrome(208250)). Cloning of the *jekyll* mutation implicates proteoglycans and hyaluronic acid in another group of syndromes that affect heart, ear, and cartilage development.

A number of complex human disorders affect heart, ear and craniofacial development simultaneously. Three such disorders, Down syndrome, CHARGE association, and Kabuki syndrome (OMIM 190685, 214800, and 147920), are hallmarked by dysmorphologies analogous to those seen in zebrafish embryos mutant for the *jekyll* gene. As the human *UDP-glucose dehydrogenase* gene maps outside the region normally associated with Down and CHARGE syndromes, it is unlikely that *ugdh* itself is directly involved in these disorders. Rather, mutations in this gene may act to modify the severity

or penetrance of these and other multi-organ syndromes. It is worth noting that three SNPs have already been identified in the human *ugdh* gene (2 in 3' UTR, and 1 intronic--Fig. 13).[45] These polymorphisms may have functional relevance in human disease.

Figure 8. Mapping of the *jekyll* mutation. Integrated genetic and radiation hybrid (RH) maps of the *jekyll* region illustrate the relationships between genes and CA-repeat "z" markers. Numbers underneath the line indicate the number of recombination events seen in 1150 diploid and 176 haploid embryos tested. Four zebrafish ESTs were chosen for RH mapping as they encode homologues of genes near *SLIT2, LDB3* and *UCHL1* on human chromosome 4p. One of the four, a clone encoding a protein with 84% amino acid identity to human UGDH, maps between *slit2* and *ldb3*, two genes that flank the *jekyll* locus.

Figure 8

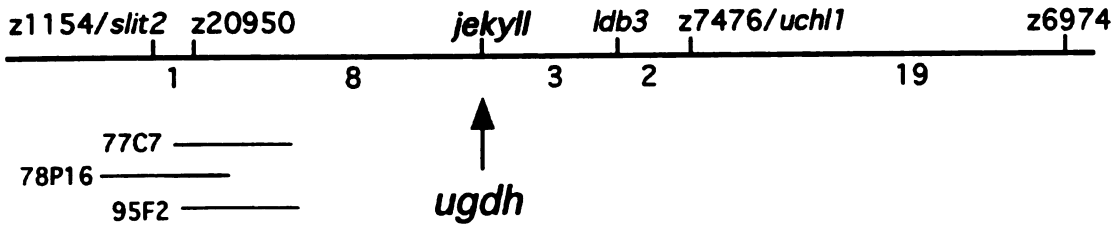
z1154/slit2
z20950
jekyll
ldb3
z7476/uchl1
z6974
1
8
3
2
19
77C7
78P16
95F2
ugdh

Figure 9. Sequence analysis of zebrafish *ugdh*. Full cDNA sequence of the *ugdh* gene with jekyll lesion, sequencing and genotyping primers indicated. The zebrafish *ugdh* cDNA sequence was deposited in Genbank under accession number AF361478.

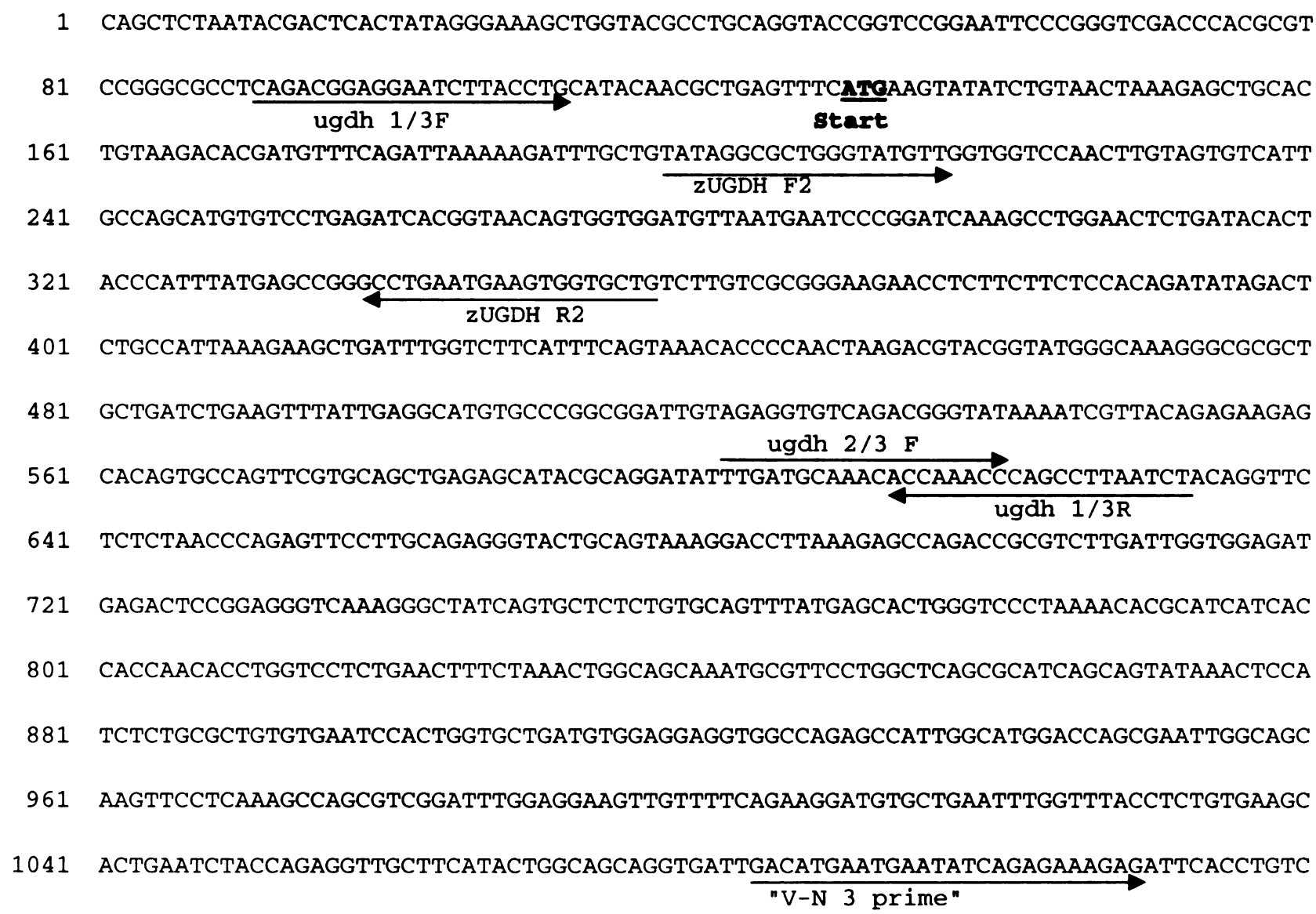
1 CAGCTCTAATACGACTCACTATAGGGAAAGCTGGTACGCCTGCAGGTACCGGTCCGGAATTCCCGGGTCGACCCACGCGT
81 CCGGGCGCCTCAGACGGAGGAATCTTACCTGCATACAACGCTGAGTTTCATGAAGTATATCTGTAACTAAAGAGCTGCAC
ugdh 1/3F
Start
161 TGTAAGACACGATGTTTCAGATTAAAAAGATTTGCTGTATAGGCGCTGGGTATGTTGGTGGTCCAACTTGTAGTGTCATT
zUGDH F2
241 GCCAGCATGTGTCCTGAGATCACGGTAACAGTGGTGGATGTTAATGAATCCCGGATCAAAGCCTGGAACTCTGATACACT
321 ACCCATTTATGAGCCGGGCCTGAATGAAGTGGTGCTGTCTTGTCGCGGGAAGAACCTCTTCTTCTCCACAGATATAGACT
zUGDH R2
401 CTGCCATTAAAGAAGCTGATTTGGTCTTCATTTCAGTAAACACCCCAACTAAGACGTACGGTATGGGCAAAGGGCGCGCT
481 GCTGATCTGAAGTTTATTGAGGCATGTGCCCGGCGGATTGTAGAGGTGTCAGACGGGTATAAAATCGTTACAGAGAAGAG
ugdh 2/3 F
561 CACAGTGCCAGTTCGTGCAGCTGAGAGCATACGCAGGATATTTGATGCAAACACCAAACCCAGCCTTAATCTACAGGTTC
ugdh 1/3R
641 TCTCTAACCCAGAGTTCCTTGCAGAGGGTACTGCAGTAAAGGACCTTAAAGAGCCAGACCGCGTCTTGATTGGTGGAGAT
721 GAGACTCCGGAGGGTCAAAGGGCTATCAGTGCTCTCTGTGCAGTTTATGAGCACTGGGTCCCTAAAACACGCATCATCAC
801 CACCAACACCTGGTCCTCTGAACTTTCTAAACTGGCAGCAAATGCGTTCCTGGCTCAGCGCATCAGCAGTATAAACTCCA
881 TCTCTGCGCTGTGTGAATCCACTGGTGCTGATGTGGAGGAGGTGGCCAGAGCCATTGGCATGGACCAGCGAATTGGCAGC
961 AAGTTCCTCAAAGCCAGCGTCGGATTTGGAGGAAGTTGTTTTCAGAAGGATGTGCTGAATTTGGTTTACCTCTGTGAAGC
1041 ACTGAATCTACCAGAGGTTGCTTCATACTGGCAGCAGGTGATTGACATGAATGAATATCAGAGAAAGAGATTCACCTGTC
"V-N 3 prime"

Figure 9

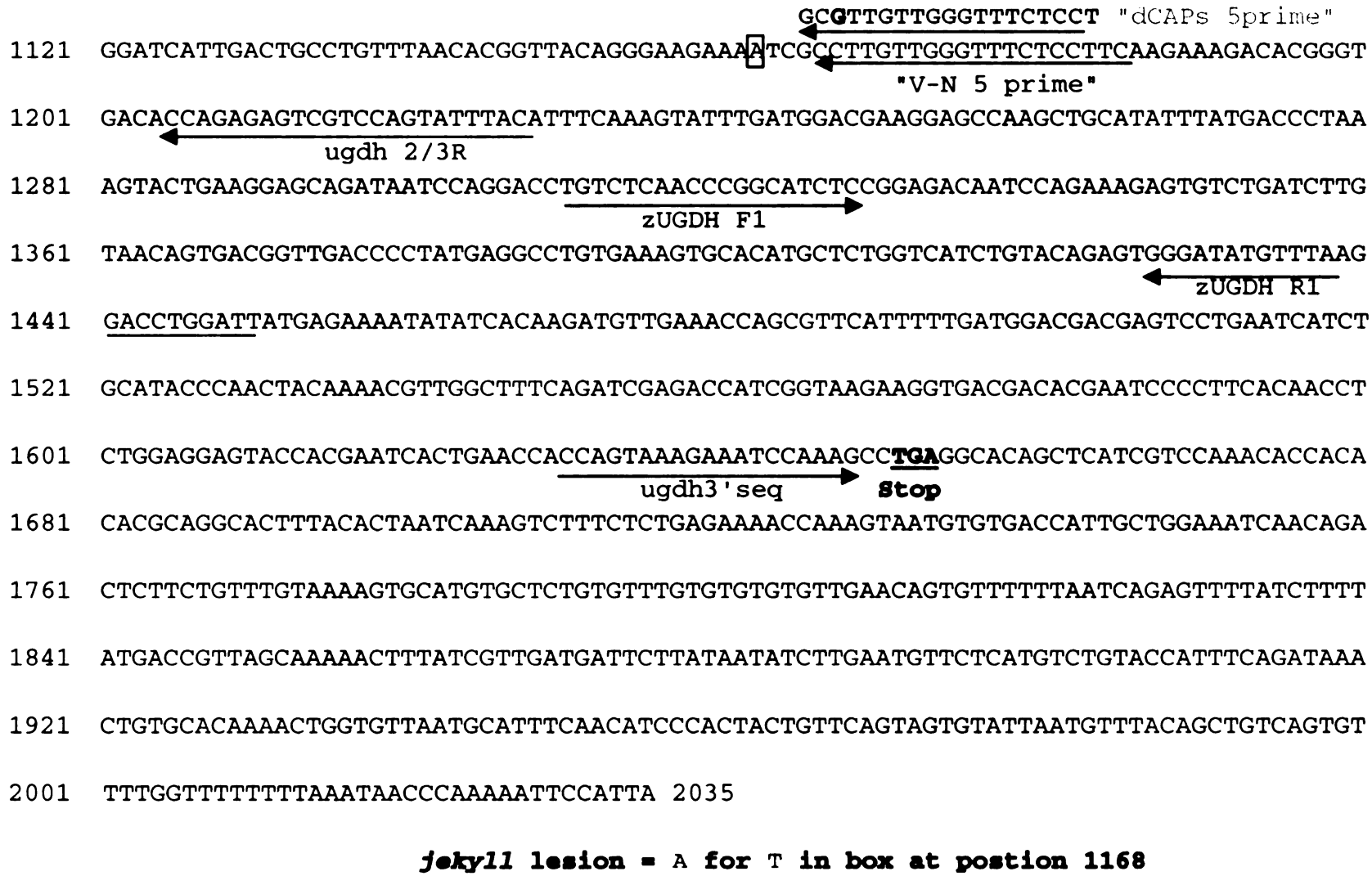

***Jekyll* lesion = A for T in box at postion 1168**

Figure 10. Protein sequence of Ugdh and *jekyll* missense mutation. (A) Sequencing of *ugdh* cDNA revealed a T to A change at base pair 992 in the *jekyll* mutant. This mutation results in an isoleucine-to-asparagine substitution at residue 331. (B) Ile 331 sits in a nonpolar pocket of the enzyme as illustrated in this rasmol image of the bovine Ugdh crystal structure.[40] The isoleucine is green, the nonpolar amino acids are white and the polar ones are blue. (C) Sequence alignment of bovine, human, mouse, zebrafish, and Drosophila Ugdh. Red arrow points to conserved isoleucine for which asparagine is substituted in *jekyll* mutants.

Figure 10

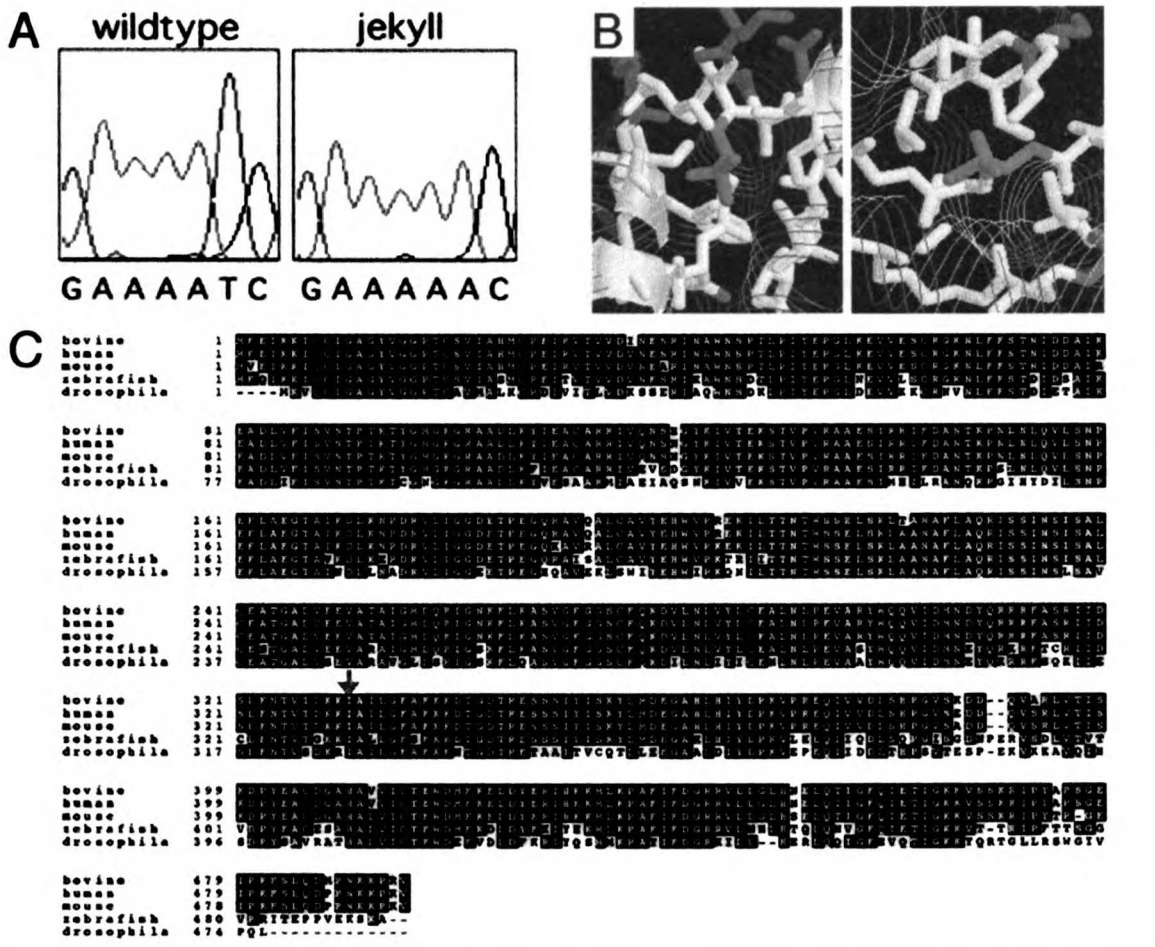
A
wildtype
jekyll
GAAAATC GAAAAAC
B
C
bovine
human
mouse
zebrafish
drosophila

Figure 11. *In situ* analysis of *ugdh* RNA expression. (A) Wholemount *in situ* hybridization[10] of a 4-cell stage embryo shows that *ugdh* mRNA is maternally provided and initially ubiquitous. (B) Dorsal mesendoderm expression of *ugdh* is apparent in a lateral view of a 90% epiboly embryo. (C) At the 6-somite stage, *ugdh* is expressed in many cells at a low level, but appears more highly expressed in the cells of the hatching gland rudiment (arrow). (D) At the same stage, a dorsal view reveals heightened expression in the adaxial cells of the developing somites (arrow). (E) An optical cross section through the hindbrain, heavy stain under brain is likely pharyngeal endoderm (arrow). Lateral expression is otic vesicle(arrowhead). (F) At 30 hpf, the developing otic vesicle (arrowhead) and branchial arches (arrow) express *ugdh* (dorsal view, anterior to the left). (G) From 37 hpf onward, a low level of *ugdh* expression can be detected in the developing heart (39 hpf shown, ventricle (V) and atrium (A) are indicated). (H) 48 hpf embryos exhibit *ugdh* expression in developing jaw elements (arrows), as well as continued expression in the otic vesicle (o) and fin bud (f) (lateral view, dorsal to the right). At 72 hpf, *ugdh* expression is present in the region of the liver, here indicated with arrows and shown in a dorsal (I) and lateral (J) view.

Figure 11

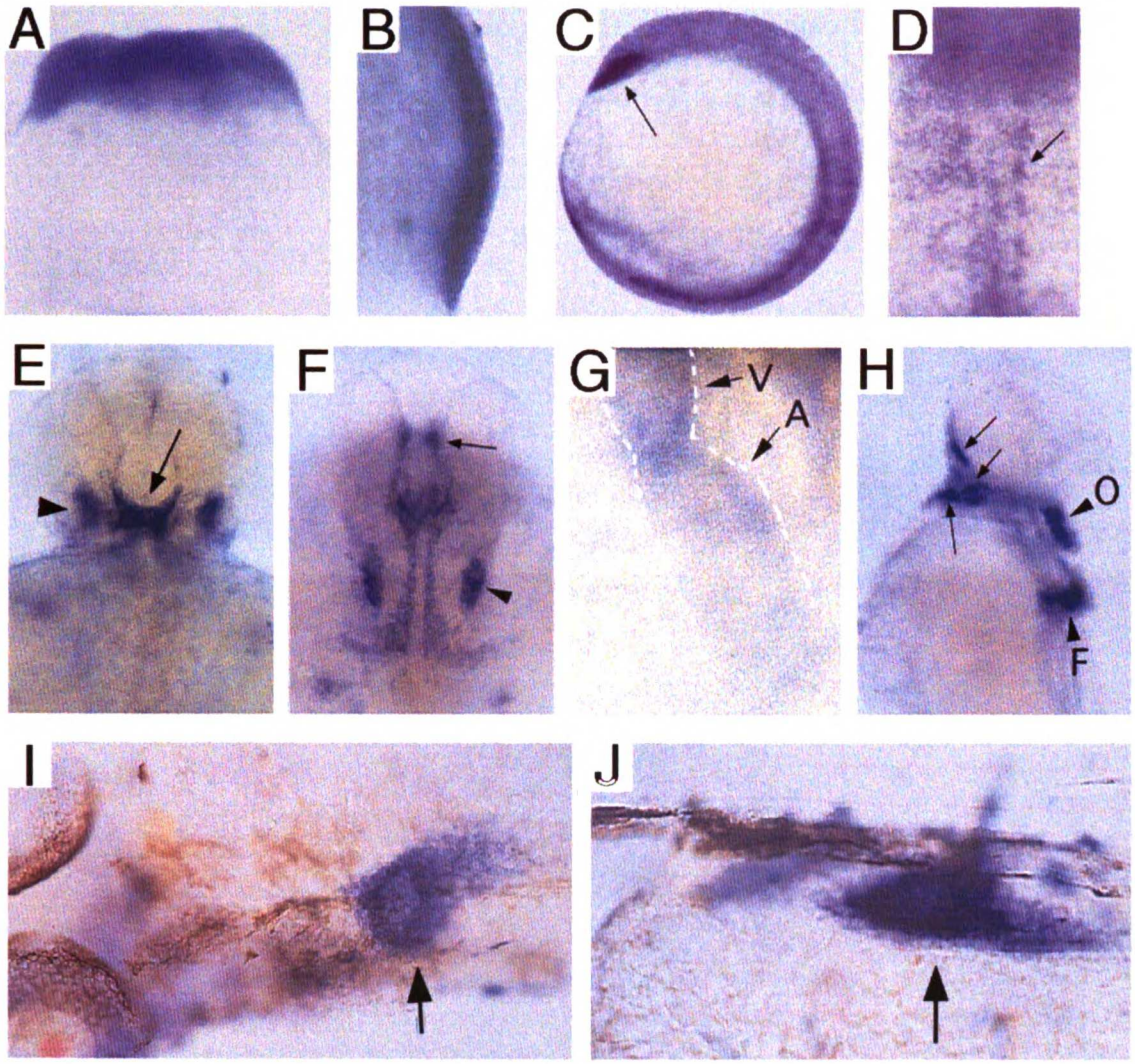

Figure 12. Morpholino antisense targeting *ugdh*. tie2-GFP transgene allows visualization of the first step in valve formation, endocardial clustering. (A-F) Antisense "knock-down" of *ugdh* phenocopies the *jekyll* mutation (A, C, E, uninjected wildtype, B, D, F morpholino-injected). (A, B) Injection of *ugdh* morpholino into sensitized embryos causes a failure of AV valve formation, here illustrated by a failure of endocardial clustering at the AV boundary in 43 hpf embryos. Examination at later stages reveals that valve formation never occurs in morpholino-injected embryos, showing that the defect at 43 hpf does not reflect a delay (C, D: 72 hpf; E, F: 96 hpf). Compare morpholino phenotype with wildtype and *jekyll* mutant at 48 hpf (G, H). Arrows indicate the AV boundary in all panels.

Figure 12

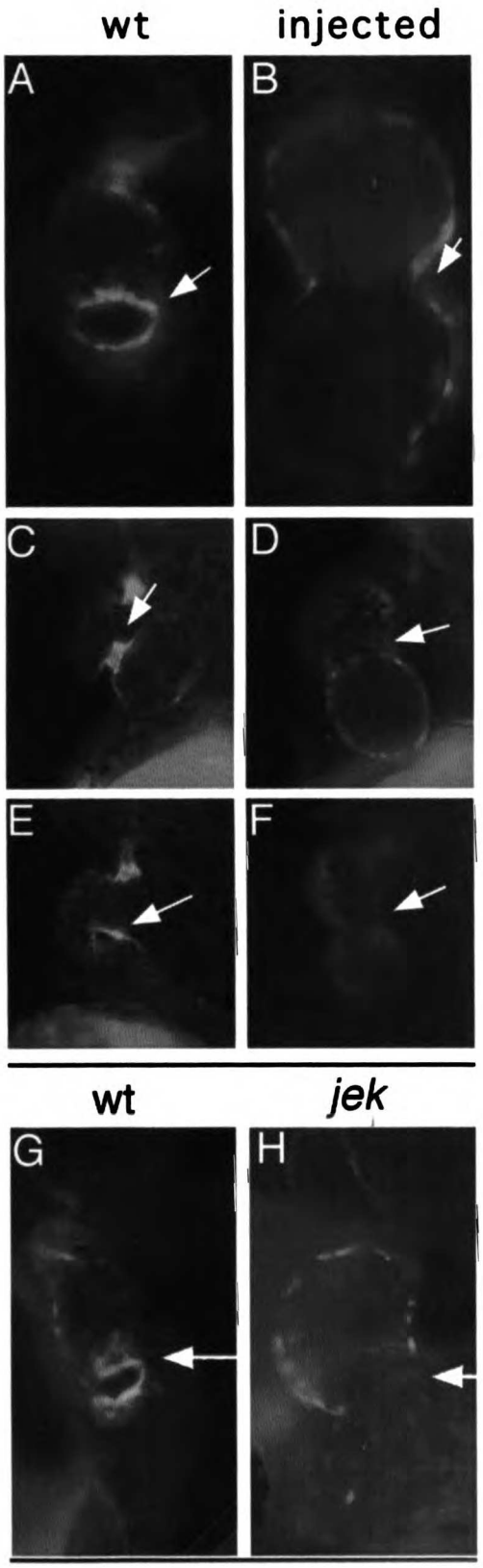

Figure 13. Common single nucleotide polymorphisms (SNPs) in human *ugdh*. Three SNPs are present in the non-coding regions of human ugdh, two in the 3' UTR and one the intron between exons 9 and 10. Sequence and polymorphisms are shown here.

Figure 13

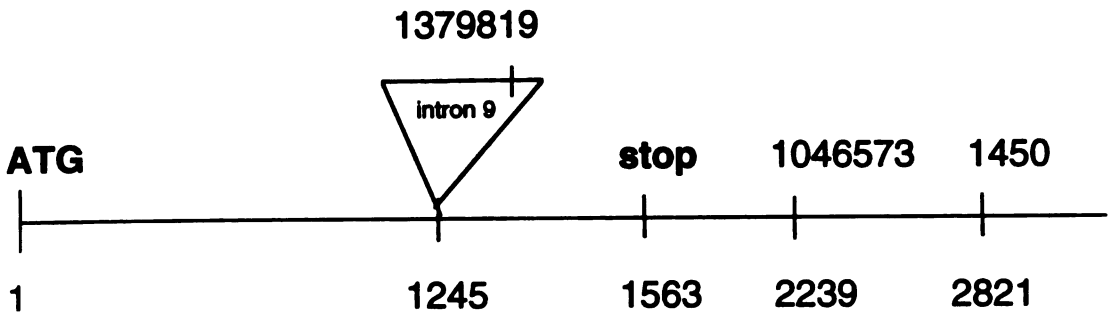

gene 1-2950 (genbank AF061016)
cds 79-1563

1379819 intron between exons 9 and 10
TTCTGTTTTTTTGTT[A/G] TTGCTATTGTTACAGTGTCCCGGCTC

1046573 3'utr bp 2239 (between 1st and 2nd polyA)
AGGGAAGGACAGTCTTCATT[T/C] CTCCTGGTTATTGGTTTGTTT

1450 3'UTR bp2821 (between 2nd and 3rd polyA)
GATGTTTAATGCAAAC[C/T] GTACATTCTCAGCAGAGCACAAGTA

jekyll mutant embryos exhibit pericardial edema and toggling of blood between the two chambers of the heart (compare Fig. 14, A and B). Together these phenotypes are generally indicative of defective AV valve function and are consistent with previous observations that *jekyll* mutant hearts lack valve tissue at 48 hours post-fertilization (hpf) (Fig. 14, C and D)[2]. To analyze endocardial morphology *in vivo*, I generated a line of *jekyll* heterozygotes bearing an integrated mouse *tie2* promoter driving green fluorescent protein (GFP) expression in the developing endocardium.[46] Normally, endocardial cells cluster at the AV boundary at the onset of valve formation at 43 hpf (Fig. 14 E). However, in mutant hearts this clustering fails to occur (Fig. 14 F) indicating that *jekyll* function is required for this early endocardial morphogenetic event.

As detailed in the introduction, explant experiments with embryonic chick tissues have shown that valve formation requires precise patterning of the myocardium and endocardium, as well as an inductive signal from the myocardium to the endocardium.[47] To determine how *jekyll* affects cardiac valve development, I assessed the expression of early differentiation markers of the valve-forming region: *bone morphogenetic protein (bmp) 4*, *notch1b*[19], and *br146* (a zebrafish *versican* homologue[48]). Initially all three genes are expressed throughout the anteroposterior extent of the heart. Later expression of these genes is restricted to the valve-forming region (*bmp4* and *br146* in the myocardium at 37 hpf and *notch1b* in the endocardium at 45 hpf). *jekyll* mutant embryos show defects in the expression of these genes (Fig. 15). While *bmp4* and *br146* expression domains become restricted from the atrium and largely from the ventricle, no heightened expression of these

genes is detectable at the AV boundary of *jekyll* mutant hearts at any stage assayed from 36-48 hpf (48 hpf shown, Fig. 15 B, D and F, H). *notch1b* expression becomes initially restricted from the atrial endocardium of mutant hearts. However, at 45 hpf, *notch1b* expression is elevated in the AV boundary of wildtype but not *jekyll* mutant embryos (appendix 6, Fig. 30).[49] At 48 hpf, atrial restriction fails to be maintained in mutant hearts and *notch1b* expression is again observed throughout the atrial and ventricular endocardium (Fig. 15 L). Thus, *jekyll* functions early in the process of AV valve formation and is required specifically in patterning the myocardium and endocardium at the AV boundary. Furthermore, the myocardial patterning defects seen in *jekyll* mutants are likely direct effects of the loss of Jekyll function as they are the first molecular defects to be observed, while the later endocardial defects may be secondary to the lack of *bmp4* restriction in the myocardium.

These data lead us to hypothesize that *jekyll* is required for cell signalling events that set aside the valve-forming region as distinct from atrium and ventricle. Perhaps similar to other boundary formation events in development, the cells at the border between the atrium and ventricle are specified to adopt a tertiary cell fate, that of the valve-forming region. In the *Drosophila* wing disc for instance, differences in *engrailed* expression between the anterior and posterior compartments restrict expression of the Hedgehog signal to the posterior and the Hedgehog receiving apparatus to the anterior. Thus, only cells on the anterior side of the compartment border can receive the Hedgehog signal coming from the posterior.[50] A similar situation exists in the vertebrate limb bud, where differences in *fringe* expression set up a domain of specific Notch signalling at the dorsoventral

border.[51,52] The cells at that boundary differentiate to form the apical ectodermal ridge, which is required for further outgrowth of the limb.

Atrial and ventricular fates are properly assigned in *jekyll* mutants, as expression of chamber specific markers appears normal (Fig. 16). Therefore, the first apparent molecular defect in *jekyll* mutants is a lack of boundary-restricted *bmp4* expression in the myocardium. A similar defect is seen in *cloche* mutant embryos, which lack endocardium altogether (Fig. 17).[12] Analysis of these two mutants suggests a model in which a primary endocardial signal to the overlying myocardium sets up a border between atrial and ventricular cells (Fig. 18). A secondary signal within the myocardium could then produce at the AV boundary a tertiary myocardial cell type with the competence to signal to the underlying endocardium. *jekyll* may be required for the primary endocardial signal or for the secondary myocardial signal that results in the tertiary cell fate.

In *Drosophila*, Sugarless has been shown to be important for Fgf and Wg signalling.[53-56] Other evidence suggests that glycosaminoglycans are important in Hedgehog and Bmp signalling as well.[41,57] The similarity of the morphological defects in the formation of the jaw elements in *jekyll*, *pipetail/wnt5a* and *knypek/glypican* mutants (chapter 4) suggests that in this process Jekyll is required for Wnt signalling, and that one substrate for Jekyll is the heparan sulfate proteoglycan, Glypican.

In the case of the heart, I have analyzed the currently available zebrafish mutations in Wg, Hedgehog, Bmp and Fgf signalling pathways (appendices 4-6) either assessing mutants for reported morphological heart defects, or through molecular analysis of mutant hearts. As a result, I have not found any overt defects in cardiac valve formation in any of

these known mutations. (However, mutants for *snailhouse/bmp7* ought to be further studied, as severely affected embryos appear to have defects in AV boundary formation, which may reflect earlier deficiencies in heart induction or something more specific (appendix 5)).

Based on these data and work in the mouse, I would like to propose that a signalling pathway heretofore not identified to require glycosaminoglycan production depends on Jekyll function during valve formation. A strong candidate for this signal is Neuregulin. Neuregulin is expressed in the ventricular endocardium, and loss of Neuregulin signalling leads to several phenotypes that are also observed in *jekyll* mutants, including the absence of myocardial proliferation in the ventricle and hypoplastic endocardial cushions.[58-60]

Neuregulin is an EGF family member that is thought to signal through ErbB2/B3 or ErbB2/B4 tyrosine kinase receptor heterodimers.[58] Neuregulin is produced in a membrane bound form and must be proteolytically processed for extracellular release. This proteolysis requires the presence of the cytoplasmic domain of the protein.[61] Loss of *neuregulin,* or two of its receptors, *erbB2,* or *erbB4* results in ventricular trabeculation defects and hypoplastic endocardial cushions at E10.5.[58-60] Mutants in another Neuregulin receptor, *erbB3,* display only mild defects in trabeculation; however, endocardial cushion development is affected.[62] The *erbB3* -/- cushions have reduced mesenchyme and are thinner than wildtype cushions at E9.5.

The differences between these phenotypes may be explained by the observed expression patterns of *neuregulin, erbB2, erbB3* and *erbB4.* The *neuregulin* gene is

expressed by the endocardium.[58,62] From there, it is thought to provide a signal required for trabeculation to the myocardium, where *erbB2* and *B4* are expressed.[4,60] Neuregulin is also believed to promote the development of the endocardial cushion where *erbB3* is expressed (presumably through an ErbB2/B3 complex[62]).

However, loss of these Neuregulin pathway members does not affect this process as severly as loss of *jekyll*. There are a number of possible reasons for this observation: 1) Functional overlap may exist within the Neuregulin pathway (i.e. more than one ligand/ receptor complex is involved), 2) *jekyll* may not act in the Neuregulin pathway at all, 3) *jekyll* may act in more than one pathway and these pathways may function in concert to delineate the AV boundary, and/or 4) *jekyll* may be required sequentially at the boundary and the cumulative loss of many consecutive signals is what gives rise to the more severe phenotype.

I have attempted to explore the involvement of Jekyll in Neuregulin signalling in three ways: expression analysis, morpholino antisense experiments, and overexpression experiments. All these experiments were made possible through a collaboration with Fabrizio Serluca in Mark Fishman's laboratory who cloned the full length *Ig-domain neuregulin* cDNA in zebrafish. Based on mouse knockout experiments, I believe that this isoform was the relevant one for heart development.[58,63]

First, I examined the zebrafish *neuregulin* expression pattern to ascertain whether there was a conserved expression of this gene between species. In fact, there was similar

expression, although the levels of expression seemed lower than one would have expected (Fig. 19).

Second, I had a morpholino designed against the 5' UTR of the *Ig-neuregulin* isoform. Injection of this morpholino yielded confusing results at best. Injection alone seemed to yield no phenotype except a slightly curled axis. Co-injection with a morpholino targeting *hyaluronic acid synthase 2* yielded more severe phenotypes than either alone, however only a few of the hearts appeared *jekyll*-like. Interestingly, injection of *has2* morpholino alone, on several occasions yielded late (3-4 dpf) *jekyll* phenotypes which may represent trabeculation defects and may implicate HA in the signalling events leading up to trabeculation.

Lastly, I have been employing a novel GalVP16-based misexpression system to drive targeted expression of neuregulin and an activated receptor in the heart. This system was pioneered by Reinhard Koester and Scott Fraser and graciously provided before publication.[64] These experiments are designed to explore whether overexpression of the *neuregulin* gene can rescue the *jekyll* phenotype, as is the case for overexpression of ligands in Drosophila *sugarless/ugdh* mutant embryos. Another result that would still implicate *jekyll* in Neuregulin signalling is if overexpression of *neuregulin* yields a phenotype in a wildtype embryo but not in a *jekyll* mutant. In this case, myocardial expression of the activated receptor ought to affect both wildtype and mutant embryos similarly, as receptor activation should be downstream of *jekyll* function.

The experimental design involves placing the *gal-vp16* gene under the control of a tissue specific promoter. I have used the *tie2* promoter for endocardial expression and the 1 kb *ctnt* promoter (graciously provided by Anja Huq and Amy Sehnert) for

myocardial expression. The tissue specific *gal-vp16* construct is then incorporated into a larger construct that includes two UAS (Gal binding site)-driven genes: *gfp* and your gene of interest. So for our *neuregulin* experiment, the final construct will be:

tie2--gal-vp16; UAS-*gfp*; UAS-*neuregulin*

or for our activated receptor experiment, the construct will be:

ctnt--gal-vp16; UAS-*gfp*; UAS-*erbB4* (Q).

Production of these constructs is ongoing. Completion is detailed in Figure 20. Benno Jungblut has been helpful in many steps of the subcloning process and will be continuing production of the remaining constructs.

This binary system was designed with transient misexpression in mind. While there is a possibility that transient injection of these constructs will provide the answers sought, it is likely that experiment-to-experiment variability will make these experiments difficult to interpret. Due to the fact that the *jekyll* heart phenotype is not fully penetrant, it is possible that these experiments will need to be performed multiple times on embryos with exact misexpression levels and spatiotemporal control. As such, I have begun creating transgenic lines bearing the *tie2/ctnt--gal-vp16*; UAS-*gfp* or the UAS-*neuregulin/erbB4* alone. To achieve this, one must inject linearized versions of these DNA constructs into single cell embryos before cytoplasmic streaming begins. Injected embryos are raised to adulthood, these fish are termed F_0. Transgenic lines can then be identified either by *gfp* expression or by PCR for the transgene in the F_1 embryos resulting from intercrossing F_0 adults.

This misexpression system will also be very useful for determining the cell autonomy of the *jekyll* heart defect, as extensive cell transplants between "wildtype" and

jekyll mutant embryos proved uninformative with regards to cell autonomy. The failure of these transplant experiments is likely due to a number of reasons.

Due to the fact that the *jekyll* heart phenotype is not fully penetrant, several measures were taken to make each transplant more informative. First the donors were either *cloche* mutants or *tie2-gfp* transgenics. In fact, the line crossed to produce the donors was a *clo;tie2-gfp* line. This was done for two reasons: 1) to increase the number of myocardium-only clones (as *clo* is cell autonomously required to form endocardium), 2) to allow the visualization of endocardial clones, as these clones are sometimes hard to differentiate from myocardial clones and often hard to see with the rhodamine dextran alone. At first, *jekyll* homozygotes were used as recipients, but variation in penetration of the phenotype yielded few informative transplants. Therefore, a second measure was taken. The recipients used were the progeny of a *jekyll* cross injected with *ugdh* MO to increase the penetrance of the heart phenotype (usually one sees a 90% penetrance in this type of experiment). However, this practice had the unforeseen consequence that genotyping was no longer reliable to determine whether an embryo was just part of the 5% wildtype or in fact rescued. Furthermore, assessing potential rescues for alcian staining of the branchial arches is also uninformative as *ugdh* MO injections have only mild effects on this process. Therefore, relying on this phenotype as a readout of a successful injection was not appropriate.

In the end, 599 transplants were performed (overall recipient survival 78%): 37 with myocardial clones and 14 with endocardial clones. Due to the aforementioned penetrance issues, as well as small clone sizes, no conclusions could be made. However use of the GalVP16 system should allow resolution of these issues. If a UAS-*ugdh* line is

Figure 14. *jekyll* heart phenotype. Wildtype (A) and mutant (B) embryos at 48 hpf, lateral view, anterior to the left. Pericardial edema surrounds the *jekyll* mutant heart and blood has accumulated in both chambers (at this stage the ventricle is anterior (to the left) and in this embryo, the atrium is slightly obscured by a skin melanocyte). Arrows point to the heart in (A) and (B). Methylene blue stained JB4 sections through wildtype (C) and *jekyll* (D) hearts at 4 dpf reveals a lack of AV valve (arrows) (reproduced from (2)). Additionally, one sees a reduction of extracellular matrix deposited between myocardial and endocardial cell layers in the *jekyll* mutant heart and a lack of muscularization/trabeculation in the *jekyll* mutant ventricle (arrowhead). *tie2*-GFP allows visualization of wildtype (E) and mutant (F) endocardial morphology at 43 hpf, lateral view, anterior to the top and dorsal to the left. Arrows indicate the AV boundary where endocardial cells cluster in wildtype embryos at the onset of valve formation. wt, wildtype; V, ventricle; A, atrium. Bars, 140 μm.

Figure 14

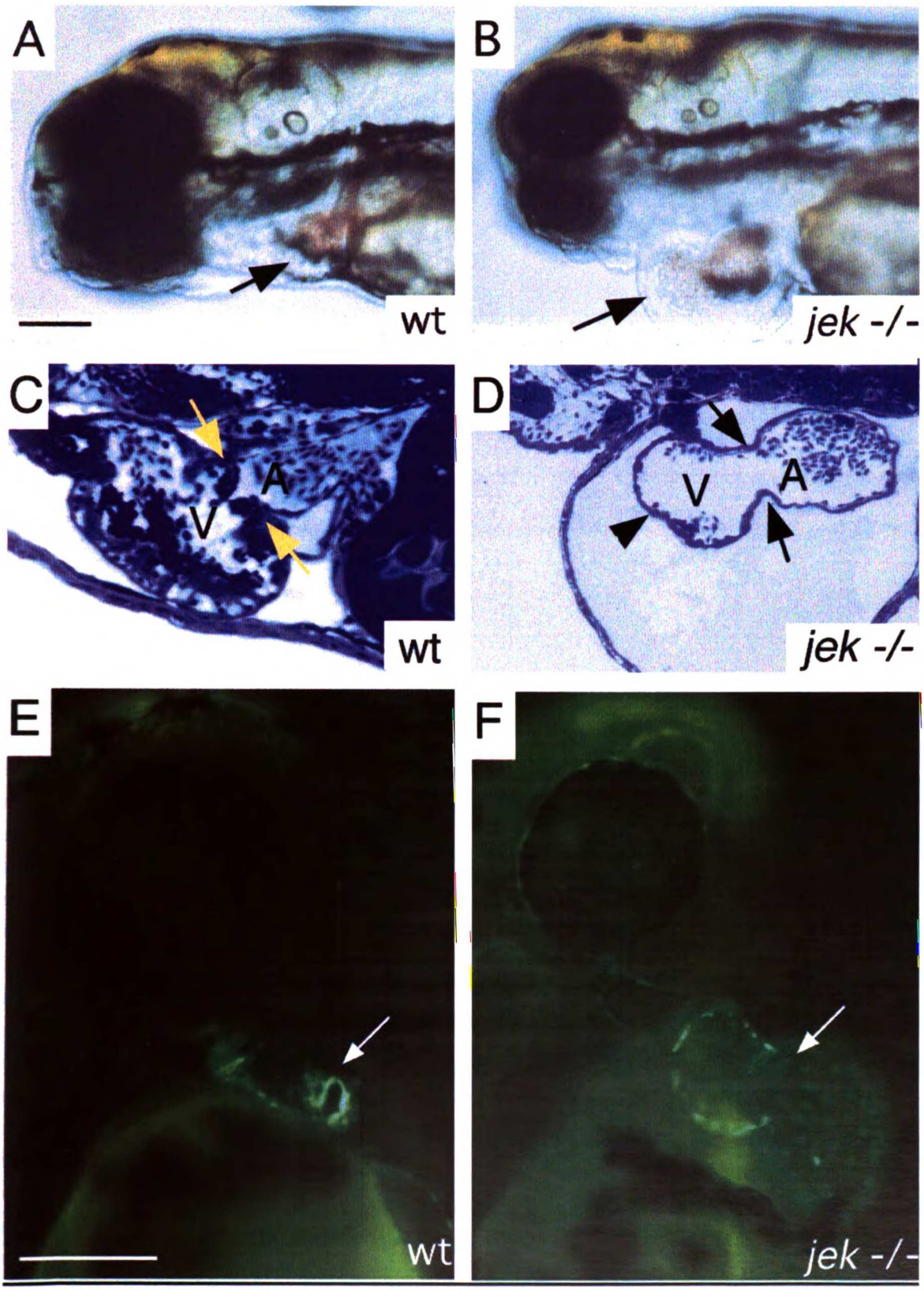

Figure 15. Atrioventricular boundary formation in *jekyll* mutants. Molecular analyses of AV valve development reveal early defects in *jekyll* mutant embryos. Schematized representations are shown to the left of the actual data. Initially expressed throughout the anteroposterior extent of the heart [49], *bmp4*, *br146* and *notch1b* become restricted to the AV boundary before the onset of valve formation. At 48 hpf, *bmp4* (A, B) and *br146* (E, F) are expressed in the myocardium and *notch1b* (I, J) in the endocardium. RNA *in situ* hybridization [10] for these genes reveals defects in *jekyll* mutant hearts. (B,D,F, and H) While expression of *bmp4* and *br146* does become restricted from the atrium and largely from the ventricle, there is no heightened expression at the valve-forming region as in wildtype. (J, L) *notch1b* expression is not increased at the AV boundary and at this stage is no longer restricted from the atrium. A, atrium; V, ventricle; wt, wildtype. Bars, 20 μm.

Figure 15

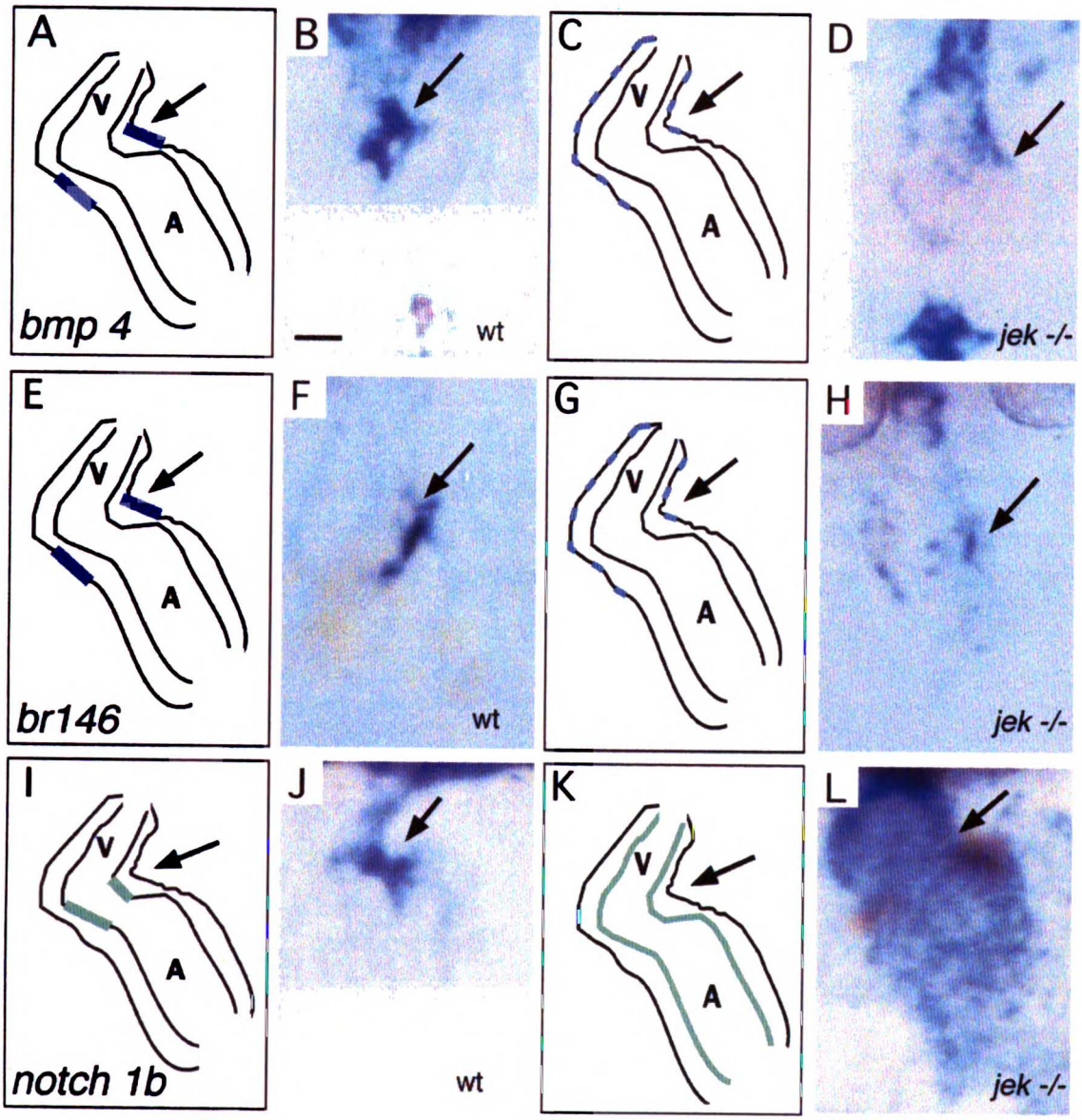
A
V
A
bmp 4
B
wt
C
V
A
D
jek -/-
E
V
A
br146
F
wt
G
V
A
H
jek -/-
I
V
A
notch 1b
J
wt
K
V
A
L
jek -/-

Figure 16. Chamber specification in *jekyll* mutants. Atrial and ventricular myocardial differentiation appears normal in *jekyll* mutant embryos. Immunofluorescence staining with MF20 (red) and S46 antibodies (green) at 48 hpf. MF20 recognizes a myosin heavy chain present throughout the heart, and S46 recognizes an atrial-specific isotype of myosin heavy chain. Co-staining allows visualization of both chambers: ventricle appears red and atrium appears yellow as a result of overlap. Although *jekyll* mutant hearts are somewhat enlarged (B) compared to wildtype (A), the staining pattern appears normal. Staining performed as described previously.[3] Chamber specification also appeared normal via *in situ* hybridization for the ventricular marker, *irx4* (data not shown). Bars, 20 μm.

Figure 16

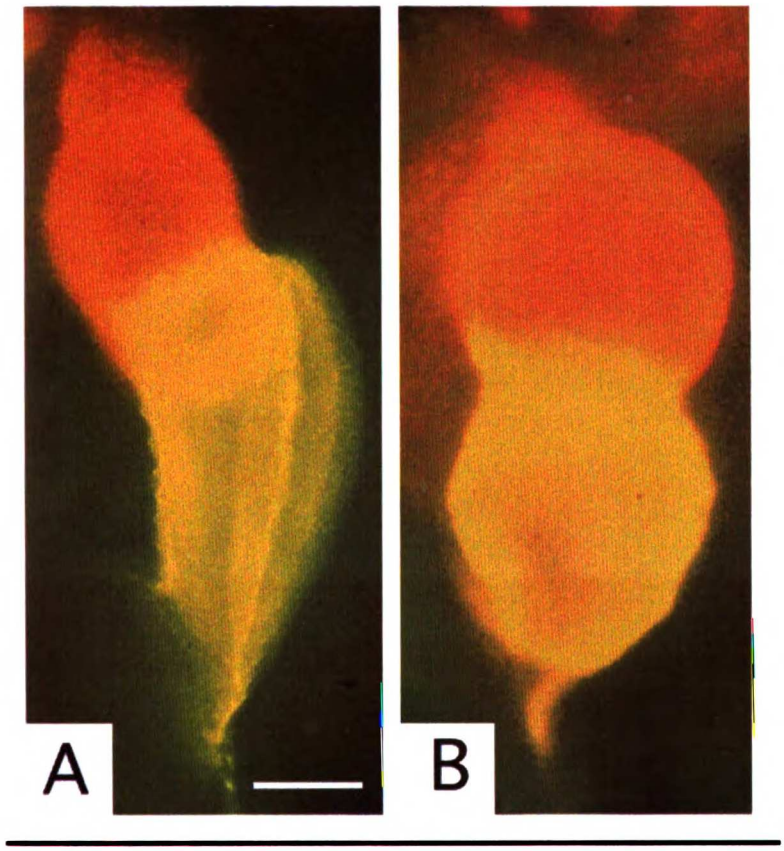

Figure 17. Atrioventricular boundary formation in *cloche* mutants. At about 48 hpf, one sees increased expression of *bmp4* at the myocardial AV boundary. Sometimes on both sides of the heart (A), and sometimes only in the inner curvature (B). This likely due to the dynamic expression of this gene. However, in *cloche* mutants (C-E), increased expression of *bmp4* is never observed at the boundary. Arrows indicate boundary in all panels.

Figure 17

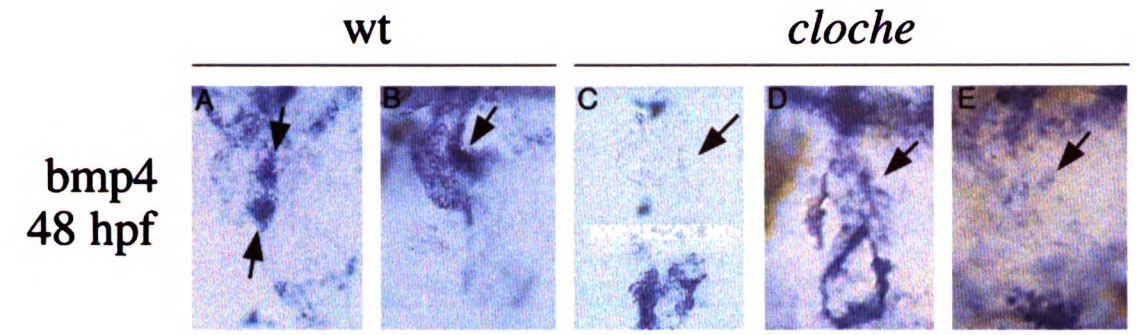

Figure 18. Model of *jekyll*'s role in atrioventricular boundary formation (A). A chamber specific primary signal (red arrows and dots) is sent from the endocardium and received by the myocardium (red X's). This establishes a border in the myocardium between the chamber that receives the signal and the chamber that does not receive the signal (**step 1**). A secondary signal (purple arrow) within the myocardium occurs as a result of the primary signal's chamber restriction (**step 2**). This second signal restricts myocardial signalling competence (orange) to the AV boundary cells (**step 3**). A subsequent myocardial-to-endocardial signal (**step 4**) induces endocardial morphogenesis and ultimately valve formation (**step 5**) (steps 4 and 5 not shown). In this model, loss of *cloche* gene function,which is required cell-autonomously for endocardial development, would prevent the primary endocardial signal in step 1. Based on our observations, *jekyll* could be required in steps 1, 2 or both. I currently favor the hypothesis that *jekyll* is required for delivery of the primary signal (**step 1**) and illustrate two possible mechanisms of *jekyll*'s involvement (B and C). HA and or proteoglycans (blue squiggles) are either acting in the extracellular matrix (B) or bound to the membranes of receiving cells (C). A, atrium; V, ventricle; E, endocardium; M, myocardium.

Figure 18

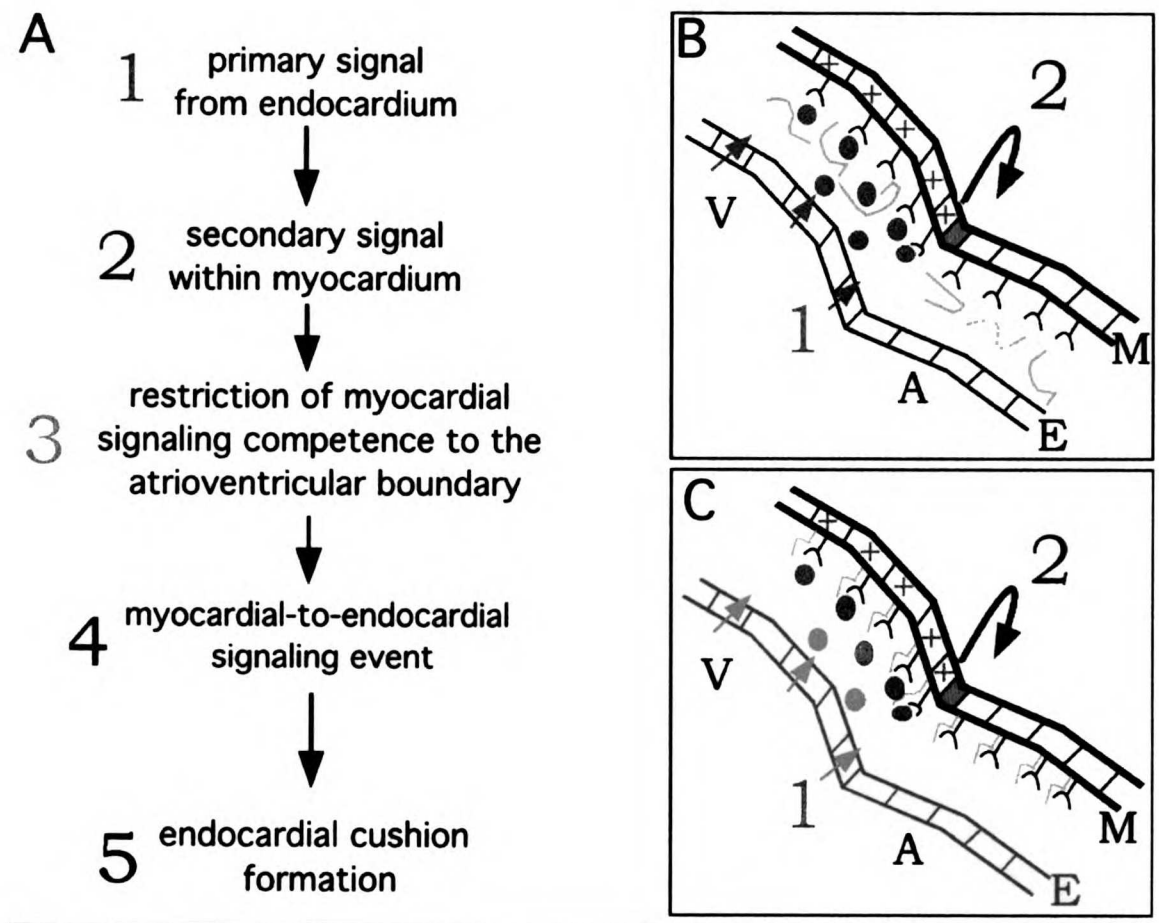
A
1 primary signal from endocardium
2 secondary signal within myocardium
3 restriction of myocardial signaling competence to the atrioventricular boundary
4 myocardial-to-endocardial signaling event
5 endocardial cushion formation
B
2
V
1
M
A
E
C
2
V
1
M
A
E

Figure 19. Expression of the zebrafish *neuregulin* gene. *neuregulin* is expressed at low levels in the endocardium of the ventricle at 36 hpf (A). Later at 48 hpf (B), *neuregulin* is restricted to the endocardial AV boundary (arrow). Oblique lateral views, anterior is up and ventral is to the right.

Figure 19.

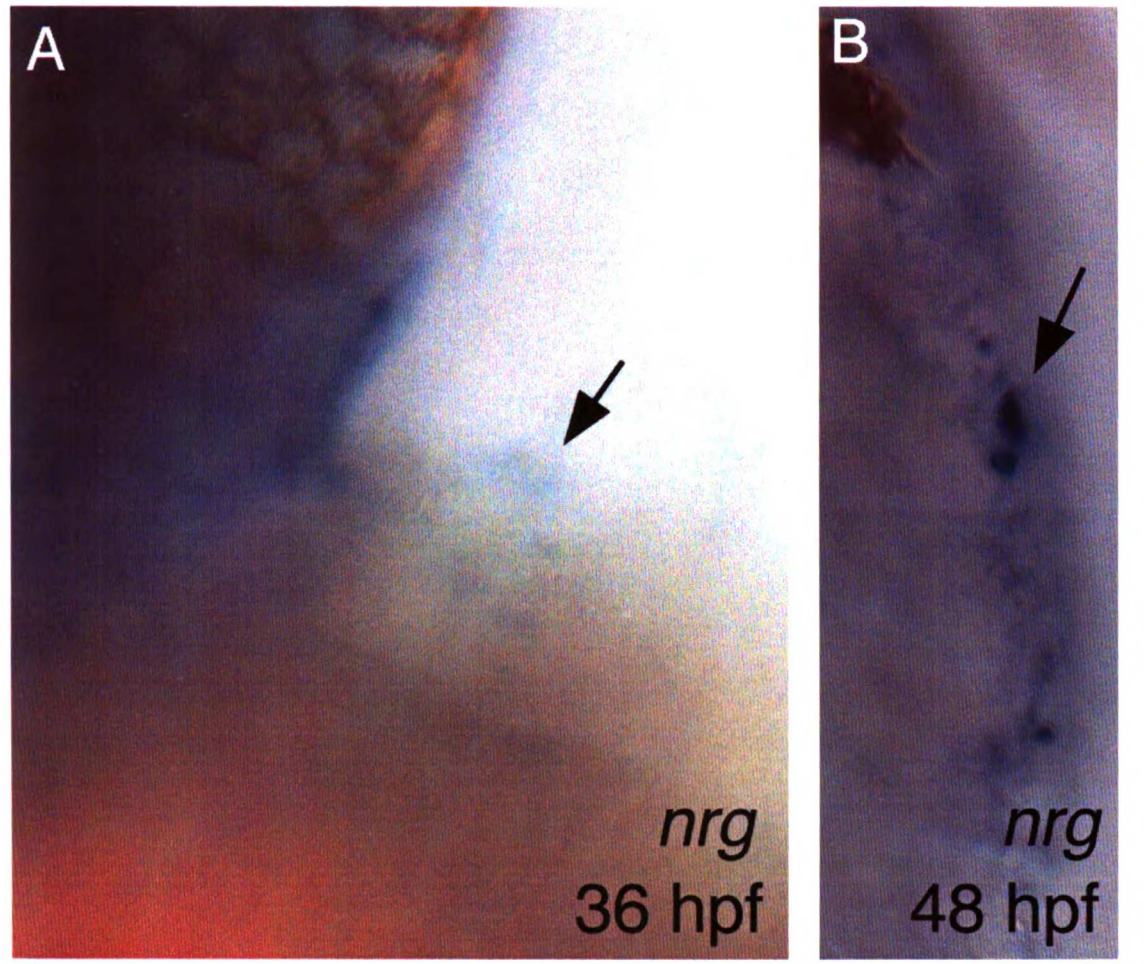

Figure 20. Gal VP16 binary system misexpression constructs to test Neuregulin's role in AV boundary formation.

As there may be more than one *neuregulin* gene in zebrafish, the failure of the morpholino antisense experiments does not necessarily indicate that Neuregulin is not the boundary formation signal. Gain of function experiments must also be performed to fully assess the role of Neuregulin at the AV boundary. Inititally transient misexpression will be employed while transgenic fish are created and identified. Two lines of experimentation will be followed. First, overexpression of *neuregulin* in the endocardium of *jekyll* embryos to attempt rescue or if overexpression of *neuregulin* in wildtype embryos produces a phenotype, overexpression in *jekyll* embryos will be assessed for that same phenotype. Presumably if *jekyll* is required for Neuregulin presentation the overexpression phenotype will not be present or will appear less severe in *jekyll* mutants. Second, Expression of an activated ErbB4 receptor will be driven in the myocardium of wildtype and *jekyll* mutant hearts. As *jekyll* presumably acts upstream of the receptor, this should either rescue the *jekyll* mutant phenotype or cause the same misexpression phenotype in wildtype and mutant embryos.

Shown in Figure 20 are the transient and transgenic constructs that are completed or in preparation (as indicated).

Figure 20

myocardial galVP16; uas-GFP

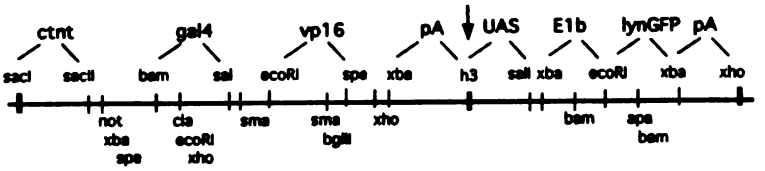

completed
"c102 145"

uas-neuregulin

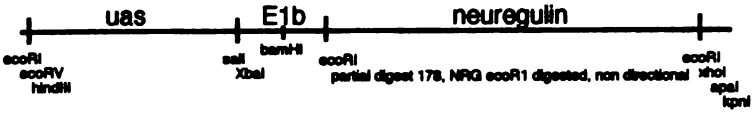

completed
"178-NRG 2.5"

uas-activated erbB4 (Q646C)

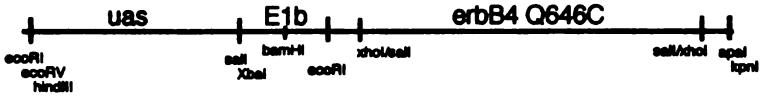

completed
"178 erbB4 Q1"

---

transient constructs to be created:

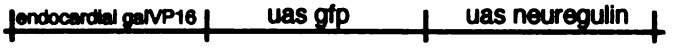

---

transgenics to be made:

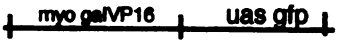

uas neuregulin

uas erbB4 Q

uas ugdh

Chapter 4 jekyll arches

Branchial arch formation begins as neural crest cells from the hindbrain migrate to occupy the pharyngeal region. In a process known as condensation, these mesenchymal cells form rolling hills of cells that eventually produce cartilage elements at their center. At early steps in this process, *jekyll* mutant arches are indistinguishable from wildtype with respect to shape, number of cells, and molecular differentiation (Fig. 21 K-M). Similarly, *in situ* hybridization analysis of late markers of differentiating chondrocytes reveals no differences between wildtype and mutant (Fig. 21 E-J).

These data are in stark contrast to the obvious defect seen from 3 dpf in alcian and methylene blue stainings of the arch elements (4 dpf shown, Fig. 21 A-D and reported previously in 36). Alcian green, which marks sulfated proteoglycans heavily deposited in developing cartilage, fails to stain the developing arches and fin buds in *jekyll* mutant embryos (Fig. 21 A, B). Similarly, methylene blue, which undergoes a metachromatic shift in the presence of negatively charged moieties like sulfated proteoglycans, fails to stain the developing chondrocytes in *jekyll* mutant arches (Fig. 21 C, D).

This severe phenotype in alcian and methylene blue staining is consistent with our finding that *jekyll* encodes an enzyme required for the production of glycosaminoglycans. Initially I believed that the main defect in the arches was this loss of staining as no other molecular defects were found. However, closer examination reveals a more subtle phenotype in the morphogenesis of the branchial arches (Fig. 22 A-F).

There are two main morphogenetic defects in the arches of *jekyll* embryos, and these defects are quite similar to those found in *knypek/glypican* and *pipetail/wnt5a* mutants.[43] First, *jekyll* arches have a wider diameter than wildtype (Fig. 22 A-C). This

defect is easily detected in the first branchial arch, here shown in comparison to a *pipetail* mutant embryo. While the first arch is only 1-2 cells in diameter in wildtype embryos, is 3-4 and 5-6 cells wide in *pipetail* and *jekyll* mutants, respectively. This broadness may reflect a lack of intercalation between chondrocytes. Additionally, methylene blue stained parasagittal sections reveal that the proper slanting of the arch elements is defective similarly in *jekyll* and *pipetail* mutants (Fig. 22 D-F). In wildtype embryos, branchial arches exhibit a dorsoanterior-ventroposterior alignment (indicated by the arrow in D). By contrast, in *pipetail* and *jekyll* mutants the arches exhibit a ventroanterior-dorsoposterior alignment (arrows in E and F respectively).

The similarity of the morphological defects in the formation of the jaw elements in *jekyll*, *pipetail/wnt5a* and *knypek/glypican* mutants suggests that in this process Jekyll is required for Wnt signalling, and that one substrate for Jekyll is Glypican. However, there may be other ligands involved as the width of the *jekyll* mutant arch is larger than that of the *pipetail/wnt5a* mutant arch. Also, it appears that *jekyll* mutant arches do not fuse correctly at the midline. This is particularly true of the first branchial arch. This phenotype is not present in *pipetail/wnt5a* mutants, further implicating another Jekyll-mediated signalling pathway in the process of branchial arch formation.

Figure 21. Molecular analysis of the *jekyll* branchial arch defect. (A-J) dorsal views, anterior to the right. (A, B) Alcian green staining for sulfated proteoglycans deposited in the developing cartilage is completely absent in *jekyll* mutant embryos at 4 dpf (remaining medial staining is in the pharynx). (C, D) Methylene blue staining of parasagittal sections allows further analysis of this defect as this dye undergoes a metachromatic shift from blue to purple in the presence of negatively charged moieties like sulfated proteoglycans. Arrow indicates the position of a purple callyx that surrounds wildtype chondrocytes in the third branchial arch (C). Arrow in D denotes the loss of this staining in a mutant sibling. A comparison of the sections also shows that *jekyll* chondrocytes are generally dysmorphic and *jekyll* arches lack an accumulation of extracellular matrix between the arch elements. (E-J) Comparative analysis of the expression of two genes associated with chondrocyte differentiation, *collagen 2a* and *sox9a*, reveals no gross defects between wildtype and mutant arches. Arrows point to gene expression in various chondrocyte populations (E, F: ethmoid plate; G, H: mandible; I, J: auditory capsule). (K) Cell number and morphology of early condensing arches is normal in *jekyll* mutant embryos at 48 hpf (lateral view, rostral to the left). (L, M) Branchial arch expression of *bmp4* and *dlx2* is indistinguishable between wildtype and *jekyll* mutant embryos at 36 hpf (wildtype staining is shown for reference, dorsal views, anterior to the top).

Figure 21

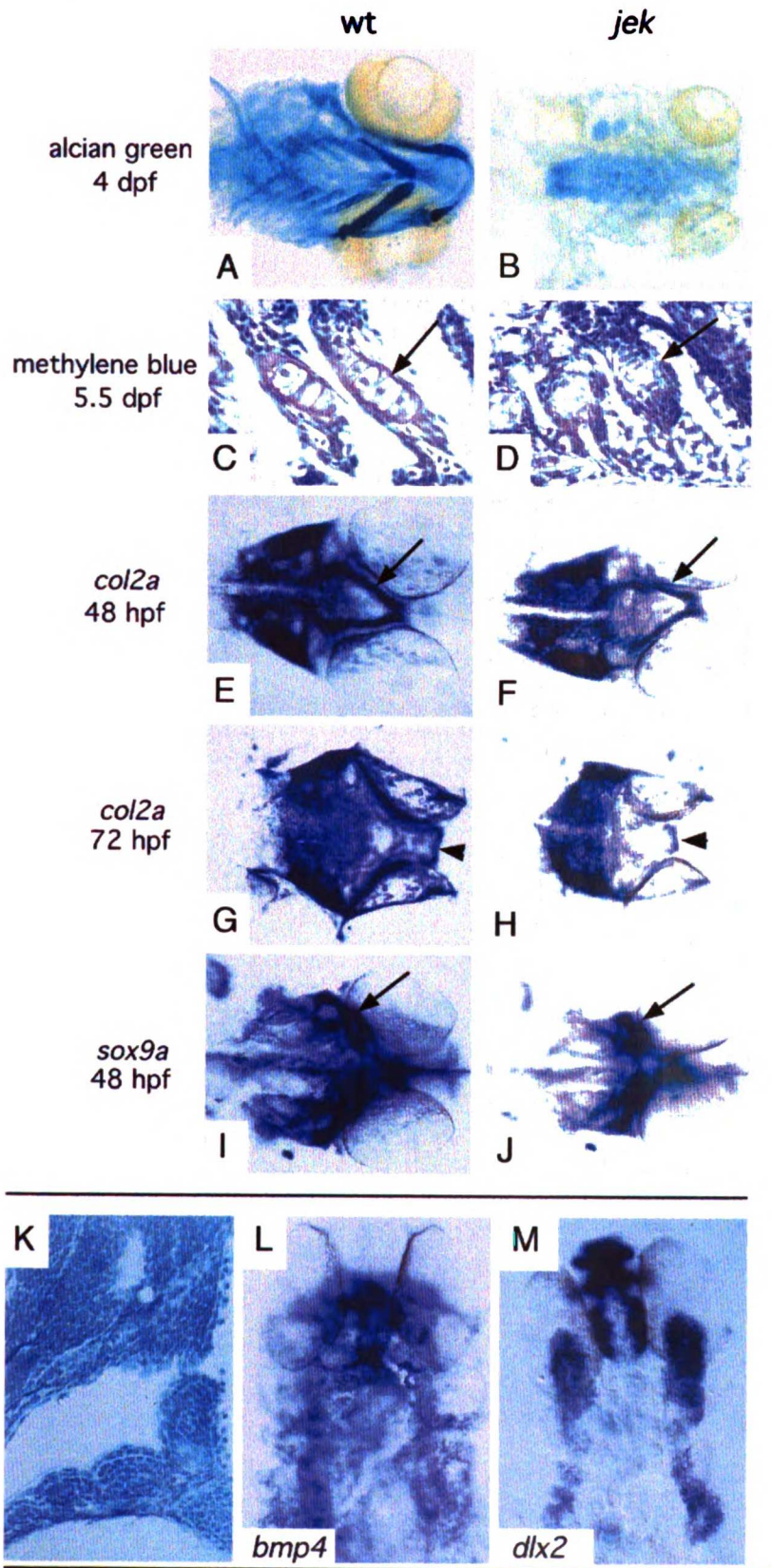
wt
jek
alcian green
4 dpf
A
B
methylene blue
5.5 dpf
C
D
col2a
48 hpf
E
F
col2a
72 hpf
G
H
sox9a
48 hpf
I
J
K
L
bmp4
M
dlx2

Figure 22. Comparison of branchial arch morphology between *jekyll* and *pipetail/wnt5a* mutant embryos. (A-C) Alcian green staining of wildtype (A), *pipetail/wnt5a* mutant (B), and *jekyll* mutant (C) embryos at 4 dpf (*39*). As noted previously (*16*), *jekyll* branchial arches are devoid of alcian staining which detects negatively charged sulfated proteoglycans deposited around developing chondrocytes. Closer examination reveals additional morphological defects in the *jekyll* mutant arches, similar to those seen in *pipetail* mutants. The first branchial arch, which is only 1-2 cells in diameter in wildtype embryos, is 3-4 and 5-6 cells wide in *pipetail* and *jekyll* mutants, respectively. Typical cells are outlined in white next to arrow (ventral view, anterior to the left). (D-F) Methylene blue staining of JB4 plastic parasagittal sections shows additional defects in the arches at 4 dpf (anterior to the left). In wildtype embryos, branchial arches exhibit a dorsoanterior-ventroposterior alignment (indicated by the arrow in D). By contrast, in *pipetail* and *jekyll* mutants the arches exhibit a ventroanterior-dorsoposterior alignment (arrows in E and F respectively). Bars, 50 μm.

Figure 22

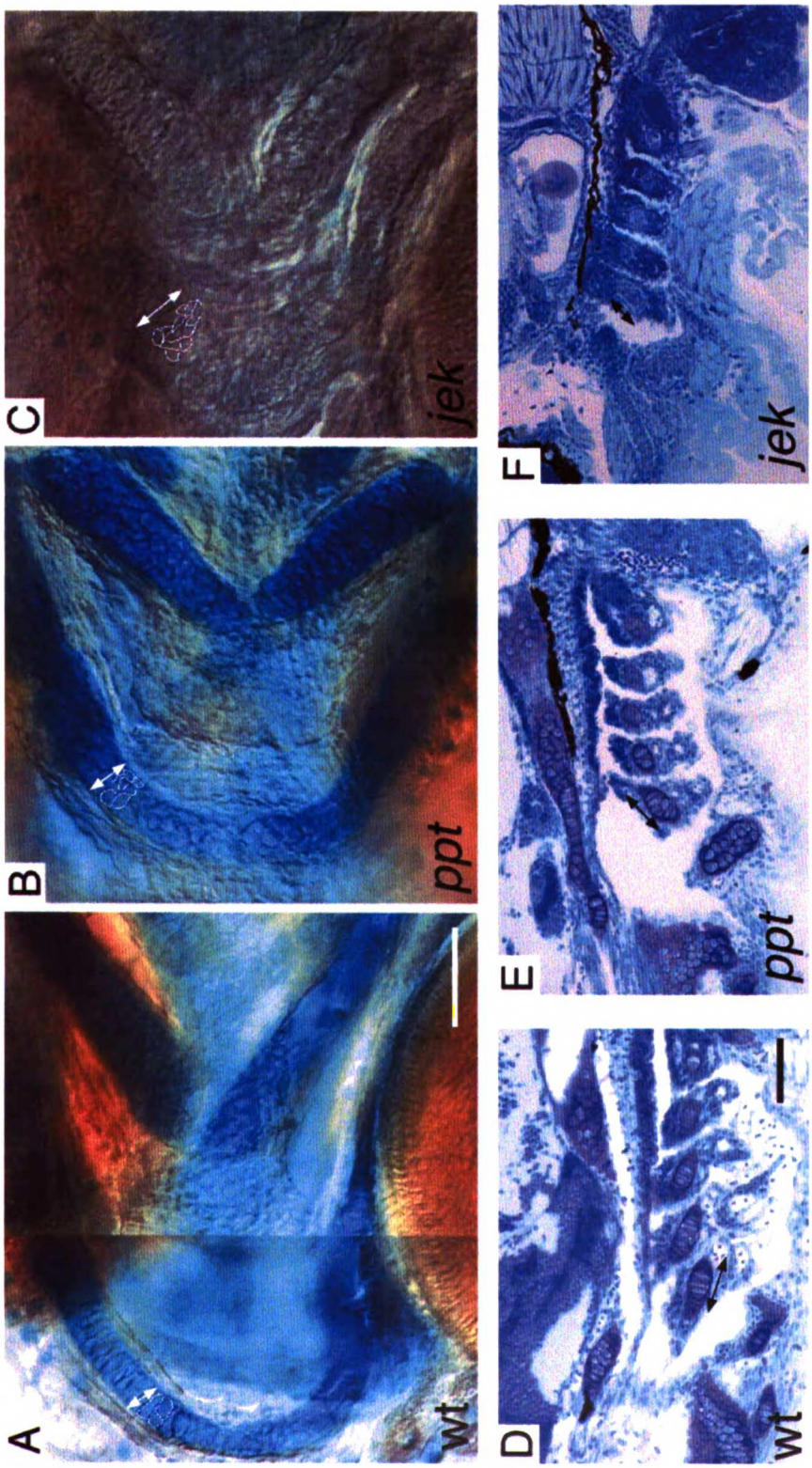

Appendix 1: ***jekyll*** **genomic organization. Figure 23. (A) Known intron-exon junctions in *ugdh*, as found using zUGDH F1/R1 and F2/R2 primer pairs (figure 9). Sequence for the F1/R1 junction is shown. The F2/R2 junction has not been sequenced. (B) PAC rescue of the jekyll branchial arch phenotype with 142J10 and 97M23, two of three PACs isolated by PCR for *ugdh* on PAC pools (142J10, 97M23, and 180A23). PAC injected embryos were stained with alcian revealing small clones of alcian positive cells in *jekyll* mutant arches. Presumably these cells contain the injected PAC as uninjected mutant embryos never stain in this way. (C) Graphical representation of PACs 142J10 and 180A23 and their approximate sizes, however end sequencing and PAC orientation have not been performed.**

Figure 23

A

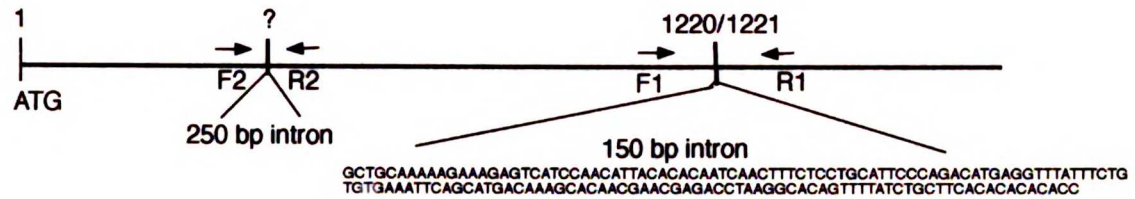

B pac 142J10 injected pac 97M23 injected

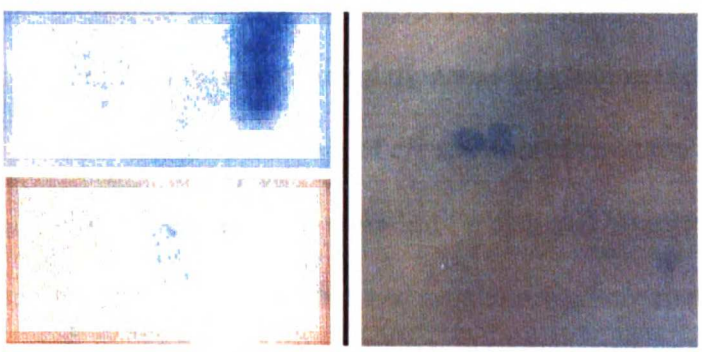

C

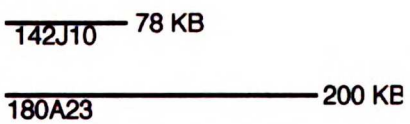

Appendix 2: Analysis of *cardiofunk* valve defects

The *cardiofunk* (*cfk*) mutation was isolated from a line of fish thought to bear a mutation that conferred reduced staining with the *nkx2.5* riboprobe. The original mutation was identified in a small scale haploid *in situ* and immunofluorescence screen for heart defects.[3] *s11* was the given line name. It has not yet been confirmed that the *cfk* mutation is the original lesion detected by the authors as *nkx2.5 in situ* analysis has proved inconclusive. Perhaps when the identity of *cfk* is known, such analysis will yield more conclusive results.

Like *jekyll* mutant embryos, *cfk* mutants lack proper formation of an AV valve as determined by blood accumulation and toggling in the two chambers of the heart at 48 hpf. Additionally, analysis of *cfk* mutants bearing the *tie2* GFP transgene reveals a lack of endocardial clustering at 43 hpf (Walsh and Stainier, data not shown). Like *jekyll* mutants, *notch1b* restriction and heightening, here shown at 48 hpf, does not occur properly (Fig. 24 A-F, arrows indicate boundary). Although earlier expression is indistinguishable from wildtype (two examples each of wildtype and mutant, as determined by slight edema at 42 hpf, are shown--Fig. 24 A-D). Also, chamber specific myosin heavy chain antibody staining using MF20 and S46 antibodies reveals that like *jekyll* mutants, chamber specification occurs normally in *cfk* mutants (Fig. 24 G-H). In one case (I), there did appear to be a few S46 expressing cells in the ventricle of the mutant heart, however this has not been observed again.

Unlike *jekyll* mutants, *cfk* mutants, do delineate an AV boundary as judged by *bmp4 in situ* analysis (arrows indicate AV boundary--Fig. 24 J-M). Compared to wildtype, this boundary appears to be reduced in staining; however, this may only reflect

the cfk valve's dysmorphology at 48 hpf. Thus, Cardiofunk activity is not required to set aside the boundary. This result suggests that Cardiofunk activity is required downstream or parallel to Jekyll in AV valve formation.

Interestingly, in spite of this seemingly downstream or parallel function, *cardiofunk* and *jekyll* mutations interact genetically. I showed that double heterozygotes exhibit a low level failure to complement or about 10-20% penetrance, this result was later confirmed by Tom Bartman.

Figure 24

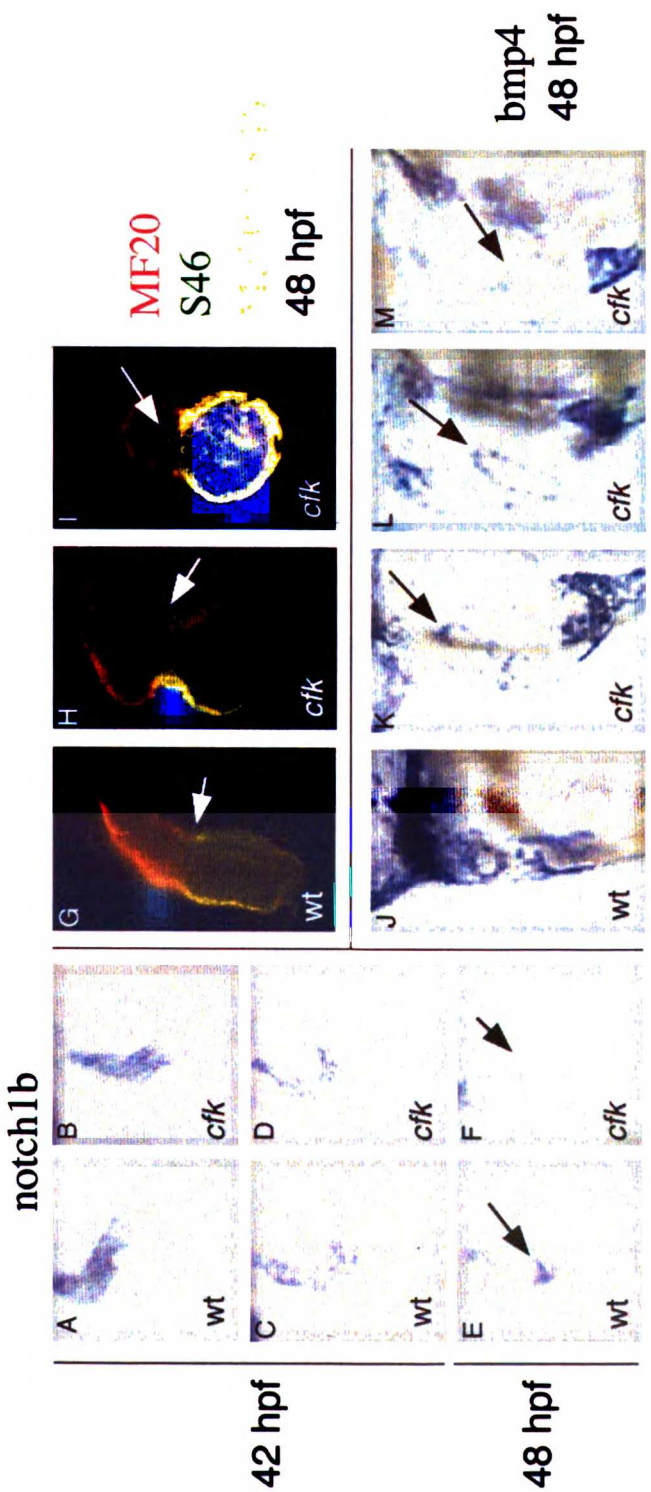
notch1b
bmp4
42 hpf
48 hpf
48 hpf
MF20
S46
A
B
C
D
E
F
G
H
I
J
K
L
M
wt
cfk

Appendix 3: β-xyloside and *has2* MO treatment of zebrafish embryos.

In characterizing *jekyll*, I explored with the help of Brian Biehs whether the jekyll phenotype was due to loss of proteoglycans or loss of hyaluronic acid. To assess this we used β-xyloside treatment to inhibit the glycosaminoglycan decoration of proteoglycans and a morpholino targeted against the embryonic hyaluronic acid synthase (*has2*).

Figure 25. (A, B) Two examples of β-xyloside treated zebrafish embryos. Hearts appear stringy in most cases, however in a few cases hearts appear *jekyll*-like (not shown). The stringy heart phenotype is almost completely penetrant at both doses of treatment (5mM and 20mM). The critical time of treatment has not yet been accurately determined but appears to be before 24 hpf.

has2 morpholino injections yield highly variable heart phenotypes. In one experiment, *has2* MO injections yield 16% mild stringy heart phenotypes and 8% *jekyll* heart phenotypes (N=50). However, two other sets of experiments produced 2-4% and 40-60% affected embryos respectively. Sometimes injecting *jekyll* heterozygote embryos has a sensitizing effect and sometimes this practice had no effect.

Clearly , additional carefully controlled experiments are warranted to determine the relative need for proteoglycans and hyaluronic acid in AV boundary and valve formation. Perhaps this work is better done in the *has2* and *hdf* mouse mutants. In situ analysis for *bmp4* expression in each of these mutants should determine the "molecular epistasis" of these mutations.

Figure 25

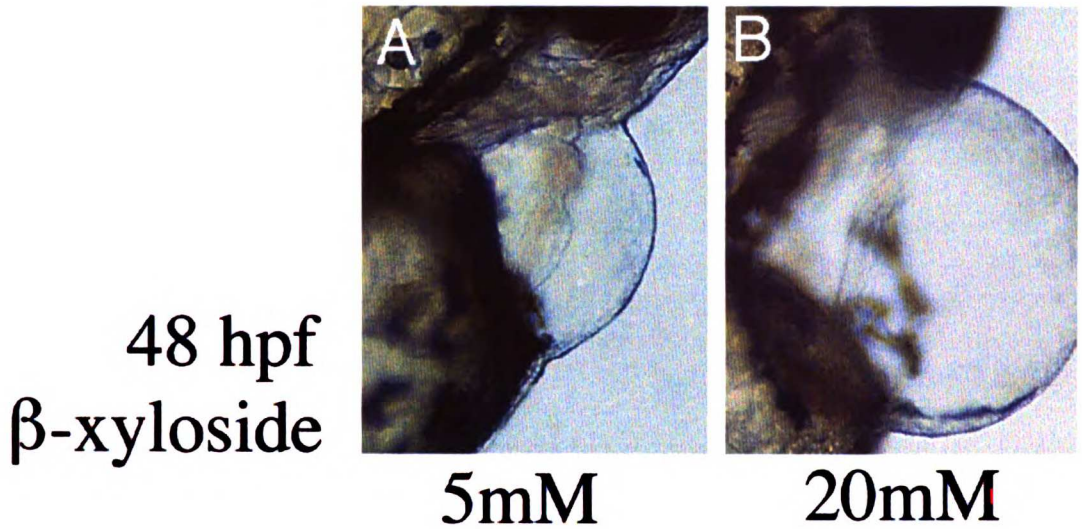

Appendix 4: Acerebellar/Fgf8 is required for zebrafish heart induction

As part of a collaboration with Phillip Crossley and Gail Martin, I was able to help isolate the zebrafish *fgf8.1* gene. Through a collaboration with Michael Brand and colleagues, it was determined that the zebrafish *acerebellar* (*ace*) mutation lies in the *fgf8.1* gene. Subsequent collaboration, in particular with Frank Reifers from Michael Brand's group, delineated the effect of the *ace* mutation on heart development. My role in this heart collaboration was to determine the ventricular reduction in *ace* mutants at 24 hpf and aid in the interpretation of the *in situ* analysis of heart development. This appendix includes those two manuscripts published in Development[65,66] as well as a figure detailing some unpublished collaborative work assessing other aspects of the role of *fgf8.1* in heart development.

ace mutants do form AV boundaries as judged by *bmp4* and *nkx2.7 in situ* analysis at 48 hpf (Fig. 26 A, B and C, D, respectively). While this result does not rule out a role for *fgf8.1* in the process (as the *ace* mutation is likely not null), it does show that mutations which affect ventricular induction do not necessarily affect the formation of a boundary at the atrial-ventricular border.

Also shown in Fig. 26, comparison of the extent of *in situ* staining for *nkx2.5*, *fgf8.1*, and *cmlc* riboprobes in the cardiac ring at 22 hpf (E, F, and G, respectively). While *nkx2.5* is not always a reliable probe, it does appear that there is a *cmlc*+, *nkx2.5*-population of cells in the outermost aspects of the cardiac ring. Furthermore, *fgf8.1* appears to be expressed heavily in only the innermost aspect of the ring with much lighter expression in the outermost portions.

Figure 26

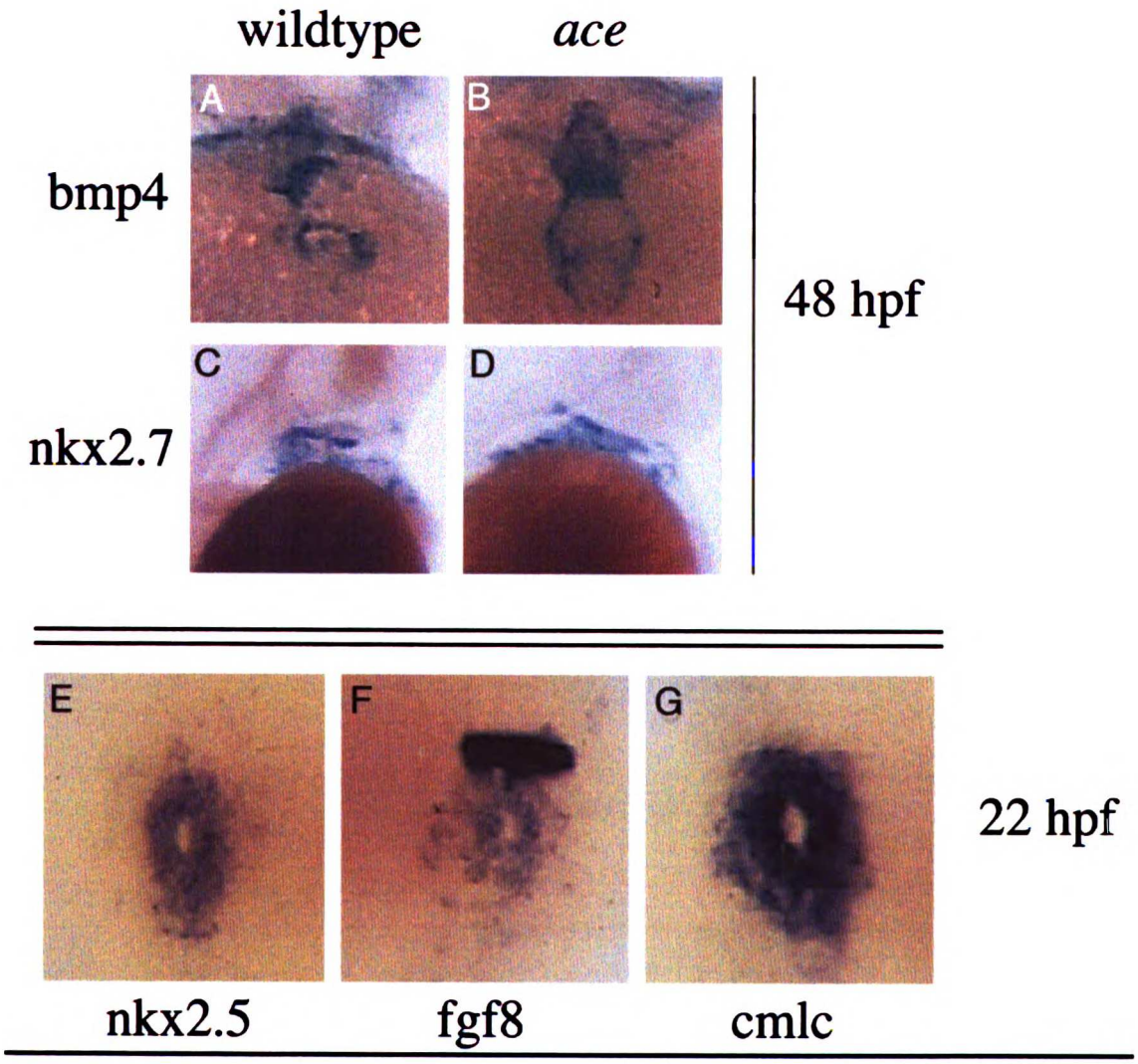
wildtype
ace
A
B
bmp4
48 hpf
C
D
nkx2.7
E
F
G
22 hpf
nkx2.5
fgf8
cmlc

Development 125, 2381-2395 (1998)
Printed in Great Britain © The Company of Biologists Limited 1998
DEV1266

Fgf8 is mutated in zebrafish *acerebellar* (*ace*) mutants and is required for maintenance of midbrain-hindbrain boundary development and somitogenesis

Frank Reifers[1], Heike Böhli[1], Emily C. Walsh[2], Phillip H. Crossley[2], Didier Y. R. Stainier[2] and Michael Brand[1,*]

[1]Department of Neurobiology, University of Heidelberg, Im Neuenheimer Feld 364, D-69120 Heidelberg, Germany
[2]Department of Biochemistry and Biophysics, University of California San Francisco, San Francisco, CA 94143-0554, USA
*Author for correspondence (e-mail: brand@sun0.urz.uni-heidelberg.de)

Accepted 2 April; published on WWW 3 June 1998

SUMMARY

We describe the isolation of zebrafish *Fgf8* and its expression during gastrulation, somitogenesis, fin bud and early brain development. By demonstrating genetic linkage and by analysing the structure of the *Fgf8* gene, we show that *acerebellar* is a zebrafish *Fgf8* mutation that may inactivate *Fgf8* function. Homozygous *acerebellar* embryos lack a cerebellum and the midbrain-hindbrain boundary organizer. *Fgf8* function is required to maintain, but not initiate, expression of *Pax2.1* and other marker genes in this area. We show that *Fgf8* and *Pax2.1* are activated in adjacent domains that only later become overlapping, and activation of *Fgf8* occurs normally in *no isthmus* embryos that are mutant for *Pax2.1*. These findings suggest that multiple signaling pathways are independently activated in the midbrain-hindbrain boundary primordium during gastrulation, and that Fgf8 functions later during somitogenesis to polarize the midbrain. *Fgf8* is also expressed in a dorsoventral gradient during gastrulation and ectopically expressed *Fgf8* can dorsalize embryos. Nevertheless, *acerebellar* mutants show only mild dorsoventral patterning defects. Also, in spite of the prominent role suggested for *Fgf8* in limb development, the pectoral fins are largely unaffected in the mutants. *Fgf8* is therefore required in development of several important signaling centers in the zebrafish embryo, but may be redundant or dispensable for others.

Key words: Neurogenesis, Regionalization, *Fgf8*, *acerebellar*, *Pax* genes, Midbrain, Hindbrain, Organizer, Zebrafish, Somitogenesis, Axis specification, *no isthmus*, *Danio rerio*, Splicing

INTRODUCTION

Generation of the large number of different cell types in the nervous system requires cell intrinsic programs and coordination between neighbouring cells. Work in recent years has established that designated cell populations exist in the neural plate that influence cell fate in surrounding neural plate cells. One such population is located at the boundary between midbrain and hindbrain (MHB), also referred to as isthmus (Alvarado-Mallart, 1993; Nakamura et al., 1994, Marin and Puelles, 1994; for review: Bally-Cuif and Wassef, 1995; Joyner, 1996; Lumsden and Krumlauf, 1996).

The midbrain derives from the mesencephalic neural plate and includes as major derivatives the optic tectum and the tegmentum. When MHB tissue is transplanted into the caudal forebrain primordium, midbrain-hindbrain markers are not only expressed in the transplanted tissue, but also in the surrounding forebrain tissue. When such transplants are allowed to develop, the induced cells show a midbrain-like character (Gardner and Barald, 1991; Martinez et al., 1991; Bally-Cuif et al., 1992). Substructures in the induced midbrain and MHB tissues are arranged in the normal sequence relative to each other, but are inverted with respect to the endogenous midbrain and cerebellum (Marin and Puelles, 1994). Similarly, transplantation of the MHB cells into the dorsal spinal chord leads to induction of a second cerebellum (Martinez et al., 1995). These experiments identify the MHB region as an important organizing center with a role in midbrain and cerebellar induction and patterning.

At the MHB, several molecules are expressed that have been implicated in cellular interaction processes and could mediate the activity of the MHB organizer. *Wnt1* is a cognate of the secreted *wingless* gene product in *Drosophila*, and is expressed from the early neural plate stage onwards at the MHB of mouse and other vertebrate embryos (Wilkinson et al., 1987). Targeted inactivation of *wnt1* has demonstrated its requirement during maintenance, but not initiation, of midbrain and cerebellar development of mouse embryos (Thomas and Capecchi, 1990; McMahon et al., 1992). In *Drosophila*, *wingless* cooperates with the Engrailed transcription factor in several cellular interaction processes, and its vertebrate homologues *En1* and *En2* are likewise expressed during and required for maintaining early MHB development (Wurst et al., 1994; Millen et al., 1994). Indeed, a major role for *wnt1* during MHB development

is to maintain expression of *En1* (Danielian and McMahon, 1996). Apart from *wnt1*, *engrailed* expression also requires the activity of the paired box gene *Pax2.1* (formerly *pax-b*, Pfeffer et al., 1998) in zebrafish and mice (Brand et al., 1996; Favor et al., 1996; Lun and Brand, unpublished data), consistent with the presence of binding sites for paired box proteins in the *En2* promoter (Song et al., 1996).

Members of the family of secreted fibroblast growth factors (*Fgfs*) signal through receptor-tyrosine kinases (Fgfrs 1 to 4) to activate ras signaling (Basilico and Moscatelli, 1992). *Fgfs* play important roles during growth and patterning in the embryo. For instance, injection of dominant negative Fgf receptor constructs in *Xenopus* and zebrafish leads to posterior truncation, demonstrating that Fgf signaling is required during gastrulation and mesoderm development (Kroll and Amaya, 1996; Griffin et al., 1995).

In this study, we describe the isolation and expression of zebrafish *Fgf8*, and its functional requirement in embryonic development. *Fgf8* was originally isolated as an androgen-induced growth factor (AIGF, Tanaka et al., 1992). *Fgf8* is expressed in chicken and mouse from early somitogenesis onwards at the MHB and in a number of other cell groups with signaling properties (Heikinheimo et al., 1994; Ohuchi et al., 1994; Crossley and Martin, 1995; Mahmood et al., 1995). Implantation of beads soaked in Fgf8 or Fgf4 in chicken induces midbrain or cerebellar tissue in a manner analogous to cells of the MHB organizer, and *Fgf8*, *En2* and *wnt1* are activated by the implantation (Crossley et al., 1996a). These experiments strongly suggested that *Fgf8* or a similar *Fgf* is an important component of MHB organizer function. Consistently, the receptors that Fgf8 and Fgf4 bind to in vitro are expressed during MHB development in mouse and zebrafish (MacArthur et al., 1995, and references therein; Thisse et al., 1995; Ornitz et al., 1996; Blunt et al., 1997).

Apart from the MHB, *Fgf8* has been suggested to be a key signaling molecule in development of the limb bud (review: Cohn and Tickle, 1996), forebrain (Shimamura and Rubenstein, 1997), tooth (Neubüser et al., 1997), among others. In the limb bud, *Fgf8* and *Fgf4* are expressed in the apical ectodermal ridge (AER), which directs outgrowth of the limb. Mesenchymal cells of the zone of polarizing activity (ZPA) impose anteroposterior pattern on the limb bud, an activity that is mimicked by Sonic hedgehog (Shh) (Riddle et al., 1993), and Fgf8 and Fgf4 are thought to act in a feedback loop controlling Shh in the ZPA. Fgf beads or Fgf-expressing cells for *Fgf1*, *Fgf2*, *Fgf4*, *Fgf8* and *Fgf10* are all able to induce an additional limb from the flank of chick embryos (review: Cohn and Tickle, 1996; Ohuchi et al., 1997a), raising questions about the relative role of the various Fgfs. Both *Fgf8* and *Fgf10* are expressed early enough in the mesenchyme that is thought to induce the limb bud. In two chicken mutants, however, limb buds are established independently of *Fgf8* expression (Niswander, 1997), and *Fgf8* may therefore mimic the action of *Fgf10* in limb induction (Ohuchi et al., 1997a).

Loss-of-function mutations for several *Fgfs* often display weaker phenotypes than anticipated from their expression patterns or misexpression experiments. Although *Fgf3* and *Fgf5* are expressed from gastrulation onwards, targeted inactivation of *Fgf3* leads only to later defects in morphogenesis and differentiation of the inner ear and somites (Mansour et al., 1993) and *Fgf5* mutants have fur alterations (Hebert et al., 1994). Others show very severe phenotypes: *Fgf4* mutants die shortly after implantation (Feldman et al., 1995). Likewise, inactivation of *Fgfr1* leads to absence of somites and expansion of notochord, suggesting that these embryos cannot respond to an unidentified, organizer-derived signal required to pattern the gastrula embryo (Deng et al., 1994; Yamaguchi et al., 1994). Also, heterozygous mutations in human *Fgfr1* to *Fgfr3* cause dominant defects in craniofacial development, vertebrae and limbs, indicative of functions in later development (review: Yamaguchi and Rossant, 1995). The effects of loss of *Fgf8* function have not been described yet in zebrafish, but a recent study in mice indicates that *Fgf8* is required in gastrulation and brain development (Meyers et al., 1998).

As in other species, zebrafish *Fgf8* is expressed during gastrulation, in mesodermal tissue, during early MHB development and several other sites in the nervous system. We show here that *Fgf8* is mutated in *acerebellar* (*ace*). A single recessive *acerebellar* allele exists, and homozygous mutant embryos lack a MHB and a cerebellum (Brand et al., 1996). We analyze the requirement for *Fgf8* in the mutants, compare the effects of misexpressing wild-type and mutant *Fgf8* transcripts, and examine *Fgf8* dependence in *no isthmus* mutants which inactivate *Pax2.1* (Brand et al., 1996; Lun and Brand, unpublished data).

MATERIALS AND METHODS

Zebrafish were raised and kept under standard conditions at about 27°C (Westerfield, 1994). Mutant carriers were identified by random intercrosses. To obtain mutant embryos, heterozygous carriers were intercrossed. Time of development at 28.5°C and morphological features were used to stage the embryos (Kimmel et al., 1995). Occasionally, 0.2 mM phenylthiourea (PTU) was added to prevent melanization. Histology is described in Kuwada et al. (1990).

Whole-mount in situ hybridisation

Digoxigenin- or fluorescein-labelled RNA probes were prepared from linearized templates using an RNA labelling and detection kit (Boehringer). Hybridisation and detection with anti-digoxigenin or anti-fluorescein antibodies coupled to alkaline phosphatase (Boehringer) was modified from Thisse et al. (1994). Hybridisation was at 68.5°C, and Boehringer DIG blocking agent was used during detection as specified by the supplier. To determine overlap in double stains with BM purple and FastRed fluorescent substrate (Boehringer), the BM purple reaction was allowed to proceed until it quenched but did not obliterate the fluorescent FastRed signal. Antibodies were preabsorbed against fixed embryo powder. Stained embryos were dissected and thick sections were prepared with sharpened tungsten needles, mounted in glycerol, photographed on a Zeiss Axioskop and assembled using Adobe Photoshop.

Isolation of *Fgf8* cDNA

Fgf8 was isolated from a λgt11 library (kindly provided by Kai Zinn) using as probe the coding sequence of mouse *Fgf8* variant 4 during the initial screen, and a chicken *Fgf8* cDNA during rescreen (Crossley et al., 1996b). Candidates were subcloned into pCRII and sequenced (accession number AF051365). One additional zebrafish gene of uncertain relationship resembles *Fgf8*, but also other Fgfs; in contrast to the *Fgf8* gene reported here, this gene is expressed much later in development than *Fgf8* (S. Schulte-Merker, personal communication, and F. R. and M.B., unpublished data).

Molecular analysis of acerebellar

To determine linkage, heterozygous carriers for *acerebellar* (induced in the Tübingen strain) were crossed to AB wild-type strain. Carriers were identified in F_1 and intercrossed. Embryos from such crosses were separated into homozygous *acerebellar* mutants (n=100 and 108 for two independent experiments) and their siblings (n=100), and DNA and cDNA was prepared from each pool. cDNA synthesis with SuperScriptII reverse transcriptase (GibcoBRL) was according to manufacturers instructions. Intron sequences between exons 1 and 2 (1.6 kb) were amplified from both pools and from Tübingen and AB strains, assuming that exon/intron structure would be conserved relative to mouse *Fgf8* (Crossley and Martin, 1995). This assumption was confirmed by our results, and by sequencing of the amplified introns (not shown). Amplified fragments were digested with *Bgl*II, which detects a restriction fragment length polymorphism (RFLP) between the Tübingen and AB strains; the resulting gel was blotted and probed with a fragment containing only intron sequences to confirm that the fragments are derived from the *Fgf8* locus (not shown). Linkage was also observed for a second RFLP (not shown). Equivalent amplifications were carried out to obtain and sequence the exon 2/3 intron. cDNA was isolated by RT-PCR with nested primers flanking the coding region in two independent amplifications from cDNA pools of homozygous Tübingen wild-type and *acerebellar* embryos, and was subcloned and sequenced on an ALF sequenator. RT-PCR to detect presence of exon2 was carried out on cDNA from wild-type and *acerebellar* embryos under standard PCR conditions.

Injections

Wild-type and *acerebellar* mutant versions of *Fgf8* were subcloned into pCS2+ (Rupp et al., 1994) and transcribed using the SP6 message machine kit (Ambion). The amount of RNA injected was estimated from the concentration and volume of a sphere of RNA injected into oil at the same pressure settings. Typically, about 25 pg of *Fgf8* RNA were injected; higher concentrations cause more severe dorsalizations that lead to rupture of the embryos during somitogenesis (not shown). RNA was dissolved in 0.25 M KCl with 0.2% of phenol red and backloaded into borosilicate capillaries prepared on a Sutter puller. During injection, RNA was deposited into the cytoplasm of 1- to 8-cell-stage embryos; in embryos after the first cleavage, the RNA usually stays in the progeny of the injected blastomere, as judged from the unilateral distribution of control *lacZ* RNA, as detected with anti-β-gal antibody (Promega, 1:500) after ISH (Dornseifer et al., 1997).

RESULTS

Cloning and expression of zebrafish *Fgf8*

We have isolated zebrafish *Fgf8* from an embryonic cDNA library. The aminoacid sequence of zebrafish *Fgf8* is 79% identical to mouse and human *Fgf8*, and 84% identical to chicken *Fgf8* (Fig. 1). Amino acids encoded by exon 2 are diagnostic for *Fgf8* relative to other *Fgf* family members (Lorenzi et al., 1995); here the identity is 83% to mouse and human, and 91% to chicken *Fgf8*, with other similarities being much lower (e.g. *Fgf7*, 37% and *Fgf4*, 29%).

Expression during gastrulation

To study possible functions of *Fgf8*, we examined expression in wild-type embryos using whole-mount in situ hybridisation (ISH; Fig. 2). Expression becomes detectable at 30% epiboly in the marginal zone, and develops at 50% epiboly into a gradient with a highpoint in the dorsal embryonic shield, the zebrafish equivalent of Spemann's organizer (Fig. 2A-C). During gastrulation, dorsoventrally graded expression continues in the marginal zone. At 70% epiboly, expression starts in two transverse stripes in the anterior hindbrain primordium (Fig. 2D,E), and towards the end of epiboly at the anterior margin of the forebrain primordium (Fig. 2F).

Somitogenesis

During somitogenesis, expression continues in the prospective MHB (see below) and the tailbud, and is initiated in presomitic mesoderm in segmental expression domains (Fig. 2H,J). Expression is found throughout newly formed somites (Fig. 2J), but eventually becomes confined to the anterolateral margin of the maturing somite (Figs 2K, 10R). Transient expression occurs in the floorplate as it emerges from the tailbud (not shown). Posterior to the MHB, three additional stripes are detected in the hindbrain neural keel during early somitogenesis (Fig. 2H). In the forebrain primordium, a dorsomedian stripe is observed in the presumptive telencephalon with an anterior high point of intensity (Fig. 2H,I).

Expression in the brain

In the brain of pharyngula stage embryos (24-48 hours), expression is still prominent in the MHB, excluding the floorplate (Fig. 2O), and in the optic stalks, retina, a pair of paramedian telencephalic stripes that forms the commissural plate and in the dorsal diencephalon (Fig. 2N-R). Additional expression is seen in the dorsal hypothalamus ventral to the optic recess, in the area where the postoptic commissure will form (Fig. 2P). Around 36 hours, expression is detected in addition near the ventral midline of the hypothalamus in the hypophysis and infundibulum (Fig. 2P,Q), and in the nasal placodes (Fig. 2S). Expression continues in these tissues until 48 hours, the latest stage that we have examined (not shown).

Outside of the brain, expression is found in tissues of the

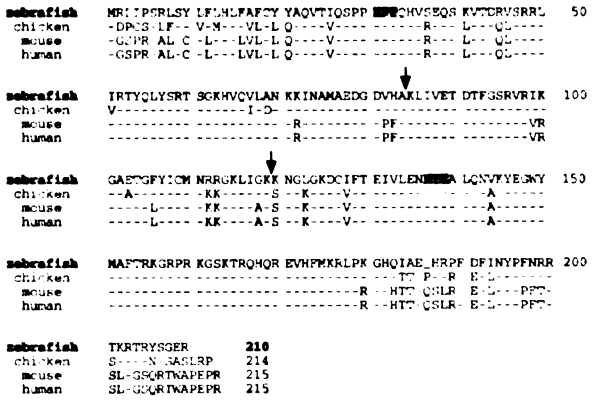

Fig. 1. Sequence comparison between the predicted amino acid sequences of zebrafish, chicken, mouse and human Fgf8 proteins. Horizontal bars indicate identical residues; arrows mark exon boundaries; consensus N-linked glycosylation sites are shaded.

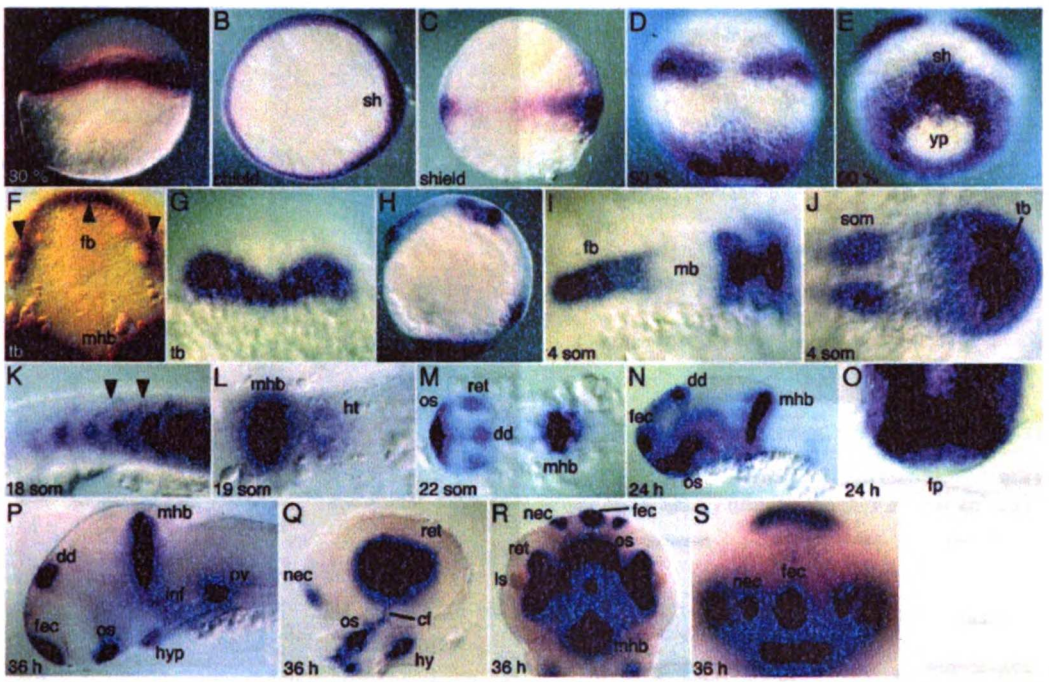

Fig. 2. Expression of *Fgf8* in wild-type embryos. (A) *Fgf8* in the blastoderm margin at 30% epiboly. (B,C) At shield stage, *Fgf8* is expressed in a dorsoventral gradient in the germ ring with a high point of expression in the shield (B, vegetal pole view; C, lateral view). (D,E) Graded expression persists in the margin of the blastoderm at 90% epiboly. Prospective anterior hindbrain expresses *Fgf8* (D, dorsal view; slightly tilted in E). (F) Forebrain expression in a tailbud stage embryo (arrowheads point to high points of expression). (G) Prospective MHB domains fuse at the midline at tailbud stage. (H) 4-somite stage, lateral view. Expression in forebrain, mid-hindbrain region, segmental plate and tailbud. (I,J) Flat mount of H, depicting anterior and posterior expression domains. (K) *Fgf8* expression at the anterior somite border (arrowheads). (L) Flat-mounted 19-somite embryo. Expression in the heart ring posterior to the MHB. (M) Flat mount at 22 somites; expression in the brain is detected at the MHB, dorsal diencephalon, retina and optic stalks. (N) Lateral view of a 24 hours embryo. Additional expression occurs in the facial ectoderm. (O) Thick cross section through the MHB demonstrating absence of expression in floorplate. (P) Lateral view of a dissected brain at 36 hours of development. Additional expression in the infundibulum, hypophysis and otic vesicle (eyes are removed). (Q) Details of expression in the retina, choroid fissure and the optic stalks. Additional expression is detected in nasal ectoderm and the hyoid. (R) Ventral view of head at 36 hours demonstrating expression in the retinal epithelium, but not in the lens. (S) Frontal view, expression in the facial and nasal ectoderm. cf, choroid fissure; dd, dorsal diencephalon; fb, forebrain; fec, facial ectoderm; fp, floorplate; ht, heart; hy, hyoid; hyp, hypophysis; inf, infundibulum; ls, lens; mb, midbrain; mhb, mid-hindbrain boundary; nec, nasal ectoderm; os, optic stalks; ov, otic vesicle; ret, retina; sh, shield; som, somites; tb, tailbud, yp, yolk plug.

developing head, such as the hyoid, heart, inner ear (Fig. 2L, P-S) and the fin buds (Fig. 1I).

Fgf8 expression at the MHB

Because of its possible patterning function in development of the MHB territory, we have examined the expression in this area in more detail. *Fgf8* activation is seen initially as a bilateral stripe at 70% epiboly (Fig. 3A-D). Relative to Krox-20, a marker for rhombomeres 3 and 5 (Oxtoby and Jowett, 1993; Fig. 3A,B), this stripe encompasses by tailbud stage the anterior hindbrain up to and including rhombomere 4. At 5 somites, this domain has become subdivided into several stripes lying at the MHB, in rhombomeres 1 and 4 and ventral rhombomere 2 (Figs 3C-D, 2H). In double stainings with the midbrain marker *Pax2.1*, *Fgf8* expression (Fig. 3E-H) is localized posterior to the domain of *Pax2.1* expression at 90% epiboly, with very little, if any, overlap. At 6 somites, however, the MHB stripe is completely contained within the posterior part of the *Pax2.1* domain (Fig. 3I,J).

Fgf8 is mutated in acerebellar

Fgf8 expression occurs in several tissues that are defective in *acerebellar* mutant embryos. Mutant larvae older than 2 days are retarded and eventually die with severe oedemas (not shown), but develop without significant retardation during the first 48 hours of development. In particular, homozygous *acerebellar* mutants lack a MHB and a cerebellum (see below). By testing candidate genes, we found that *Fgf8* is linked to the

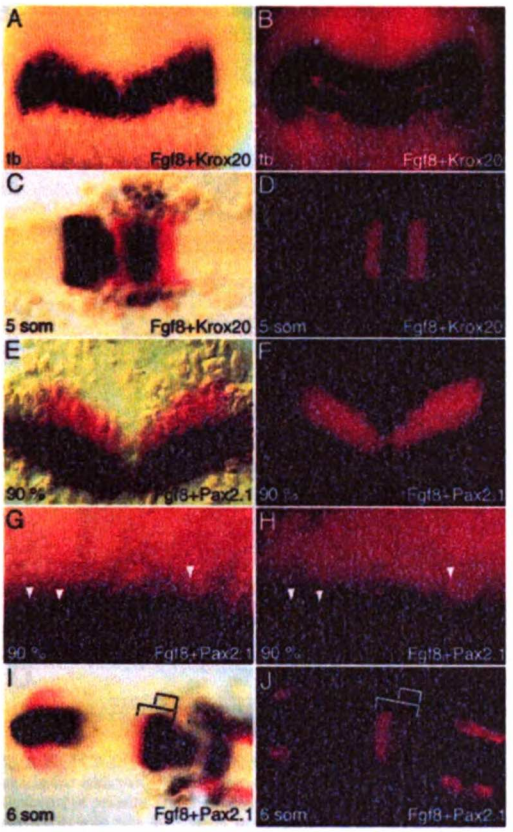

Fig. 3. *Fgf8* expression in early midbrain and anterior hindbrain development. (A-D) Double ISH with *Fgf8* (blue) and *Krox20* (red, fluorescent) of wild-type embryo at tailbud stage (A,B) and 5 somites (C,D). At tailbud stage, *Fgf8* expression extends throughout the anterior hindbrain incl. rhombomere 4 (r4) posteriorly. At 5 somites, expression of *Fgf8* is detected at the MHB, in r1, r4 and in ventral r2 (see also Fig. 2H). (E-J) Double ISH with *Fgf8* (blue) and *Pax2.1* (red, fluorescent) at 90% epiboly (E-H) and 6 somites (I,J). At 90% epiboly, the *Fgf8* expression domain is located posterior to the *Pax2.1* domain with very little overlap (E,F; higher magnification: G,H), while at 6 somites the *Fgf8* domain at the MHB is completely included in the *Pax2.1* expression domain (visible as quenching of the fluorescent *Pax2.1* signal). Embryos in C-J are flat mounted, A,C,E,G and I show bright field, B,D,F,H and J show fluorescent images of the same embryos.

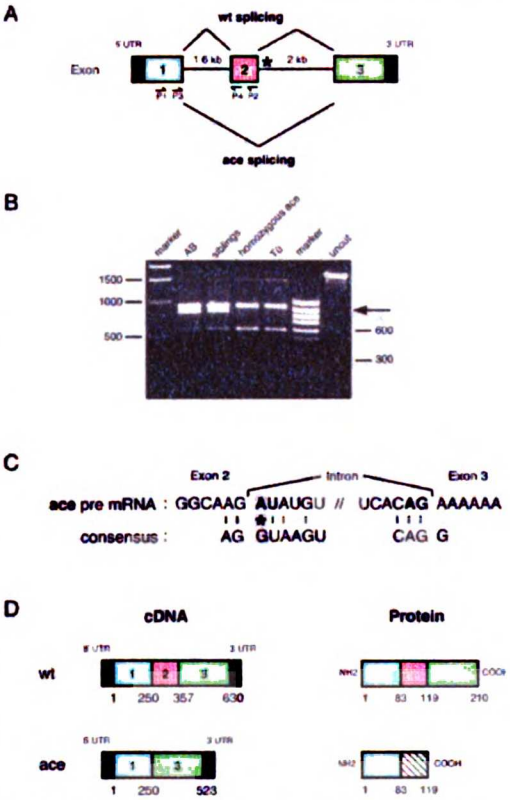

Fig. 4. *Fgf8* is mutated in *acerebellar*. (A) Genomic structure of the zebrafish *Fgf8* gene and possible splicing variations in wild-type and *acerebellar* embryos (asterisk depicts mutated 5′ splice site). (B) The intron between exon 1 and 2 was amplified and digested with *Bgl*II. An RFLP was identified for AB versus 'Tübingen' strain zebrafish (compare lane 'AB' with lane 'Tü'; arrow points to the polymorphic band). The homozygous *acerebellar* mutation was induced in a Tü strain and shows the Tü restriction pattern (compare lane 'homozygous ace' with lane 'Tü'), while their siblings show the AB pattern (compare lane 'siblings' with lane 'AB'). Therefore the *acerebellar* phenotype is linked to the *Fgf8* gene. (C) A 100% conserved G in the 5′ splice site following exon 2 is changed to an A, leading to skipping of exon 2. (D) cDNA from *acerebellar* embryos lacks exon 2 (red). This causes a frame shift in the open reading frame, leading to altered amino acids (hatched) and a premature stop in translation.

acerebellar mutation. In a test cross with two segregating RFLPs of *Fgf8*, the RFLP characteristic for the 'Tübingen' strain (in which *acerebellar* was induced) is linked to the *acerebellar* phenotype (Fig. 4). This RFLP was located in intron one and was lost during subsequent generations. However, by RT-PCR with single embryos, we found that the *acerebellar* phenotype and the lesion in *Fgf8* (see below) could not be separated in 101 embryos representing 202 meiotic events (0±0.5 cM; Fig. 5D).

acerebellar mutant transcripts lack exon 2

Through characterizing the *Fgf8* gene in *acerebellar* embryos, we found that *acerebellar* is a mutation that strongly or completely inactivates the *Fgf8* gene. We used RT-PCR to

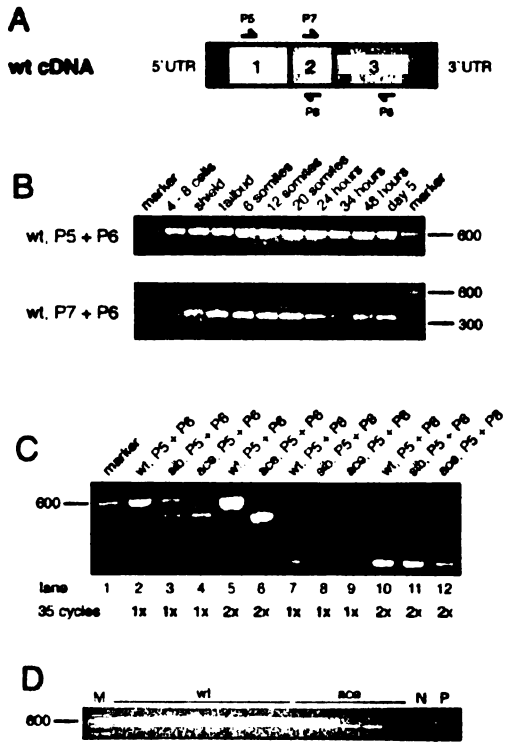

Fig. 5. RT-PCR analysis of *Fgf8* transcripts in wild-type and *acerebellar* embryos. (A) Structure of wild-type cDNA and placement of primers. (B) Only transcripts containing exon 2 are detected in wild type throughout development either with primers spanning exon 2 (P5 + P6) or with one primer located in exon 2 (P7 + P6). (C) Exon 2 is missing in *Fgf8* transcripts of *acerebellar* embryos. RT-PCR with primers spanning exon 2 (P5 + P6) yields a single band of 612 bp in wild-type embryos. In *acerebellar* embryos, no transcripts of wild-type size are detected; instead only transcripts without exon 2 are seen, which are shorter by 107 bases (compare lanes 2 and 4, and lane 5 and 6). In heterozygous siblings, bands of both sizes are detectable (lane 3). With one primer located in exon 2 (P5 + P8), amplification is only possible in *acerebellar* embryos after reamplification (compare lane 9 and 12), while in wild-type embryos and siblings one round of amplification is sufficient (lanes 7, 8), demonstrating the low abundance of exon 2 containing transcripts in *acerebellar* embryos. (D) *acerebellar* mutant embryos and their siblings were sorted by phenotype, indicated by bars. Single embryo RT-PCR with primers spanning exon 2 (P5 + P6) was performed for 101 *acerebellar* embryos and 13 siblings. Phenotypically wild-type siblings show either a wild-type or a heterozygous pattern. In all phenotypically *acerebellar* embryos tested, only exon 2-less transcript is detected, confirming genetic linkage (0 ± 0.5 cM).

amplify *Fgf8* cDNAs from homozygous *acerebellar* embryos and compared them to wild-type cDNA (Fig. 4). In two independent amplifications of the coding region, we find a deletion of 107 bases exactly corresponding to exon 2 in the mutant cDNAs; no other amino acid changes were detected. In order to study how this deletion is generated, we examined genomic DNA of *acerebellar* embryos and found that exon 2 is both present and of normal sequence. Upon sequencing of the 1.6 kb intron between exons 1 and 2, no conspicuous changes were detected and, in particular, the splicing consensus sequences were found to be intact (not shown). However, in the 5′ splice donor site following exon 2, a G residue was mutated to an A (Fig. 4C). Since this G is 100% conserved in all 5′ splice donor sites (Padgett et al., 1986), this mutation may inactivate this splice site, leading to skipping of exon 2 in the mutants.

As a result of skipping exon 2, the open reading frame runs into a premature stop codon (Fig. 4D). The predicted protein fragment in *acerebellar* embryos therefore lacks the aminoacids encoded in exons 2 and 3, which are required to activate the receptor and which are conserved between different *Fgf8*s and other *Fgf* family members (Lorenzi et al., 1995). The protein fragment in *acerebellar* mutants is therefore presumably non-functional, a notion that is confirmed by our injection experiments (see below).

Exon 1, but not exon 2, is alternatively spliced in murine *Fgf8* (Crossley and Martin, 1995; MacArthur et al., 1995). We find no evidence for differential splicing of exon 2 of *Fgf8* in zebrafish : in a timecourse up to day 5, we detect in wild-type embryos a single transcript of the size predicted for transcripts containing exon 2 (Fig. 5). This transcript is also detected at the 4- to 8-cell stage, i.e. prior to activation of zygotic transcription (Kane and Kimmel, 1993), showing that maternal *Fgf8* message is present in these embryos (Fig. 5B). We could not, however, detect any maternal RNA by in situ hybridisation (not shown), suggesting that these RNAs are rare.

To assess the strength of the *acerebellar* allele, it was crucial to determine if any wild-type *Fgf8* transcript is present in the mutants. We therefore performed RT-PCR on cDNA from *acerebellar* embryos. With primers flanking exon2, we detect a single band of the size predicted for transcripts lacking exon 2, but no transcripts of wild-type size (Fig. 5C). With one primer in exon 2 and another in the flanking exons, exon-2-containing transcripts can be detected in *acerebellar* embryos, but only after two rounds of amplification (Fig. 5C). These transcripts could be of maternal origin (see above), or they could be due to partially spliced mRNA in our cDNA pools; although partially spliced transcripts are usually unstable and confined to the nucleus (Padgett et al., 1986; Khoury et al., 1979). We can at present not distinguish between these possibilities. In either case, wild-type transcripts containing exon 2 must be rare, since they are not detectable with primers flanking exon 2 or by in situ hybridisation. We conclude that *acerebellar* partially or completely inactivates the *Fgf8* gene (see Discussion).

ace mutant Fgf8 is unable to dorsalize embryos

In order to determine whether the Fgf8 protein left in *acerebellar* mutants has any functional properties, we developed a functional assay for *Fgf8* activity. When wild-type *Fgf8* RNA is injected into developing embryos, we observe dorsalization and axis duplication (Fig. 6A-F; Table 1). We monitored adaxial and somitic development with *myoD* probe, and the location of the injected cells by coinjection of *lacZ* RNA. Embryos with a secondary axis formed in 12% of the

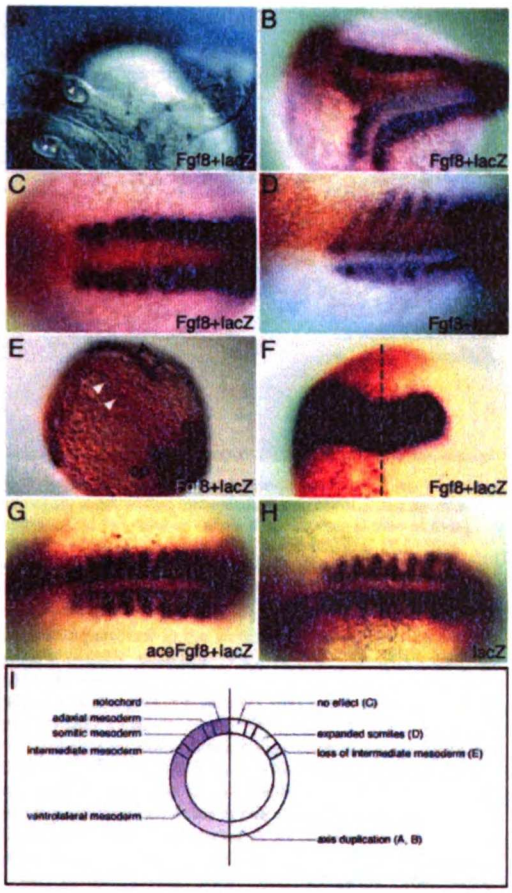

Fig. 6. Function of wild-type and mutant *Fgf8* in dorsoventral patterning of the gastrula. Adaxial and somitic mesoderm is visualized with *myoD* (blue), or intermediate mesoderm and MHB with *Pax2.1*, and location of the *lacZ* co-injected cells with an antibody to β-gal (brown). RNA distribution is mostly restricted to one side, allowing comparison with the contralateral side as a control. (A-F) Misexpression of *Fgf8* in wild-type embryos by RNA injection. (A,B) Live 28 h embryo with axis duplication (A) and stained for *myoD* (B). (C) Axial location of the injected RNA yields no obvious defect in mesoderm patterning. (D) Expansion of somitic mesoderm on the injected side of embryo. (E) *Pax2.1*-positive intermediate mesoderm (black arrowheads) is missing on the injected side (white arrowheads). (F) *Fgf8* misexpression alters the d/v, but not the a/p extent of the *Pax2.1* expression domain on the left, injected side (midline is given by a dashed line; op, otic placode). (G) No effect is seen after injection of the *acerebellar* version (lacking exon2) of *Fgf8* RNA, showing that the *acerebellar* transcript is inactive in vivo. (H) *lacZ* control injections had no effect. (I) Summary of the effects observed after injection of *Fgf8*. Left: schematic fate map of a gastrula, and the *Fgf8* gradient in the germ ring. Right: consequence of misexpressing *Fgf8* in the respective area. All embryos shown are at early to midsomitogenesis stages; B-D, G, H show *myoD* in situ stainings of injected embryos, E and F show *Pax2.1* in situ stainings; β-gal was detected by antibody staining.

cases (Table 1). Invariably, the cells of the secondary axis were the injected cells (Fig. 6B), and failed to form a head, notochord and adaxial cells. Exclusively dorsal location of the injected cells in the notochord primordium has little or no effect, suggesting that this tissue is not competent to respond (Fig. 6C). In dorsolateral levels, *Fgf8* misexpression causes severe expansion of the somites to ventral levels (Fig. 6D), which in some cases encircle the embryo (not shown). Consistent with the expansion of dorsal cell fates, *Pax2.1* expression in the intermediate mesoderm is suppressed or shifted to more ventral levels (Fig. 6E). Notably, although MHB expression of *Pax2.1* is expanded ventrally, it is *not* expanded along the anteroposterior axis (Fig. 6F), showing that *Fgf8* is not sufficient to induce *Pax2.1* expression. These findings are summarized in Fig. 6I. Our misexpression studies do not necessarily imply that Fgf8 normally functions in dorsoventral patterning, but they do provide a sensitive assay for functional activity of ectopically expressed *Fgf8* transcripts. In contrast to the severe effects of misexpressing wild-type *Fgf8*, injections of the *ace* mutant *Fgf8* at the same or a tenfold higher concentration causes no effect (Fig. 6G; Table 1). We conclude that the *Fgf8* transcript lacking exon 2 is inactive.

Requirement for *Fgf8* in MHB development

Examination of living embryos and of histological sections shows that the MHB fold and the cerebellum are absent in *acerebellar* embryos (Fig. 7). In living embryos, the MHB fold and the posteriorly adjacent cerebellar primordium are missing (Fig. 7A,B). In histological sections, the MHB tissue is

Table 1. Summary of Fgf8 and aceFgf8 overexpression

Experiment	Injected RNA	Normal	Dorsoventral effect	Double axis	Necrotic/ disorganized	Σ embryos (n = 100%)
Fgf8 overexpression	25 pg Fgf8	35%	29%	15%	21%	34
	25 pg Fgf8 + 250 pg *lacZ*	27%	49%	12%	12%	41
	250 pg *lacZ*	60%	0%	4%	36%	25
aceFgf8 overexpression	25 pg aceFgf8 + 500 pg *lacZ*	65%	0%	1%	34%	168
	500 pg *lacZ*	78%	0%	0%	22%	77
	250 pg aceFgf8 + 500 pg *lacZ*	83%	0%	0%	17%	59
	25 pg aceFgf8 + 500 pg *lacZ*	79%	0%	2%	19%	53

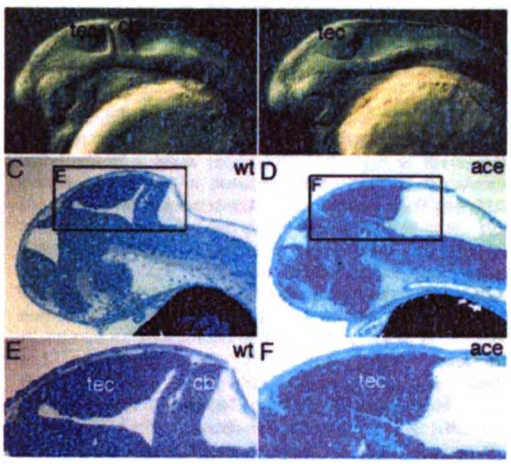

Fig. 7. Brain phenotype of *acerebellar* embryos. (A,B) At pharyngula stage, mutant embryos lack a cerebellum and the mid-hindbrain fold, but show an enlarged tectum (lateral view of living embryos). (C,D) Sagittal section of 36 hour embryos. (E,F) High magnification view of area depicted in C and D, showing the mid-hindbrain phenotype in more detail. cb, cerebellum; tec, tectum.

eliminated posterior to the tectum opticum, which itself often appears slightly enlarged (Fig. 7C-F). The MHB can be subdivided into an anterior portion (probably still part of the midbrain) and a posterior portion, which is thought to give rise to cerebellum (Kimmel et al., 1995). Both portions are absent in *acerebellar* mutants, showing that the defect is not restricted to the cerebellar primordium. We do not know the fate of the prospective fold tissue in *acerebellar* mutants but, since we have not detected cell death in this region previously (Brand et al., 1996), the apparent increase in the tectal tissue could reflect a transformation to a midbrain fate.

Our above results show that cerebellar and MHB development fail during embryonic stages in *acerebellar* mutants. We therefore examined the expression of marker genes of this area in a detailed time course (Fig. 8, Table 2). Like *Fgf8* itself, *wnt1*, *Pax2.1*, *Eng1*, *Eng2*, *Eng3* and *Her5* are expressed during normal development of the MHB primordium (Krauss et al., 1991; Molven et al., 1991; Ekker et al., 1992; Müller et al., 1996). After initially widespread expression in the midbrain primordium, expression of these genes is restricted during mid-somitogenesis towards the posterior midbrain and MHB. Expression of all marker genes that we examined is initiated normally in *acerebellar* mutant embryos. During early to mid-somitogenesis stages, however, expression gradually fades in *acerebellar* mutants, but continues in wild-type siblings. The expression domains of all markers gradually narrow and seem to persist longest in dorsoposterior parts of the MHB; eventually, expression is completely eliminated in the mutants (Fig. 8, Table 2). The earliest defect is seen for *Her5* at the 5-somite stage (Fig. 8G,J). These results show that maintenance, but not initiation of gene expression at the MHB, is affected in *acerebellar* mutant embryos.

Early *Fgf8* expression does not require *Pax2.1*

To examine if establishment of *Fgf8* signalling is dependent on *Pax2.1*, a gene required for early midbrain development (Brand et al., 1996; Lun and Brand, unpublished data), we examined *Fgf8* expression in *no isthmus* (*noi*) mutant embryos for noi^{tu29a}, which lack a functional *Pax2.1* gene (Fig. 9). Up until the 10 somites stage, we observe no difference in *Fgf8* expression between wild-type and *noi* embryos (Fig. 9A). At 18 somites, expression is eliminated at the MHB, but not in several other tissues (Fig. 9B,C). Since *noi* mutants lack the isthmus at this stage (Brand et al., 1996), this is most likely a secondary consequence of elimination of the tissue. We conclude that *Fgf8* signalling in the early MHB primordium is activated independently of *Pax2.1*/Noi.

Requirement during dorsoventral patterning and mesodermal development

To study whether *Fgf8* functions during development of the mesodermal derivatives that it is expressed in, we examined *ace* mutants with marker genes for axial, paraxial and intermediate mesoderm, and found defects that are probably due to weakly abnormal dorsoventral patterning (Fig. 10). *myoD* is expressed in adaxial cells lateral to the notochord from

Table 2. Marker gene expression at MHB in ace

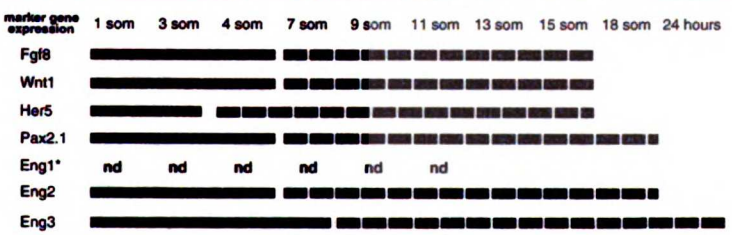

Expression of markers at the MHB during shown time course of zebrafish development.
Black bar shows normal expression at MHB, while dashed bar indicates decreasing expression domain as compared to wild type.
*Eng1 transcripts could be detected only from 12 somites onwards in wild type and *ace* embryos using non-radioactive in situ hybridization.
MHB, mid-hindbrain boundary; som, somites; nd, not detectable.

80% epiboly onwards, and later spreads to the forming somites in the paraxial mesoderm (Weinberg et al., 1996). *myoD* expression in adaxial cells of *acerebellar* mutants is strongly reduced at 80% to tailbud stages, and is interrupted during somitogenesis stages (Fig. 10A-F).

Since *Fgf8* is not yet expressed in adaxial cells or notochord between 80% and tailbud, the early failure to express *myoD* could reflect a weak requirement for *Fgf8* in dorsoventral patterning. To test a possible requirement in dorsoventral patterning, we examined expression of *eve1*, *fkd3* and *BMP4* as markers for ventral and dorsal cell fates (Joly et al., 1993; Chen et al., 1997; J. Odenthal, unpublished) and found no difference at 50%, 80% and tailbud stages (not shown). Likewise, *Pax2.1* expression in the intermediate mesoderm is normal at 7 somites (Fig. 10I,J). The tailbud is viewed as a site of continuing gastrulation and patterning (Gont et al., 1993) and expresses *Fgf8*. We find *snail1* expression (Hammerschmidt and Nüsslein-Volhard, 1993) to be absent in the vicinity of the tailbud, possibly reflecting another weak function for *Fgf8* in gastrulation or patterning (Fig. 10K,L). We conclude that early defects of *myoD* and *snail1* expression in *acerebellar* mutants could reflect a weak requirement in dorsoventral patterning. Notably, this requirement is most apparent in the future adaxial and somitic mesoderm, close to the site of highest *Fgf8* expression on the dorsal side.

Following activation throughout the somites and adaxial cells, *Fgf8* expression is successively confined to anterior-lateral cells of wild-type somites (Fig. 10Q,R). Both somite and adaxial cell development is affected in *acerebellar* mutants. During midsomitogenesis, *myoD* and *snail1* are expressed in condensing somites of the wild type, but are reduced and patchy in *acerebellar* mutants (Fig. 10E,F,M,N). Towards the end of the segmentation period, wild-type somites assume a distinct chevron shape and continue to express *myoD* and *snail1* (Fig. 10G,O). In *acerebellar* mutants, the somites appear more block-shaped, and have strongly reduced levels of *myoD* and *snail1* (Fig. 10H,P).

To examine development of adaxial cells, we studied expression of *Eng* in muscle pioneers that are derived from a subset of adaxial cells (Devoto et al., 1996). Expression of *Eng1* (not shown) and *Eng2* is reduced in *acerebellar* mutants at 24 hours (Fig. 10S,T). Adaxial cells themselves depend on signals from the notochord (Halpern et al., 1993). Brachyury/T expression as a marker for notochord (Schulte-Merker et al., 1992) was however unaffected at 80%, tailbud and 5-somite stages (not shown). In zebrafish *you-too* mutants, adaxial cells are missing, without affecting overall *myoD* expression in the early somites (van Eeden et al., 1996). In contrast, *acerebellar* mutants are defective both in early adaxial cell development (Fig. 10A-D) and in somitic expression of *myoD* and *snail1* (see above). *Fgf8* may therefore function independently in development of both cell types; alternatively, the defect could be an indirect consequence of the earlier abnormal expression of paraxial mesoderm genes like *myoD* and *snail1*. Given its anteriorly restricted expression pattern at later stages, Fgf8 might also function in polarization of somites along the craniocaudal axis (Hrabe de Angelis et al., 1997). However, in mutant somites, *Fgf8* itself is still expressed anteriorly, and *snail1* is more highly expressed posteriorly as in wild type, suggesting that the mutant somites are still patterned along the rostrocaudal axis (not shown).

Fgf8 in pectoral fin development

Teleost pectoral fins are homologous to tetrapod forelimbs (Sordino et al., 1995). Fgf8 is discussed as an important regulator of limb development, possibly by maintaining or inducing expression of *sonic hedgehog* (*shh*) in the zone of polarizing

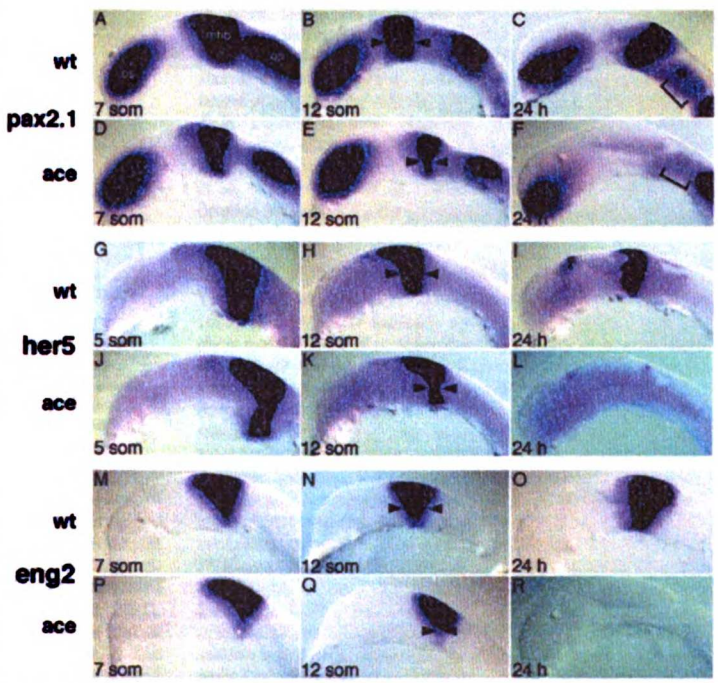

Fig. 8. *Fgf8* is required for the maintenance of MHB marker genes. Lateral views of dissected brain primordia. Stages and markers as indicated. (A-F) Expression of *Pax2.1* in wild-type (A-C) and *acerebellar* (D-F) embryos. Notice the gradual reduction in width at the MHB in B, E, and the reduction of otic placode (A,D), optic stalk and anterior hindbrain expression in C versus F. (G-L) Expression of *Her5* in wild-type (G-I) and *acerebellar* (J-L) embryos. Expression of *Eng2* in wild-type (M-O) and *acerebellar* (P-R) embryos. Arrowheads depict the width of the MHB, brackets mark anterior hindbrain. op, otic placode.

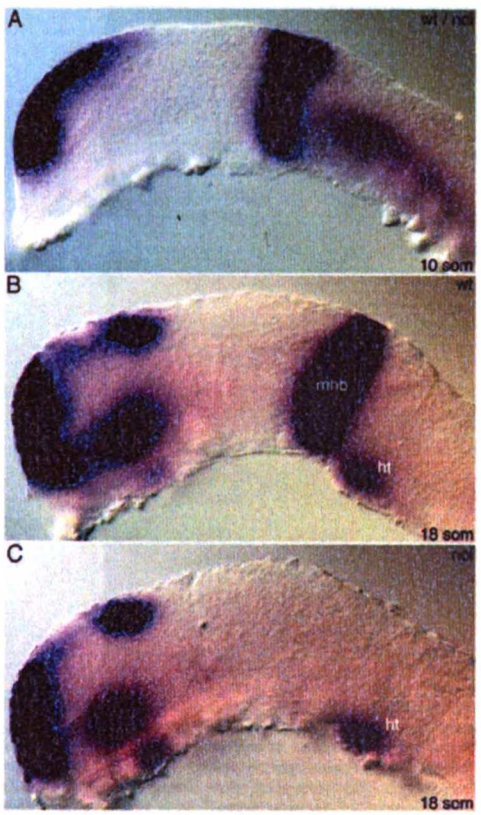

Fig. 9. *Fgf8* expression at the MHB is independent of *Pax2.1*. (A) Expression of *Fgf8* at the MHB in *noi/Pax2.1* mutant embryos cannot be distinguished from their wild-type siblings at the 10-somite stage. (B,C) At 18 somites, the expression of *Fgf8* is absent from the MHB in *noi/Pax2.1* mutant embryos, due to the loss of MHB territory. A-C show lateral views of *Fgf8* in situ-stained embryos. ht, heart; mhb, mid-hindbrain boundary.

activity (ZPA; see Cohn and Tickle, 1996, for review). In contrast to chicken and mice, *Fgf8* expression starts in the pectoral fin bud ectoderm only after initial fin bud formation, at 36 hours (Fig. 11B). At 48 hours, *Fgf8* is confined to the distal-most ridge of the developing fin (Fig. 11C,M), the equivalent of the apical ectodermal ridge of other vertebrates (Wood, 1982). *engl* and *shh* are activated earlier than *Fgf8* in the fin bud of wild-type embryos (Hatta et al., 1991; Krauss et al., 1993), and *Fgf8* is therefore probably not involved in the induction and early patterning of the fin bud in zebrafish (Fig. 11A,E,H). To examine if *Fgf8* could function in later stages of fin development, we analysed *shh* expression in the ZPA, and *engl* expression in the ventral-anterior fin bud, but could not detect an effect in *acerebellar* embryos (Fig. 11F,G,I,J). Furthermore, the overall structure of fins on day 5 of development appears normal in living *acerebellar* larvae (Fig. 11K,L). We do, however, consistently observe a slight increase in *Fgf8* expression in the mutants at 48 hours, possibly reflecting a later function for *Fgf8* (Fig. 11D). Although there are no obvious defects, our data do not exclude a late function for Fgf8 in development of the fin bud, since other Fgfs could compensate for missing Fgf8 activity, as reported for other vertebrates (Cohn et al., 1995; Crossley et al., 1996b; Ohuchi et al., 1997a).

DISCUSSION

We have described the isolation and expression pattern of zebrafish *Fgf8* and have shown that *acerebellar* is a mutation in *Fgf8*. Unexpectedly, our analysis demonstrates a requirement for *Fgf8* in maintenance, but not initiation, of MHB development. In addition, *Fgf8* is weakly required for normal dorsoventral patterning and in somite development. Other tissues, like the pectoral fins, apparently require *Fgf8* to a lesser degree. Maternally supplied *Fgf8* or other *Fgfs* may compensate for the loss of *Fgf8*.

Cloning and expression

Within the *Fgf* family, zebrafish *Fgf8* is most closely related, by sequence, expression pattern and genomic structure, to the *Fgf8* subgroup. During development, *Fgf8* is expressed in many cell populations that are known to be important signaling centers, such as the shield (Spemann's organizer), the anterior edge of the neural plate, the MHB and the limb bud. A similar association of *Fgf8* expression with signaling centers occurs in other vertebrates, often combined with expression of other *Fgfs* (Heikinheimo et al., 1994; Crossley and Martin, 1995; Mahmood et al., 1995; Bueno et al., 1996; Neubüser et al., 1997). Our detailed analysis of *Fgf8* expression at the MHB shows that even within a given domain expression can be very dynamic.

Strength of the *acerebellar* allele

The combined data of our linkage studies, analysis of the *Fgf8* locus in *acerebellar* mutants, and of our phenotypic studies show that *acerebellar* is mutated in *Fgf8*. A key issue is to what extent *Fgf8* activity is inactivated in *acerebellar*. Our analysis shows that mutation of a 100% conserved residue in a splice donor site following exon 2 leads to skipping of exon 2 in mutant embryos (Fig. 4). In a direct comparison of the prevalence of transcripts containing or lacking exon 2 with flanking primers, only transcripts lacking this exon are detectable in *acerebellar* mutants (Fig. 5). In the more sensitive assay where one primer is located in exon 2, also transcripts containing exon 2 are detectable, but only after two rounds of PCR amplification; such transcripts are therefore probably rare. They could be maternal transcripts, or transcripts resulting from incomplete inactivation of the mutated splice site. Absence of exon 2 results in a frameshift and premature chain termination of the predicted mutant protein. The conserved amino acids encoded by exons 2 and 3 that are thought to be important for Fgf function (Basilico and Moscatelli, 1992) are absent, and the resulting truncated protein is therefore probably inactive. This prediction is confirmed by the results of our injection experiments with RNA encoding the *ace* mutant version of *Fgf8*, which even at 10-fold higher RNA concentration does not have a biological effect (Fig. 6G). While these results show that transcripts lacking exon 2 do not

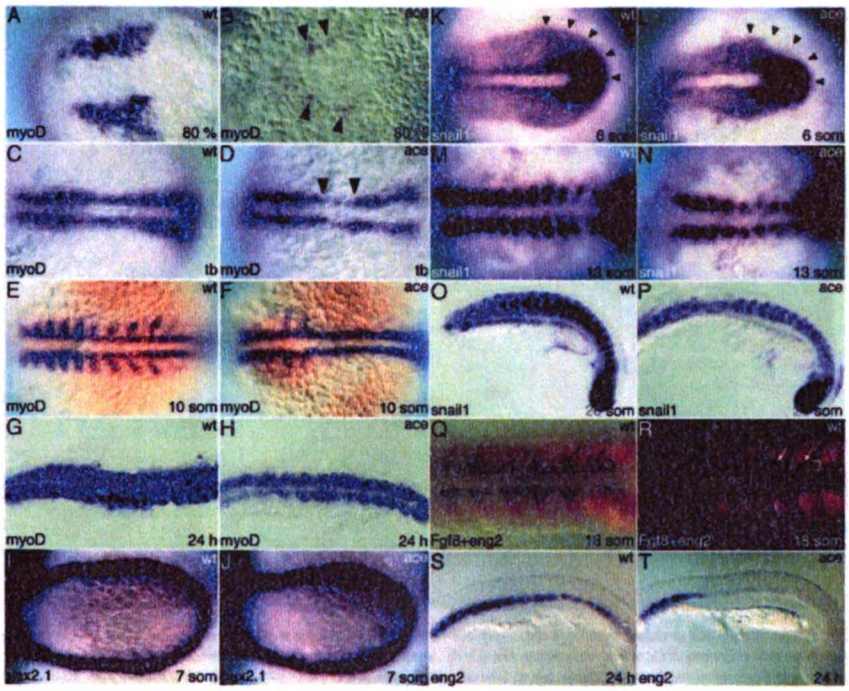

Fig. 10. *Fgf8* is involved in mesoderm and somite patterning. (A,B) Expression of *myoD* is strongly reduced in adaxial mesoderm of *acerebellar* embryos at 80% epiboly (arrowheads point to remnants of expression). (C,D) At tailbud stage, *myoD* expression in adaxial mesoderm is interrupted in *acerebellar* (arrowheads). (E,F) *myoD* staining in the somitic mesoderm is strongly reduced in mutants at the 10-somite stage. (G,H) At 24 hours, the expression of *myoD* is weak in the smaller and less-well-differentiated somites of *acerebellar* embryos. (I,J) No obvious difference could be detected between wild-type and *acerebellar* embryos in formation of intermediate mesoderm, shown here with *Pax2.1* staining at the 7-somite stage. (K,L) Expression of *snail1* is reduced in *acerebellar* embryos in the region around the tailbud at 6-somite stage (arrowheads point to the wild-type border of expression). (M,N) At the 13-somite stage and (O,P) 20-somite stage, snail1 transcripts are strongly reduced in the somites of mutant embryos. (Q,R) Dorsal view of wild-type embryo stained for *eng2* (blue) and *Fgf8* (red, fluorescent) showing partial overlap of these expression domains at an early stage of somite development (arrows). Note the restriction of *Fgf8* expression to anterolateral cells of the somites over time (anterior is to the left; brackets depict adaxial cells; nc, notochord). (S,T) Muscle pioneers are reduced in *acerebellar* embryos, as shown here for 24 hours embryos with *Eng2* staining.

produce functional Fgf8 protein, the fact that we do observe a minor amount of wild-type message containing exon 2 means that *acerebellar* may not cause complete inactivation of Fgf8. Elimination of the maternal component and isolation of further alleles of *Fgf8* can be used to address this issue.

Fgf8 function in dorsoventral patterning

In contrast to the drastic effect of misexpressing *Fgf8* on patterning of the gastrula, *acerebellar* mutants display a surprisingly mild phenotype. One possibility is that *ace* is not a null allele. A stronger phenotype was recently described for mouse *Fgf8* mutants: homozygous null *Fgf8* mutants fail to gastrulate and have no mesodermal derivatives, whereas weaker alleles display phenotypes more akin to what is seen in *acerebellar* mutants, including deletions of the posterior midbrain and cerebellum (Meyers et al., 1998).

Other explanations are, however, also possible for the weaker phenotype of *acerebellar* mutants. The maternal *Fgf8* RNA that we have observed (which contains exon 2, Fig. 5) could partially ameliorate the phenotype of *acerebellar* mutants, thus 'masking' a requirement for *Fgf8* in zebrafish, but not in mice, which have little maternal cytoplasm. We do not consider this possibility very likely: in contrast to zygotic RNA, maternal RNA is only detectable using the much more sensitive PCR assay, but not by in situ hybridisation, and maternal RNA may not be localized.

A more likely possibility is offered by the observation that *Fgf8* is often coexpressed with other members of the *Fgf* family in gastrulation (reviewed by Yamaguchi and Rossant, 1995). Prior to and during mouse gastrulation, *Fgf3*, *Fgf4*, *Fgf5* and *Fgf8* are expressed in distinct but overlapping patterns in the primitive streak: whereas *Fgf5* is found throughout the gastrula ectoderm, *Fgf3* is found in future mesodermal cells in the streak, and *Fgf4* is at the anterior end of the streak. While the expression patterns of these genes are suggestive, only *Fgf4* is required during gastrulation, whereas *Fgf3* and *Fgf5* are not (Feldman et al.,

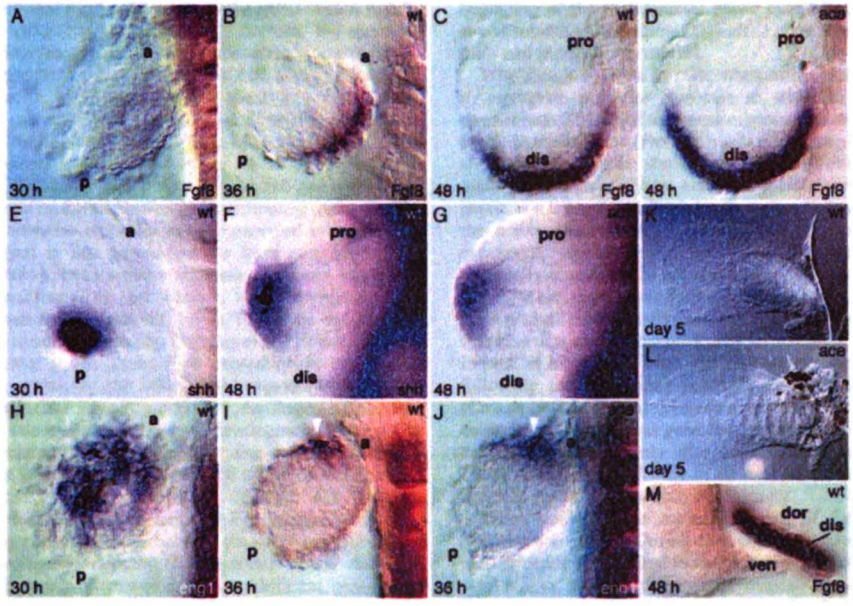

Fig. 11. *acerebellar* embryos show no severe defects in pectoral fin development. (A-D,M) *Fgf8* expression in the finbud. (A-C) Wild type. (D) *acerebellar*. No *Fgf8* expression is detected at 30 hours of development. (E-G) *shh* expression in the ZPA precedes *Fgf8* expression and is not affected in *acerebellar*. (E,F) Wild type. (G) *acerebellar*. (H-J) *eng1* (arrowheads) in the ventral fin bud precedes *Fgf8* and is normal in *acerebellar*. (H,I) Wild type. (J) *acerebellar*. (K,L) Fins of wild-type (K) and *acerebellar* (L) embryos on day 5 of development are of similar size and shape. (M) *Fgf8* expression in the distalmost ridge, AER, of the developing fin at 48 hours of development (viewed from posterior). a, anterior; dis, distal; dor, dorsal; p, posterior; pro, proximal; ven, ventral.

1995; Mansour et al., 1993; Hebert et al., 1994). An alternative explanation for the absence of severe gastrulation defects in *ace* mutants is therefore that other Fgfs can compensate for lack of Fgf8, or that Fgf8 has only a weak function.

Inactivation of *Fgfr1* causes absence of somites, expanded notochords and primitive streak defects. Fgfr1 was therefore proposed to be the receptor for an organizer-derived signal that patterns paraxial mesoderm (Yamaguchi et al., 1994; Deng et al., 1994). Based on its expression pattern and the phenotypes seen after misexpression and loss of function, Fgf8 or a similar Fgf could be this signal. Similar observations on the effects of *Fgf8* misexpression were made by M. Fürthauer, C. Thisse and B. Thisse, who also showed that *Fgf8* misexpression alters the distribution of the Bmp4 morphogen (Fürthauer et al., 1997). We note that the mild defect in activation and overall expression of *myoD* in the *acerebellar* mutants is consistent with a function of *Fgf8* in dorsoventral patterning, in keeping with the stronger gastrulation defect of the mouse mutant (Meyers et al., 1998).

Fgf8 in MHB development

The dynamic pattern of expression of *Fgf8* at the MHB is compatible with the functional requirement that we have observed. In chicken, beads containing Fgf8 or Fgf4 protein placed into the posterior forebrain or alar hindbrain primordium are able to induce ectopic isthmic, midbrain and cerebellar structures, strongly suggesting a role for Fgfs in MHB development (Crossley et al., 1996a). Our analysis of *Fgf8* requirement is generally compatible with these results. However, the bead experiments have raised the possibility that Fgf8 is the endogenous molecule which *induces* the midbrain, a notion that is not supported by several observations. (i) At the time *Fgf8* is activated at late gastrulation stages, it clearly marks the anterior hindbrain (Fig. 3). Posteriorly, its expression extends to the rhombomere 4/5 boundary and, anteriorly, it abuts the *Pax2.1* expression domain. Since the *Fgf8* and *Pax2.1* domains are largely non-overlapping at this stage, the early expression of *Fgf8* is clearly not sufficient to induce MHB markers such as *Pax2.1*. (ii) Secreted Fgf8 might act on the anteriorly adjacent cells at a distance to induce midbrain fate. We have observed, however, that misexpression of *Fgf8* leads to severe expansion of *Pax2.1* only along the d/v direction during gastrulation (as a consequence of altered dorsoventral patterning, see Fig. 6), but not to an expansion along the anteroposterior axis as would be expected if anterior cells could respond to *Fgf8*. Similarly, delocalized *Fgf8* expression does not alter early *En1* and *wnt1* midbrain expression in mice with altered *Otx* gene dosage; instead, the later restriction of *wnt1* and *Fgf8* to the posterior midbrain is affected (Acampora et al., 1997), similar to our findings in *acerebellar*. (iii) We find that *Fgf8* and *Pax2.1* expression come to gradually depend on each other only during mid-somitogenesis, after the time when

the anterior-most *Fgf8* subdomain in the MHB region is fully contained within the posterior *Pax2.1* domain. We speculate that this time may coincide with the establishment of the isthmus organizer in the region of overlap. (iv) In mice, *Fgf8* activation at the MHB occurs only at the 3- to 4-somite stage, and is thus preceded by activation of *wnt1* and *En1* as midbrain markers (Crossley and Martin, 1995; Mahmood et al., 1995). Taken together, Fgf8 is unlikely to act as the endogenous inducer of midbrain development in zebrafish and mice.

What could be the real inducer? Experimental manipulations in mouse, zebrafish and chicken have provided evidence for a vertical signal in late gastrula stages from mesendoderm to overlying ectoderm to activate expression of some, but not all midbrain markers (Ang and Rossant, 1993; Miyagawa et al., 1996; Darnell and Schoenwolf, 1997). To explain the ability of Fgf8 beads to induce midbrain, Crossley et al. (1996a) proposed that in normal development *Fgf8* expression in cardiogenic mesoderm underlying the MHB could provide, by a vertical path, the inductive signal. In zebrafish, cardiogenic precursors have been fate mapped throughout development. They derive from ventrolateral levels of the germ ring and migrate during gastrulation into a longitudinal domain which moves closer to the axis during early somitogenesis (Stainier and Fishman, 1992). Because we have not seen any *Fgf8* expression in these cells during gastrulation and because the shape and orientation of the cardiogenic domain (longitudinal) versus the *Fgf8* ectodermal domains (transverse) are very different, cardiogenic precursors are unlikely to provide the inductive signal for the ectodermal expression at the MHB in zebrafish gastrulae. We cannot rule out, however, that part of these cell populations are adjacent to each other at some stage during development and that signaling may occur between them.

An alternative source for the midbrain-inducing signal is the germ ring from which mesendodermal tissues derive. Fate-mapping studies in zebrafish have shown that a midbrain primordium is already separately established at late gastrulation stages (Woo and Fraser, 1995). Transplantation studies have suggested that an unknown signal responsible for hindbrain induction is present in the germ ring. This signal is not mimicked by bFgf beads and is absent from the dorsal shield (which has high levels of *Fgf8*), and may therefore not be a member of the *Fgf* family (Woo and Fraser, 1997). During gastrulation, *Fgf8*-expressing and *Pax2.1*-expressing domains in the neural primordium look quite similar in shape and width. By analogy to the hindbrain, the germ ring could therefore also provide the signal responsible for midbrain induction.

Establishment and maintenance phases

On the basis of the evidence presented here, we suggest that early MHB development occurs in at least two phases. During the establishment phase in late gastrulation, midbrain and hindbrain primordia are set up independently, in a process that does not require *Fgf8*. Given that *Fgf8* and *pax2.1* are activated independently of each other, at least two independent signalling pathways must act in parallel during early MHB development. The establishment phase is followed during early somitogenesis by a maintenance phase during which gene expression in the midbrain depends on signal(s) from the MHB. The gain- and loss-of-function experiments in chicken and fish together suggest that *Fgf8* is required for the maintenance phase, possibly in combination with *wnt1*. The beginning of the maintenance phase may be coincident with establishment of the isthmus organizer at the interface between mid- and hindbrain territories.

Why then is *Fgf8* on its own, when misexpressed, sufficient to reprogram posterior forebrain to midbrain and/or MHB development? Many of the genes expressed in the maintenance phase in the isthmus (*Pax2.1*, *wnt1*, *Eng2*, *Eng3*, *Fgf8*, *Her5*) are also active earlier during the establishment phase in the midbrain. We have shown here that MHB expression of *Eng* genes, *wnt1*, *Her5* and *Pax2.1*, all require *Fgf8* activity during the maintenance phase, since they all start to fail in their expression around early to midsomitogenesis and are eventually eliminated in *acerebellar* mutants. It is thus likely that *Fgf8* can impinge on their regulation. Thus, misexpressing *Fgf8* probably ectopically activates the complement of genes that also acts during establishment of midbrain development. Indeed, at least *Fgf8*, *wnt1* and *En2* are ectopically activated following the Fgf8 bead insertion into neural plate tissue (Crossley et al., 1996a). Moreover, ectopic *Fgf8* expression in embryos with altered *otx* gene dosage recruits *En1* and *wnt1* to the ectopic position only after some delay (Acampora et al., 1997). Once re-established in an ectopic position, the gene program could then develop accordingly.

What would be the normal function of Fgf8 during the maintenance phase? During this phase, expression of many marker genes is restricted to the posterior part of the midbrain primordium, towards the zone of overlap between *Fgf8* and *Pax2.1* at the isthmus. A crucial function for *Fgf8*, and possibly for the isthmus organizer in general, may therefore be to ensure polarized expression of midbrain markers, rather than initial induction. In keeping with this possibility, we find that all posterior midbrain markers we examined are absent from the midbrain of *acerebellar* mutants at later stages.

A distinction between establishment and maintenance functions for *Fgfs* has also been made for development of the chick limb bud (for a review, see Cohn and Tickle, 1996; Niswander, 1997). Similar to the situation at the MHB and as with other Fgfs, Fgf8 bead implantation is able to activate the full limb development program ectopically (Crossley et al., 1996b; Vogel et al., 1996). The earliest signal to establish limb development is thought to derived from the mesenchyme of the prospective limb bud. *Fgf10* is expressed in the mesenchyme at the right time, preceding *Fgf8* expression, and is able to induce complete limbs (Ohuchi et al., 1997a), so Fgf8 could mimic the limb-inducing action of Fgf10. Consistent with this possibility, in two chicken mutants, *limbless* and *wingless*, limb buds are established independently of *Fgf8* expression (Grieshammer et al., 1996; Ros et al., 1996; Ohuchi et al., 1997b), and Fgf8 is only weakly required in mouse limb bud development (Meyers et al., 1998). In zebrafish, *Fgf8* is neither expressed nor required during pectoral fin bud formation (Fig. 11), arguing that also in fish Fgf8 is not involved in fin bud establishment.

We thank M. Fürthauer, B. Thisse, Ch. Thisse, G. Martin, S. Martinez, S. Schulte-Merker and D. Ornitz for sharing unpublished results, Dave Willison for substantial contribution to the cloning of Fgf8, and C. Nichrs, F. Pelegri, P. Sordino, S. Wilson and members of the Brand laboratory for comments. F. R., H. B. and M. B. are funded by the Förderprogramm Neurobiologie, Baden-Württemberg, and the Deutsche Forschungsgemeinschaft (SFB 317). D. Y. R. S. is funded by the NIH and the Packard foundation, E. C. W. is a Howard Hughes Medical Institute predoctoral fellow.

REFERENCES

Acampora, D., Avantaggiato, V., Tuorto, F. and Simeone, A. (1997). Genetic control of brain morphogenesis through Otx gene dosage requirement. *Development* **124**, 3639-3650.

Alvarado-Mallart, R. M. (1993). Fate and potentialities of the avian mesencephalic/metencephalic neuroepithelium. *J. Neurobiol.* **24**, 1341-1355.

Ang, S. L. and Rossant, J. (1993). Anterior mesendoderm induces mouse Engrailed genes in explant cultures. *Development* **118**, 139-149.

Bally-Cuif, L., Alvarado-Mallart, R. M., Darnell, D. K. and Wassef, M. (1992). Relationship between *Wnt-1* and *En-2* expression domains during early development of normal and ectopic met-mesencephalon. *Development* **115**, 999-1009.

Bally-Cuif, L. and Wassef, M. (1995). Determination events in the nervous system of the vertebrate embryo. *Curr Opin Genet Dev* **5**, 450-458.

Basilico, C. and Moscatelli, D. (1992). The FGF family of growth factors and oncogenes. *Adv. Cancer Res.* **59**, 115-165.

Blunt, A. G., Lawshe, A., Cunningham, M. L., Seto, M. L., Ornitz, D. M. and MacArthur, C. A. (1997). Overlapping expression and redundant activation of mesenchymal fibroblast growth factor (FGF) receptors by alternatively spliced FGF-8 ligands. *J. Biol. Chem* **272**, 3733-3738.

Brand, M., Heisenberg, C.-P., Jiang, Y.-J., Beuchle, D., Lun, K., van Eeden, F. J. M., Furutani-Seiki, M., Granato, M., Haffter, P., Hammerschmidt, M., Kane, D. A., Kelsh, R. N., Mullins, M. C., Odenthal, J. and Nüsslein-Volhard, C. (1996). Mutations in zebrafish genes affecting the formation of the boundary between midbrain and hindbrain. *Development* **123**, 179-190.

Bueno, D., Skinner, J., Abud, H. and Heath, J. K. (1996). Spatial and temporal relationships between Shh, Fgf4, and Fgf8 gene expression at diverse signalling centers during mouse development. *Dev. Dyn.* **207**, 291-299.

Chen, J. N., van Eeden, F. J. M., Warren, K. S., Cahin, A., Nüsslein-Volhard, C., Haffter, P. and Fishman, M. C. (1997). Left-right pattern of cardiac *BMP4* may drive asymmetry of the heart in zebrafish. *Development* **124**, 4373-4382.

Cohn, M. J., Izpisua Belmonte, J. C., Abud, H., Heath, J. K. and Tickle, C. (1995). Fibroblast growth factors induce additional limb development from the flank of chick embryos. *Cell* **80**, 739-746.

Cohn, M. J. and Tickle, C. (1996). Limbs: a model for pattern formation within the vertebrate body plan. *Trends in Genetics* **12**, 253-257.

Crossley, P. H. and Martin, G. R. (1995). The mouse Fgf8 gene encodes a family of polypeptides and is expressed in regions that direct outgrowth and patterning in the developing embryo. *Development* **121**, 439-451.

Crossley, P. H., Martinez, S. and Martin, G. R. (1996a). Midbrain development induced by FGF8 in the chick embryo. *Nature* **380**, 66-68.

Crossley, P. H., Minowada, G., MacArthur, C. A. and Martin, G. R. (1996b). Roles for FGF8 in the induction, initiation, and maintenance of chick limb development. *Cell* **84**, 127-136.

Danielian, P. S. and McMahon, A. P. (1996). *Engrailed-1* as a target of the *Wnt-1* signalling pathway in vertebrate midbrain development. *Nature* **383**, 332-334.

Darnell, D. K. and Schoenwolf, G. C. (1997). Vertical induction of engrailed-2 and other region-specific markers in the early chick embryo. *Dev. Dyn.* **209**, 45-58.

Deng, C. X., Wynshaw Boris, A., Shen, M. M., Daugherty, C., Ornitz, D. M. and Leder, P. (1994). Murine FGFR-1 is required for early postimplantation growth and axial organization. *Genes. Dev.* **8**, 3045-3057.

Devoto, S. H., Melancon, E., Eisen, J. S. and Westerfield, M. (1996). Identification of separate slow and fast muscle precursor cells in vivo, prior to somite formation. *Development* **122**, 3371-3380.

Dornseifer, P., Takke, C. and Campos-Ortega, J. A. (1997). Overexpression of a zebrafish homologue of the *Drosophila* neurogenic gene *Delta* perturbs differentiation of primary neurons and somite development. *Mech. Dev.* **63**, 159-171.

Ekker, M., Wegner, J., Akimenko, M. A. and Westerfield, M. (1992). Coordinate embryonic expression of three zebrafish *engrailed* genes. *Development* **116**, 1001-1010.

Favor, J., Sandulache, R., Neuhäuser-Klaus, A., Pretsch, W., Chatterjee, B., Senft, E., Wurst, W., Blanquet, V., Grimes, P., Spörle, R. and Schughart, K. (1996). The mouse Pax2 1Neu mutation is identical to a human PAX2 mutation in a family with renal-coloboma syndrome and results in developmental defects of the brain, ear, eye and kidney. *Proc. Natn Acad. Sci., USA* **93**, 13870-13875.

Feldman, B., Poueymirou, W., Papaioannou, V. E., DeChiara, T. M. and Goldfarb, M. (1995). Requirement of FGF-4 for postimplantation mouse development. *Science* **267**, 246-249.

Fürthauer, M., Thisse, C. and Thisse, B. (1997). A role for Fgf-8 in the dorsoventral patterning of the zebrafish gastrula. *Development* **124**, 4253-4264.

Gardiner, C. A. and Harald, K. F. (1991). The cellular environment controls the expression of engrailed-like protein in the cranial neuroepithelium of quail-chick chimeric embryos. *Development* **113**, 1037-1048.

Gont, L. K., Steinbeisser, H., Blumberg, B. and de Robertis, E. M. (1993). Tail formation as a continuation of gastrulation: the multiple cell populations of the Xenopus tailbud derive from the late blastopore lip. *Development* **119**, 991-1004.

Grieshammer, U., Minowada, G., Pisenti, J. M., Abbott, U. K. and Martin, G. R. (1996). The chick limbless mutation causes abnormalities in limb bud dorsal-ventral patterning: implications for the mechanism of apical ridge formation. *Development* **122**, 3851-3861.

Griffin, K., Patient, R. and Holder, N. (1995). Analysis of FGF function in normal and no tail zebrafish embryos reveals separate mechanisms for formation of the trunk and the tail. *Development* **121**, 2983-2994.

Halpern, M. E., Ho, R. K., Walker, C. and Kimmel, C. B. (1993). Induction of muscle pioneers and floor plate is distinguished by the zebrafish no tail mutation. *Cell* **75**, 99-111.

Hammerschmidt, M. and Nüsslein-Volhard, C. (1993). The expression of a zebrafish gene homologous to Drosophila snail suggests a conserved function in invertebrate and vertebrate gastrulation. *Development* **119**, 1107-1118.

Hatta, K., Bremiller, R., Westerfield, M. and Kimmel, C. B. (1991). Diversity of expression of engrailed-like antigens in zebrafish. *Development* **112**, 821-32.

Hebert, J. M., Rosenquist, T., Gotz, J. and Martin, G. R. (1994). FGF5 as a regulator of the hair growth cycle: evidence from targeted and spontaneous mutations. *Cell* **78**, 1017-1025.

Heikinheimo, M., Lawshe, A., Shackleford, G. M., Wilson, D. B. and MacArthur, C. A. (1994). Fgf-8 expression in the post-gastrulation mouse suggests roles in the development of the face, limbs and central nervous system. *Mech. Dev.* **48**, 129-138.

Hrabe de Angelis, M., McIntyre, J. n. and Gossler, A. (1997). Maintenance of somite borders in mice requires the Delta homologue DII1. *Nature* **386**, 717-721.

Joly, J. S., Joly, C., Schulte-Merker, S., Boulekbache, H. and Condamine, H. (1993). The ventral and posterior expression of the zebrafish homeobox gene eve1 is perturbed in dorsalized and mutant embryos. *Development* **119**, 1261-1275.

Joyner, A. L. (1996). Engrailed, Wnt and Pax genes regulate midbrain-hindbrain development. *TIG* **12**, 15-20.

Kane, D. A. and Kimmel, C. B. (1993). The zebrafish midblastula transition. *Development* **119**, 447-456.

Khoury, G., Gruss, P., Dahr, R. and Lai, C. J. (1979). Processing and expression of early SV40 mRNA: a role for RNA conformation in splicing. *Cell* **18**, 85-92.

Kimmel, C. B., Ballard, W. W., Kimmel, S. R., Ullmann, B. and Schilling, T. F. (1995). Stages of embryonic development of the zebrafish. *Dev. Dyn.* **203**, 253-310.

Krauss, S., Johansen, T., Korzh, V. and Fjose, A. (1991). Expression of the Zebrafish Paired Box Gene pax<zf-b> During Early Neurogenesis. *Development* **113**, 1193-1206.

Krauss, S., Concordet, J. P. and Ingham, P. W. (1993). A functionally conserved homolog of the Drosophila segment polarity gene hh is expressed in tissues with polarizing activity in zebrafish embryos. *Cell* **75**, 1431-1444.

Kroll, K. L. and Amaya, E. (1996). Transgenic Xenopus embryos from sperm nuclear transplantations reveal FGF signaling requirements during gastrulation. *Development* **122**, 3173-3183.

Kuwada, J. Y., Bernhardt, R. R. and Chitnis, A. B. (1990). Pathfinding by identified growth cones in the spinal cord of zebrafish embryos. *J. Neurosci.* **10**, 1299-1308.

Lorenzi, M. V., Long, J. E., Miki, T. and Aaronson, S. A. (1995). Expression cloning, developmental expression and chromosomal localization of fibroblast growth factor-8. *Oncogene* **10**, 2051-2055.

Lumsden, A. and Krumlauf, R. (1996). Patterning the vertebrate neuraxis. *Science* **274**, 1109-1123.

MacArthur, C. A., Lawshe, A., Xu, J., Santos Ocampo, S., Heikinheimo, M., Chellaiah, A. T. and Ornitz, D. M. (1995). FGF-8 isoforms activate receptor splice forms that are expressed in mesenchymal regions of mouse development. *Development* **121**, 3603-3613.

Mahmood, R., Bresnick, J., Hornbruch, A., Mahony, C., Morton, N., Colquhoun, K., Martin, P., Lumsden, A., Dickson, C. and Mason, I. (1995). A role for FGF-8 in the initiation and maintenance of vertebrate limb bud outgrowth. *Curr. Biol.* **5**, 797-806.

Mansour, S. L., Goddard, J. M. and Capecchi, M. R. (1993). Mice homozygous for a targeted disruption of the proto-oncogene int-2 have developmental defects in the tail and inner ear. *Development* **117**, 13-28.

Marin, F. and Puelles, L. (1994). Patterning of the embryonic avian midbrain after experimental inversions: a polarizing activity from the isthmus. *Dev. Biol.* **163**, 19-37.

Martinez, S., Wassef, M. and Alvarado-Mallart, R. M. (1991). Induction of a mesencephalic phenotype in the 2-day-old chick prosencephalon is preceded by the early expression of the homeobox gene *en*. *Neuron* **6**, 971-981.

Martinez, S., Marin, F., Nieto, M. A. and Puelles, L. (1995). Induction of ectopic *engrailed* expression and fate change in avian rhombomeres: intersegmental boundaries as barriers. *Mech. Dev.* **51**, 289-303.

McMahon, A. P., Joyner, A. L., Bradley, A. and McMahon, J. A. (1992). The midbrain-hindbrain phenotype of *Wnt-1*$^{-}$/*Wnt-1*$^{-}$ mice results from stepwise deletion of engrailed-expressing cells by 9. 5 days postcoitum. *Cell* **69**, 581-595.

Meyers, E. N., Lewandoski, M. and Martin, G. R. (1998). An Fgf8 mutant allelic series generated by Cre- and Flp-mediated recombination. *Nat. Genet.* **18**, 136-142.

Millen, K. J., Wurst, W., Herrup, K. and Joyner, A. (1994). Abnormal embryonic cerebellar development and patterning of postnatal foliation in two mouse *Engrailed-2* mutants. *Development* **120**, 695-706.

Miyagawa, T., Amanuma, H., Kuroiwa, A. and Takeda, H. (1996). Specification of posterior midbrain region in zebrafish neuroepithelium. *Genes to Cells* **1**, 369-377.

Molven, A., Njolstad, P. R. and Fjose, A. (1991). Genomic structure and restricted neural expression of the zebrafish wnt-1 (int-1) gene. *EMBO J.* **10**, 799-807.

Müller, M., v. Weizsäcker, E. and Campos-Ortega, J. A. (1996). Transcription of a zebrafish gene of the *hairy-Enhancer of split* family delineates the midbrain anlage in the neural plate. *Dev. Genes Evol.* **206**, 153-160.

Nakamura, H., Itasaki, N. and Matsuno, T. (1994). Rostrocaudal polarity formation of chick optic tectum. *Int. J. Dev. Biol.* **38**, 281-286.

Neubüser, A., Peters, H., Balling, R. and Martin, G. R. (1997). Antagonistic interactions between FGF and BMP signaling pathways: a mechanism for positioning the sites of tooth formation. *Cell* **90**, 247-255.

Niswander, L. (1997). Limb mutants: what can they tell us about normal limb development? *Curr. Op. Genet. Dev.* **7**, 530-536.

Ohuchi, H., Yoshioka, H., Tanaka, A., Kawakami, Y., Nohno, T. and Noji, S. (1994). Involvement of androgen-induced growth factor (FGF-8) gene in mouse embryogenesis and morphogenesis. *Biochem. Biophys. Res. Commun.* **204**, 882-888.

Ohuchi, H., Nakagawa, T., Yamamoto, A., Araga, A., Ohata, T., Ishimaru, Y., Yoshioka, H., Kuwana, T., Nohno, T., Yamasaki, M., Itoh, N. and Noji, S. (1997a). The mesenchymal factor, FGF10, initiates and maintains the outgrowth of the chick limb bud through interaction with FGF8, an apical ectodermal factor. *Development* **124**, 2235-2244.

Ohuchi, H., Shibusawa, M., Nakagawa, T., Ohata, T., Yoshioka, H., Hirai, Y., Nohno, T., Noji, S. and Kondo, N. (1997b). A chick wingless mutation causes abnormality in maintenance of Fgf8 expression in the wing apical ridge, resulting in loss of the dorsoventral boundary. *Mech. Dev.* **62**, 3-13.

Ornitz, D. M., Xu, J., Colvin, J. S., McEwen, D. G., MacArthur, C. A., Coulier, F., Gao, G. and Goldfarb, M. (1996). Receptor specificity of the fibroblast growth factor family. *J. Biol. Chem.* **271**, 15292-15297.

Oxtoby, E. and Jowett, T. (1993). Cloning of the zebrafish krox-20 gene (krx-20) and its expression during hindbrain development. *Nucleic Acids Res.* **21**, 1087-1095.

Padgett, R. A., Grabowski, P. J., Konarska, M. M., Seiler, S. and Sharp, P. A. (1986). Splicing of messenger RNA precursors. *Ann. Rev. Biochem.* **55**, 1119-1150.

Pfeffer, P. L., Gerster, T., Lun, K., Brand, M. and Busslinger, M. (1998). Characterization of three novel members of the zebrafish *Pax2/5/8* family: dependency of *Pax5* and *Pax8* expression on the *Pax2. 1* (*noi*) function. *Development*, in press.

Riddle, R. D., Johnson, R. L., Laufer, E. and Tabin, C. (1993). Sonic hedgehog mediates the polarizing activity of the ZPA. *Cell* **75**, 1401-1416.

Ros, M. A., Lopez Martinez, A., Simandl, B. K., Rodriguez, C., Izpisua Belmonte, J. C., Dahn, R. and Fallon, J. F. (1996). The limb field mesoderm determines initial limb bud anteroposterior asymmetry and budding independent of sonic hedgehog or apical ectodermal gene expressions. *Development* **122**, 2319-2330.

Rupp, R. A. W., Snider, L. and Weintraub, H. (1994). Xenopus embryos regulate the nuclear localization of XMyoD. *Genes Dev.* **8**, 1311-1323.

Schulte-Merker, S., Ho, R. K., Herrmann, B. G. and Nusslein-Volhard, C. (1992). The protein product of the zebrafish homologue of the mouse T gene is expressed in nuclei of the germ ring and the notochord of the early embryo. *Development* **116**, 1021-1032.

Shimamura, K. and Rubenstein, J. L. (1997). Inductive interactions direct early regionalization of the mouse forebrain. *Development* **124**, 2709-2718.

Song, D. L., Chalepakis, G., Gruss, P. and Joyner, A. L. (1996). Two Pax-binding sites are required for early embryonic brain expression of an Engrailed-2 transgene. *Development* **122**, 627-635.

Sordino, P., van-der-Hoeven, F. and Duboule, D. (1995). Hox gene expression in teleost fins and the origin of vertebrate digits. *Nature* **375**, 678-81.

Stainier, D. Y. R. and Fishman, M. C. (1992). Patterning the zebrafish heart tube: acquisition of anteroposterior polarity. *Dev. Biol.* **153**, 91-101.

Tanaka, A., Miyamoto, K., Minamino, N., Takeda, M., Sato, B., Matsuo, H. and Matsumoto, K. (1992). Cloning and characterization of an androgen-induced growth factor essential for the androgen-dependent growth of mouse mammary carcinoma cells. *Proc. Natl. Acad. Sci. USA* **89**, 8928-8932.

Thisse, B., Thisse, C. and Weston, J. A. (1995). Novel FGF receptor (Z-FGFR4) is dynamically expressed in mesoderm and neurectoderm during early zebrafish embryogenesis. *Dev. Dyn.* **203**, 377-391.

Thisse, C., Thisse, B., Halpern, M. E. and Postlethwait, J. H. (1994). Goosecoid expression in neurectoderm and mesendoderm is disrupted in zebrafish cyclops gastrulas. *Dev. Biol.* **164**, 420-429.

Thomas, K. R. and Capecchi, M. R. (1990). Targeted disruption of the murine *int-1* proto-oncogene resulting in severe abnormalities in midbrain and cerebellar development. *Nature* **346**, 847-850.

van Eeden, F. J. M., Granato, M., Schach, U., Brand, M., Furutani-Seiki, M., Haffter, P., Hammerschmidt, M., Heisenberg, C.-P., Jiang, Y.-J., Kane, D. A., Kelsh, R. N., Mullins, M. C., Odenthal, J., Warga, R. M., Allende, M. L., Weinberg, E. S. and Nüsslein-Volhard, C. (1996). Mutations affecting somite formation and patterning in the zebrafish *Danio rerio*. *Development* **123**, 153-164.

Vogel, A., Rodriguez, C. and Izpisua Belmonte, J. C. (1996). Involvement of FGF-8 in initiation, outgrowth and patterning of the vertebrate limb. *Development* **122**, 1737-1750.

Weinberg, E. S., Allende, M. L., Kelly, C. S., Abdelhamid, A., Murakami, T., Andermann, P., Doerre, O. G., Grunwald, D. J. and Riggleman, B. (1996). Developmental regulation of zebrafish MyoD in wild-type, no tail and spadetail embryos. *Development* **122**, 271-280.

Westerfield, M. (1994). *The Zebrafish Book*. Edition 2. 1, Oregon: University of Oregon Press.

Wilkinson, D. G., Bailes, J. A. and McMahon, A. P. (1987). Expression of the proto-oncogene int-1 is restricted to specific neural cells in the developing mouse embryo. *Cell* **50**, 79-88.

Woo, K. and Fraser, S. E. (1995). Order and coherence in the fate map of the zebrafish nervous system. *Development* **121**, 2595-609.

Woo, K. and Fraser, S. E. (1997). Specification of the zebrafish nervous system by nonaxial signals. *Science* **277**, 254-257.

Wood, A. (1982). Early pectoral fin development and morphogenesis of the apical ectodermal ridge in the killifish, *Aphyosemion scheeli*. *Anat. Rec.* **204**, 349-356.

Wurst, W., Auerbach, A. B. and Joyner, A. L. (1994). Multiple developmental defects in Engrailed-1 mutant mice: an early mid-hindbrain deletion and patterning defects in forelimbs and sternum. *Development* **120**, 2065-2075.

Yamaguchi, T. P., Harpal, K., Henkemeyer, M. and Rossant, J. (1994). fgfr-1 is required for embryonic growth and mesodermal patterning during mouse gastrulation. *Genes Dev.* **8**, 3032-3044.

Yamaguchi, T. P. and Rossant, J. (1995). Fibroblast growth factors in mammalian development. *Curr. Opin. Genet. Dev.* **5**, 485-489.

Development 127, 225-235 (2000)
Printed in Great Britain © The Company of Biologists Limited 2000
DEV1488

Induction and differentiation of the zebrafish heart requires fibroblast growth factor 8 (*fgf8/acerebellar*)

Frank Reifers[1], Emily C. Walsh[2], Sophie Léger[1], Didier Y. R. Stainier[2] and Michael Brand[1,*]

[1]Department of Neurobiology, University of Heidelberg, Im Neuenheimer Feld 364, D-69120 Heidelberg, Germany
[2]Department of Biochemistry and Biophysics, University of California San Francisco, San Francisco, CA 94143-0554, USA
*Author for correspondence (e-mail: brand@sun0.urz.uni-heidelberg.de)

Accepted 1 November; published on WWW 20 December 1999

SUMMARY

Vertebrate heart development is initiated from bilateral lateral plate mesoderm that expresses the *Nkx2.5* and *GATA4* transcription factors, but the extracellular signals specifying heart precursor gene expression are not known. We describe here that the secreted signaling factor Fgf8 is expressed in and required for development of the zebrafish heart precursors, particularly during initiation of cardiac gene expression. *fgf8* is mutated in *acerebellar* (*ace*) mutants, and homozygous mutant embryos do not establish normal circulation, although vessel formation is only mildly affected. In contrast, heart development, in particular of the ventricle, is severely abnormal in *acerebellar* mutants. Several findings argue that Fgf8 has a direct function in development of cardiac precursor cells: *fgf8* is expressed in cardiac precursors and later in the heart ventricle. Fgf8 is required for the earliest stages of *nkx2.5* and *gata4*, but not *gata6*, expression in cardiac precursors. Cardiac gene expression is restored in *acerebellar* mutant embryos by injecting *fgf8* RNA, or by implanting a Fgf8-coated bead into the heart primordium. Pharmacological inhibition of Fgf signalling during formation of the heart primordium phenocopies the *acerebellar* heart phenotype, confirming that Fgf signaling is required independently of earlier functions during gastrulation. These findings show that *fgf8/acerebellar* is required for induction and patterning of myocardial precursors.

Key words: Cardiogenesis, Heart, Ventricle, *fgf8*, *acerebellar*, *nkx2.5*, *gata4*, BMP, Zebrafish (*Danio rerio*)

INTRODUCTION

The heart is the first organ to form and function during vertebrate embryogenesis. The fish heart can be viewed as a prototypical vertebrate heart, since the process of heart formation occurs in a similar way in all vertebrates (DeHaan, 1965; DeRuiter et al., 1992; Stainier and Fishman, 1992; Stainier et al., 1993; Fishman and Chien, 1997). In zebrafish, cardiogenic precursors involute shortly after the onset of gastrulation and migrate medially as part of the lateral plate mesoderm. The myocardial precursor cells form two tubular primordia on each side of the midline at early somitogenesis. These primitive tubes then fuse by the 20-somite stage and enclose the endocardial precursor cells to give rise to the definitive heart tube consisting of an inner, endocardial layer and an outer, myocardial layer (Stainier and Fishman, 1992; Stainier et al., 1993; Fishman and Chien, 1997). Around 24 hours post-fertilization (hpf), the heart starts beating and circulation begins. The definitive heart tube is subsequently divided into different chambers, with the atrium and the ventricle being the most prominent heart structures. The atrium can be distinguished from the ventricle by differential expression of myosin heavy chains already at 24 hpf, and a morphological distinction becomes apparent soon thereafter (Stainier and Fishman, 1992; Stainier et al., 1993).

Although heart development has been well described morphologically, the molecular events underlying this process are only beginning to be understood (for reviews see Lyons, 1996; Olson and Srivastava, 1996; Fishman and Chien, 1997; Mohun and Sparrow, 1997). Several families of transcription factors have been implicated in heart development. A key family are the vertebrate *Nkx2.5* genes, which are homologues of the *Drosophila* gene *tinman*. In *Drosophila*, *tinman* is expressed in the heart (or dorsal vessel) and visceral mesoderm, and is required for heart formation (Azpiazu and Frasch, 1993; Bodmer, 1993; Harvey, 1996). In vertebrates, *Nkx2.5* is the earliest marker for heart precursors in the lateral plate mesoderm (Lints et al., 1993; Komuro and Izumo, 1993; Chen and Fishman, 1996). Overexpression of *nkx2.5* in *Xenopus* or zebrafish causes a general increase in heart size (Chen and Fishman, 1996; Cleaver et al., 1996). Targeted disruption of *Nkx2.5* in the mouse does not prevent formation of the heart tube, but cardiac looping is absent and the expression of downstream cardiac transcription factors is disturbed (Lyons et al., 1995; Tanaka et al., 1999). At least two more *Nk2* class homeobox genes, *nkx2.7* and *Nkx2.8*, are expressed early in the developing heart, with *nkx2.7* being expressed even before *nkx2.5* in the zebrafish (Lee et al., 1996; Brand et al., 1997).

A direct target gene regulated by *tinman* is the myocyte enhancer binding factor-2 (*D-mef2*) of the MADS box-

containing proteins, and loss of D-MEF2 function prevents formation of cardiac muscle (Lilly et al., 1994; Bour et al., 1995; Lilly et al., 1995; Olson et al., 1995; Gajeweski et al., 1997). Likewise, the four *mef2* genes in vertebrates are expressed in precardiac mesoderm and mouse mutants for *MEF2C* exhibit heart abnormalities (Edmondson et al., 1994; Molkentin et al., 1996; Ticho et al., 1996; Lin et al., 1997). In addition, several members of the GATA family of zinc finger domain transcription factors are involved in cardiac development. *GATA4* is expressed in the presumptive heart mesoderm and overexpression of *GATA4* in mouse embryonic stem cells enhances cardiogenesis (Kelley et al., 1993; Heikinheimo et al., 1994; Laverriere et al., 1994; Jiang and Evans, 1996; Grepin et al., 1997). In contrast, the failure of the bilateral heart primordia to migrate medially and to fuse in *GATA4* knock-out mice is thought to be a secondary consequence of a defective endoderm (Kuo et al., 1997; Molkentin et al., 1997; Narita et al., 1997a,b). Finally, basic region helix-loop-helix (bHLH) domain proteins play important roles at later stages of cardiac morphogenesis, e.g. in chamber-specific gene expression (Srivastava et al., 1995).

Although localized expression of transcription factors is important for heart development, little is known about the signaling molecules that control this expression. Endoderm, ectoderm and Spemann's organizer have been implicated as sources for cardiac mesoderm inducing signals (Lyons, 1996; Fishman and Chien, 1997; Mohun and Sparrow, 1997). Misexpression of *BMPs* in anterior mesoderm of chick embryos suggested that BMPs may induce expression of the cardiac transcription factors *Nkx2.5* and *GATA4*, and *BMPs* are expressed close to the heart primordium (Schultheiss et al., 1997; Andrée et al., 1998). In *Drosophila*, *tinman* is indeed regulated by the *BMP* homologue *decapentaplegic* (*dpp*) (Frasch, 1995). In addition, tissue culture studies have demonstrated cardiogenic effects for Activin-A and FGF2, and treatment of non-precardiac mesodermal explants from early

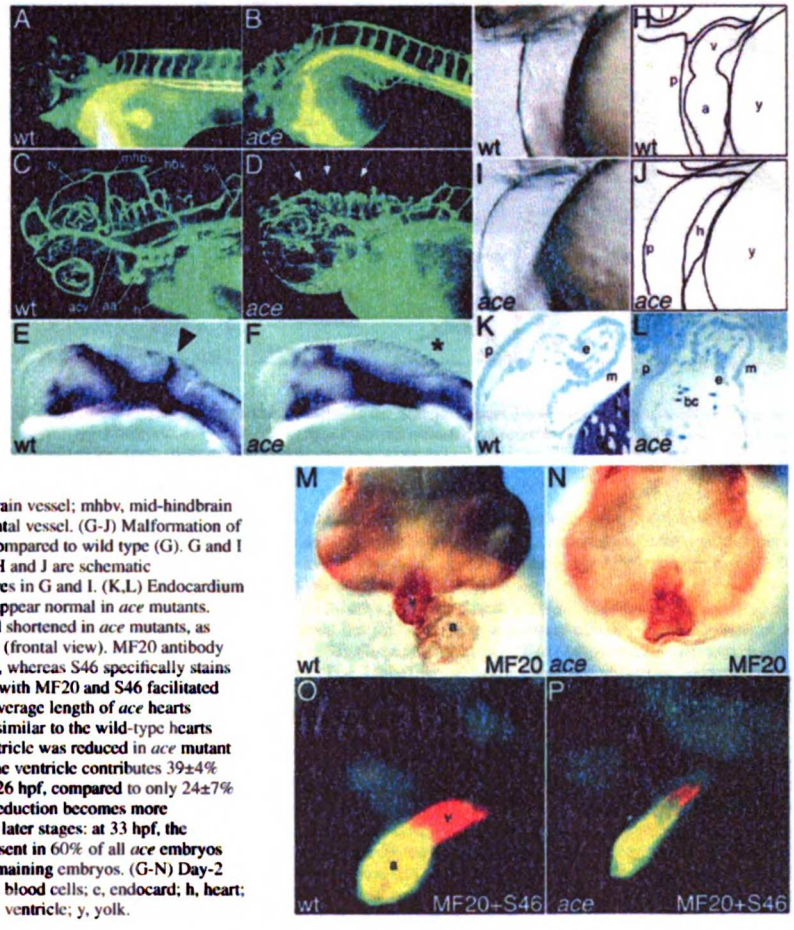

Fig. 1. Circulation, blood vessel formation and abnormal heart morphology in *acerebellar* mutants. (A,B) Overview of blood vessel system in a day-2 wild-type (A) and an *ace* (B) larva. (C,D) Confocal close-up of the blood vessels in the head in a wild-type (C) and an *ace* (D) larva on day 2, with the main vessels in the tectum, at the mid-hindbrain boundary and in the hindbrain being affected in *ace* mutants (arrows). The dashed circle in D marks the position of the eye. (E,F) The vessel at the mid-hindbrain boundary (E, arrowhead) is missing in *ace* mutant embryos (F, asterisk) at 24 hpf, detected by in situ hybridization with *flk-1*. aa, aortic arches; acv, anterior cardinal vein; h, heart; hbv, hindbrain vessel; mhbv, mid-hindbrain vessel; tv, tectal vessel; sv, segmental vessel. (G-J) Malformation of the heart in *acerebellar* larva (I) compared to wild type (G). G and I are lateral views of living larvae, H and J are schematic representation of the main structures in G and I. (K,L) Endocardium and myocardium are present and appear normal in *ace* mutants. (M,N) The heart is malformed and shortened in *ace* mutants, as shown by MF20 antibody staining (frontal view). MF20 antibody reacts with both cardiac chambers, whereas S46 specifically stains the atrium. (O,P) Double staining with MF20 and S46 facilitated measuring the chambers and the average length of *ace* hearts (83±16%, n=19) was found to be similar to the wild-type hearts (100±8%, n=10), whereas the ventricle was reduced in *ace* mutant embryos. In wild-type embryos, the ventricle contributes 39±4% (n=10) to the total heart length at 26 hpf, compared to only 24±7% (n=19) in *ace* mutants. Ventricle reduction becomes more pronounced, but is still variable at later stages: at 33 hpf, the ventricle is severely reduced or absent in 60% of all *ace* embryos (n=55), and less affected in the remaining embryos. (G-N) Day-2 larvae, (O,P) 26 hpf. a, atrium; bc, blood cells; e, endocard; h, heart; l, lens; m, myocard; p, pericard; v, ventricle; y, yolk.

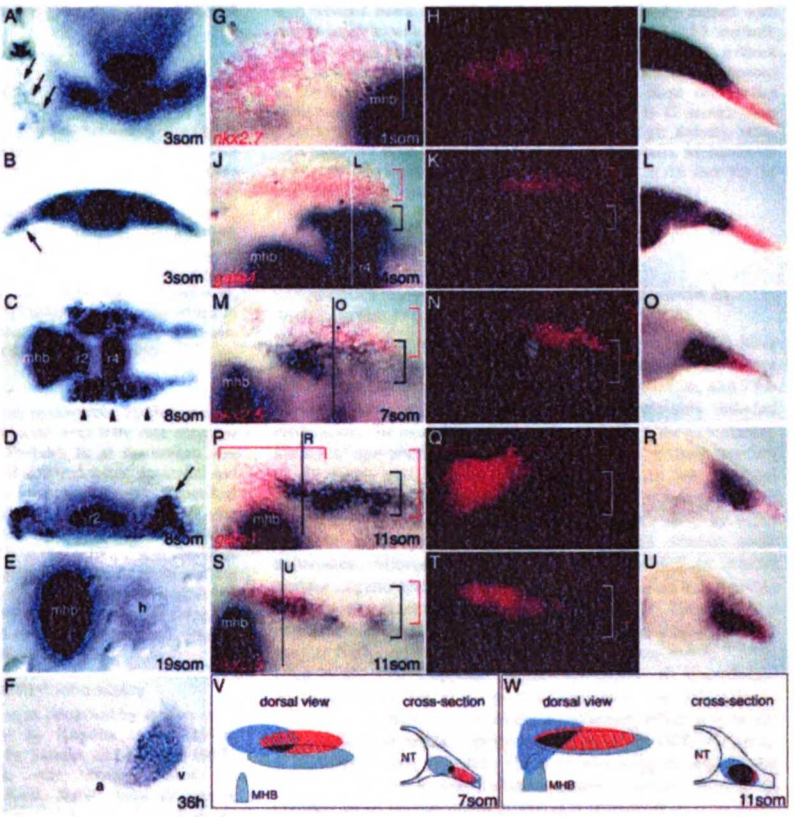

Fig. 2. Cardiac expression of *fgf8* in relation to heart marker genes in wild-type embryos. (A-F) *fgf8* expression at various stages of development, as indicated. B and D are cross sections of A and C, respectively. (A,B) Cells in lateral plate mesoderm express *fgf8* (arrows) at the 3-somite stage. (C,D) Expression bilaterally to the neural tube including cardiogenic fields (arrowheads in C and arrow in D) at the 8-somite stage. (E) Ring-shaped expression in the heart at 19-somite stage. (F) Expression is predominantly in the ventricle at 36 hpf. (F) Dissected heart. (A) Anterior to the top; (C,E) anterior to the left; a, atrium; h, heart; mhb, mid-hindbrain boundary; os, optic stalks; r2, rhombomere 2; r4, rhombomere 4; v, ventricle. (G-U) Double in situ hybridization with *fgf8* (black) and indicated heart markers (red fluorescence) of wild-type embryo at given stages. (G-I) *fgf8* is expressed in close proximity to *nkx2.7*. (J-L) *fgf8* is expressed close to *gata4*. (M-O) *fgf8* expression partially overlaps *nkx2.5* expression (star marks the same cell in M and N). (P-R) *fgf8* expression partially overlaps *gata4* expression. (S-U) *fgf8* expression strongly overlaps *nkx2.5* expression. Brackets indicate the two expression domains. (V,W) Summary of *fgf8* expression relative to the described heart marker genes at given stages (grey, *fgf8*; red, *nkx2.5*; blue, *gata4*, black, triple overlap). Embryos in G,H,J,K,M,N,P,Q,S,T are flat mounted, anterior to the left; G,J,M,P,S are bright-field images, H,K,N,Q,T are fluorescent images of the same embryos; I,L,O,R,U are cross sections at the indicated levels, lateral is to the right. mhb, mid-hindbrain boundary; r4, rhombomere 4.

chick embryos with a combination of FGF4 and BMP2 is able to induce cardiogenesis in vitro (Sugi and Lough, 1995; Lough et al., 1996).

Here we show that the secreted signaling factor Fgf8 is required in vivo for heart development of the zebrafish. Although expression of several *Fgfs* has been described in the developing heart (Parlow et al., 1991; Spirito et al., 1991; Engelmann et al., 1993; Mason et al., 1994; Crossley and Martin, 1995; Zhu et al., 1996; Hartung et al., 1997; Miyake et al., 1998), studying the function of Fgfs in development of the vertebrate heart has been difficult, often due to early lethality of the mutants or possible functional redundancy. Analysis of the available loss-of-function mutations has not revealed a specific function for Fgf signaling in the developing heart so far (Feldman et al., 1995; Dono et al., 1998; Meyers et al., 1998). Similarly, 3 out of 4 vertebrate Fgf receptors are expressed during heart development, but their inactivation in mouse embryos has not been informative with respect to cardiac development (Orr-Urtreger et al., 1991; Yamaguchi et al., 1991; Peters et al., 1992; Deng et al., 1994; Arman et al., 1995; Sugi et al., 1995; Thisse et al., 1995; Colvin et al., 1996; Weinstein et al., 1998).

In contrast, functional studies in *Drosophila* do suggest a role for Fgf signaling in cardiac development (Beiman et al., 1996; Gisselbrecht et al., 1996; Michelson et al., 1998).

The isolation of many mutants affecting zebrafish heart development in the systematic screens for embryonic zebrafish mutants opens up the possibility to study the genetic control of vertebrate heart development in great detail (Haffter et al., 1996). The zebrafish mutant *acerebellar (ace)* was orginally classified as a brain mutant (Brand et al., 1996) in which the *fgf8* gene is inactivated (Reifers et al., 1998). Here we show that analysis of this mutant unexpectedly reveals a pivotal role for Fgf8 in myocardial induction. We examine in detail the expression and function of Fgf8 in the developing zebrafish heart, and propose that Fgf8 functions together with Bmps in

induction of heart-specific gene expression upstream of *nkx2.5* and *gata4*.

MATERIALS AND METHODS

Zebrafish were raised and kept under standard laboratory conditions at about 27°C (Westerfield, 1994; Brand and Granato, 1999). Mutant carriers were identified by random intercrosses. To obtain embryos showing the mutant phenotype, two heterozygous carriers for a mutation were crossed to one another. Typically, the eggs were spawned synchronously at dawn of the next morning, and embryos were collected, sorted, observed and fixed at different times of development at 28.5°C. In addition, morphological features were used to determine the stage of the embryos, as described by Kimmel et al. (1995). In some cases, 0.2 mM phenylthiourea (PTU) was added to prevent melanization. Isolation and characterization of *acerebellar* is described by Brand et al. (1996) and Reifers et al. (1998).

Microangiography

Microangiography was essentially done as described by Weinstein et al. (1995). Briefly, embryos were injected with 0.01 mm diameter fluorescent latex beads (Molecular Probes). Bead suspension was diluted 1:1 with 2% BSA in deionized distilled water, sonicated and subjected to centrifugation for 2 minutes in an Eppendorf microcentrifuge. Dechorionated embryos were anaesthetized with tricaine as described and placed on an injection platform (Westerfield, 1994). A large bolus of bead suspension was injected into the sinus venosus. The fluorescent beads were uniformly distributed throughout the vasculature of the embryo within minutes. Specimens were either photographed on a Zeiss Axioskop microscope or scanned using the confocal microscope (Leica TCS4D) as rapidly as possible. Images were assembled using Adobe Photoshop.

In situ hybridization and immunohistochemistry

In situ hybridizations (ISH) were done as described by Reifers et al. (1998), and histology is described by Kuwada et al. (1990). Immunohistochemistry is described by Stainier and Gilbert (1990). MF20, anti-myosin heavy chain, was obtained from the Developmental Studies Hybridoma Bank. MF20 stains all cardiac chambers. S46 was a kind gift from Frank Stockdale, Stanford University. S46 specifically reacts with the atrium and the sinus venosus. Double-labeled embryos were stained with monoclonal antibodies S46 (IgG1) and MF20 (IgG2b) followed by fluoresceinated goat anti-mouse IgG1 and rhodaminated goat anti-mouse IgG2b. Heart length was measured on photographs of individually mounted wild-type and *acerebellar* embryos, heart length is given as percentage of wild-type length.

RNA injections

fgf8, subcloned into pCS2+ (Rupp et al., 1994), and XFD (Amaya et al., 1991) were linearized and transcribed using the SP6 message machine kit (Ambion). The amount of RNA injected was estimated from the concentration and volume of a sphere of RNA injected into oil at the same pressure settings. Typically, about 25 pg of *fgf8* RNA or XFD RNA were injected; RNA was dissolved in 0.25 M KCl with 0.2% phenol red and backloaded into borosilicate capillaries prepared on a Sutter puller. During injection, RNA was deposited into the cytoplasm of 2-cell stage embryos; in embryos after the first cleavage, the RNA usually stays in the progeny of the injected blastomere, as judged from the often unilateral distribution of control *lacZ* RNA, as detected with anti-β-gal antibody (Promega, 1:500) after ISH (Dornseifer et al., 1997). The embryos were fixed at the 6- to 8-somite stage prior to ISH and antibody staining.

Bead implantations and inhibitor treatment

Heparin acrylic beads (Sigma) were washed in ethanol for 30 minutes, then washed twice in PBS for 5 minutes and finally coated with recombinant mouse FGF8 protein (R&D Systems; 0.25 mg/ml). Protein-coated beads were stored for several weeks at 4°C without detectable loss of activity. FGF8 or PBS control beads were implanted in the lateral plate mesoderm of 5- to 7-somite stage *acerebellar* mutant embryos, the embryos were fixed at the 10- to 12-somite stage prior to ISH. For pharmacological inhibition of Fgfr activity, wild-type embryos were treated with SU5402 (Calbiochem; Mohammadi et al., 1997) at 8 μm in embryo medium at 28.5°C in the dark for the indicated time periods.

RESULTS

Circulatory system shows only minor defects in *acerebellar*

Wild-type embryos examined at 36 and 48 hpf (n=107) have successfully established normal circulation, whereas *ace* embryos fail to do so, with 23% having no circulation, and 77% of the *acerebellar* mutants (n=159) having variably reduced circulation. To examine whether the defect in the circulatory system of *acerebellar* mutant embryos is due to a malformation of the heart itself or the blood vessel system, we analysed vessel formation by microangiography, i.e. visualization of circulation by injecting fluorescent latex beads into the sinus venosus, and by staining for blood vessel marker gene expression. Microangiography at 48 hpf revealed an overall normal organization of the blood vessels in those *acerebellar* embryos that established circulation (Fig. 1A-D). Likewise, the expression pattern of *flk-1*, a receptor tyrosine kinase that is a marker for blood vessel endothelial cells (Fouquet et al., 1997; Liao et al., 1997) appears largely normal in all *acerebellar* mutants, except for an absence of vessels in the dorsal brain (Fig. 1E,F), which is most likely a secondary effect due to the brain defects in mutant embryos (Reifers et al., 1998, Picker et al., 1999). Taken together, these results suggest that blood vessel formation in *acerebellar* mutants is overall normal; in contrast heart development is severely abnormal.

Ventricle is strongly reduced in *acerebellar*

The zebrafish heart is composed of four subdivisions: the sinus venosus, the posterior atrium, the anterior ventricle and the bulbus arteriosus (Stainier and Fishman, 1992). The prominent atrium can be readily distinguished from the adjacent ventricle in living wild-type embryos (Fig. 1G,H). Heartbeat frequency is approximately normal in the mutants at 28 hpf (106±7 beats/minute, n=5) versus the wild-type (111±6 beats/min, n=5), but the heart of *acerebellar* mutant embryos is severely dysmorphic (Fig. 1I,J). Histological sections show that subdivision into an inner endocardial and outer myocardial layer occurs normally (Fig. 1K,L). In contrast, immunohistochemical analysis with the myosin heavy chain antibodies MF20 and the ventricular-specific antibody S46 and measurements of heart length shows that the heart is overall shorter, and that in particular the ventricular part is reduced (Fig. 1M-P).

fgf8 is expressed in the developing heart

Since the heart is affected in *acerebellar* mutant embryos and since *fgf8* expression during zebrafish heart development has not been analyzed previously, we examined the expression pattern of *fgf8* in the developing heart in detail, relative to several markers for cardiac precursors by double in situ

hybridisation. Already at the blastula stage, *fgf8* is expressed all around the margin of the embryo (Fürthauer et al., 1997; Reifers et al., 1998), which includes the fate map position of cardiac precursors ventrolaterally (Warga and Kimmel, 1990; Stainier and Fishman, 1992). The expression of *fgf8* at the mid-hindbrain boundary at tailbud stage (Fig. 2G-I) is located close to the posterior part of the expression domain of *nkx2.7*, which includes cardiac precursors in zebrafish (Lee et al., 1996). From the 3-somite stage onwards *fgf8*-positive cells can be observed in the lateral plate mesoderm in the area of the incipient heart field (Fig. 2A,B). At the 4-somite stage *fgf8* is expressed in the lateral plate mesoderm adjacent to the posterior part of the *gata4* expression domain (Fig. 2J-L), which includes the heart precursors (Kelley et al., 1993; Jiang and Evans, 1996; Serbedzija et al., 1998). Mesodermal *fgf8* expression partially overlaps with the expression domain of *nkx2.5* at the 7-somite stage (Fig. 2M-O), for which it has been shown that the anterior cells contribute to the heart (Serbedzija et al., 1998). At the 8-somite stage a subset of the *fgf8* expression lateral to the embryonic axis includes the myocardial precursors (Fig. 2C,D), which arrive in this region at this timepoint in development (Stainier and Fishman, 1992). The *fgf8* expression overlaps partially with the expression domains of *gata4* and almost completely with *nkx2.5* at the 11-somite stage (Fig. 2P-U). At the 19-somite stage the bilateral myocardial primordia meet caudal to the mid-hindbrain boundary to form a mesodermal ring-like structure which expresses *fgf8* (Fig. 2E). At 36 hpf atrium and ventricle can be morphologically distinguished, and *fgf8* expression is stronger in the ventricle (Fig. 2F); expression persists at least until 48 hpf, the latest stage we examined. These data suggest that Fgf8 could function during the earliest stages of cardiac precursor development, and in the differentiated heart.

Expression of heart markers is affected in *acerebellar*

Since *fgf8* is expressed early on in close association with the heart precursors and *acerebellar* embryos fail to develop proper hearts, we analysed the expression of cardiac marker genes in *acerebellar* mutant embryos (Table 1 and Fig. 3). *nkx2.7*, *gata4* and *nkx2.5* are affected from the onset of expression. Importantly, *gata6*-positive cells are present in mutant embryos, demonstrating that the lateral plate mesoderm cells that are normally destined to become cardiogenic precursors are present (Fig. 3I,J). In addition, we could not detect an increase in apoptotic cell death in the lateral plate mesoderm of *acerebellar* embryos (data not shown). Expression of *nkx2.7* is strongly reduced as early as the 1-somite stage in *acerebellar* embryos (Fig. 3A,B), but recovers quickly. Expression of the zinc-finger transcription factor *gata4* is also clearly reduced in mutant embryos at the 3- to 6-somite stage (Fig. 3C,D). The most severe effect was detected for *nkx2.5* expression, which was strongly reduced or absent between the 3-somite and 15-somite stages in *acerebellar* embryos (Fig. 3E,F). At the 11-somite stage the *fgf8* expression domain partially overlaps the *nkx2.5* domain and reaches further posterior at least to the level of rhombomere 5. In *acerebellar* mutant embryos the anterior part of *nkx2.5* expression is severely reduced and the expression in the posterior subdomain is completely absent (Fig. 3G,H). At late somitogenesis stages, all heart markers tested (*nkx2.5*, *nkx2.7*, *gata4*, *gata6* and *bmp4*) recover in the intensity of their expression in the remaining heart precursors of *acerebellar* mutant embryos (Table 1). However, a size-reduction of the mutant hearts remains detectable with these markers even at later stages (Fig. 3K,L and not shown). We conclude that *fgf8* expression partially overlaps with *nkx2.5* in heart precursor cells and that Fgf8 is required for expression of *nkx2.5*. Interestingly, the requirement may be stronger in the posterior part of the *nkx2.5* domain, since this expression is completely lost in *acerebellar* mutants (Fig. 3G,H). This early defect in mutant embryos may account for the subsequent loss of heart structures.

Fgf8 can rescue early expression of cardiac genes in *acerebellar*

The requirement of *acerebellar*/*fgf8* during the earliest stages of cardiac gene expression raised the possibility that Fgf8 is an inducer of heart development. To further examine this issue, we injected synthetic RNAs encoding *fgf8* or a dominant negative Fgf receptor into wild-type and *acerebellar* embryos. In addition to the described dorsalizing effect (Fürthauer et al., 1997; Reifers et al., 1998), *fgf8* injection can restore *gata4*, but not *nkx2.5* expression in mutant embryos at the 6-somite stage (Fig. 4A,B). 14 out of 45 (31%) *acerebellar* mutant embryos show strong *gata4* expression after *fgf8* injection on the injected side. Surprisingly, none of the injected mutant embryos re-expressed *nkx2.5* in response to *fgf8* overexpression by RNA injection (n=26; but see below); *lacZ* control injections gave no effect (not shown).

While *gata4* expression is restored in mutant embryos, neither *nkx2.5* nor *gata4* expression was induced outside their normal expression domain following *fgf8* RNA injection into wild-type or *ace* mutant embryos (Fig. 4A and not shown). This suggests that competence to respond to Fgf8 signaling is restricted to these subregions of lateral plate mesoderm including the prospective heart primordium.

We suspected that the failure to rescue *nkx2.5* expression in the mutant embryos by RNA injections could be due to the dorsalizing influence of *fgf8* overexpression during gastrula stages (Fürthauer et al., 1997; Reifers et al., 1998). To examine this possibility further and to test whether Fgf8 signaling could occur directly within the heart field during postgastrulation stages, we implanted Fgf8 protein-coated beads at the 5- to 6-somite stage into the lateral plate mesoderm of wild-type and *acerebellar* mutant embryos. 8 out of 10 operated mutant embryos strongly reexpressed *nkx2.5* on the bead side; implantation of PBS beads (n=6) gave no effect (Fig. 4E,F). Interestingly, implantation of Fgf8-soaked beads into wild-type embryos also results in a slight posterior expansion of the endogenous *nkx2.5* domain (Fig. 4G). These data indicate that *gata4* expression is dependent on Fgf8 signaling, while *nkx2.5* expression requires in addition to Fgf8 another factor, which may have been delocalized during gastrulation by the dorsalizing effect of *fgf8* RNA injections (see Discussion). Taken together, these experiments show that Fgf8 signaling is required but not sufficient for *gata4* and *nkx2.5* expression during early somitogenesis stages.

To further study the requirement of Fgf signaling for the expression of *nkx2.5* and *gata4*, we analysed the expression in wild-type embryos where Fgf signaling has been blocked either pharmacologically or by injecting RNA encoding the dominant

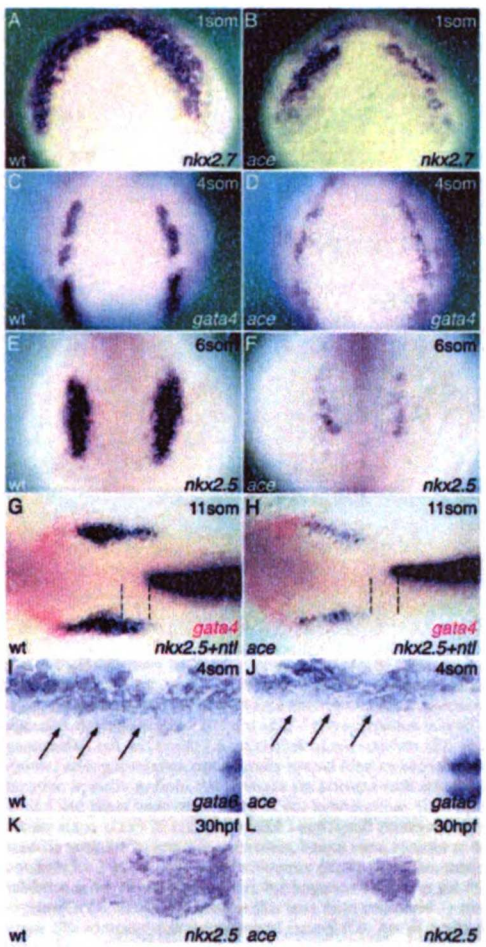

Fig. 3. Fgf8 is required for cardiac marker gene expression. Stages and markers as indicated. (A,B) Expression of *nkx2.7* in wild-type (A) and *ace* (B) embryos. (C,D) Expression of *gata4* in wild-type (C) and *ace* (D) embryos. (E-H) Expression of *nkx2.5* in wild-type (E,G) and *ace* (F,H) embryos. Notice the differential sensitivity of the posterior *nkx2.5* domain (dashed lines). (I,J) Expression of *gata6* (arrows) in wild-type (I) and *ace* (J) embryos. (K,L) Late expression of *nkx2.5* in dissected hearts of wild-type (K) and *ace* (L) embryos. A-F show dorsal views of whole embryos, anterior to the top. Embryos in G-J are flat mounted, anterior to the left. Embryos in G,H are stained for *nkx2.5* and *ntl* (black) and *gata4* (red). Embryos in I and J are double-stained for *myoD* to genotype the embryos (Reifers et al., 1998).

negative Fgf receptor XFD (Amaya et al., 1991). 32 out of 73 (44%) injected wild-type embryos show a strong reduction or even absence of *gata4* expression. In the case of *nkx2.5*, 67% (35 out of 52) of the *XFD*-injected embryos have altered gene expression (Fig. 4C,D). Interestingly, the described effects could only be observed if the misexpressed RNA was located in mesodermal cells (data not shown), suggesting that Fgf signal reception is required only within the mesodermal layer. While these results are consistent with a dependence of *nkx2.5* and *gata4* expression on Fgf signaling in the heart field, they could also be explained by an earlier requirement for Fgf signaling in dorsoventral patterning during gastrulation. To test whether Fgfs are specifically required after gastrulation during early somitogenesis for heart development, we treated wild-type embryos with SU5402, a potent inhibitor of Fgfr1 function (Mohammadi et al., 1997). Since SU5402 blocks Fgfr1 activity by binding to a region identical in all four Fgfrs (Johnson and Williams, 1993), it probably blocks all Fgf signals, including Fgf8. Inhibitor treatment during early somitogenesis results in a phenocopy of the *acerebellar* heart phenotype (not shown), including failure to initiate *nkx2.5* expression (Fig. 4I-K). This confirms that Fgf signaling is required specifically during early somitogenesis for initiation of heart development. As in *acerebellar* homozygous embryos (see above, Fig. 3F and Table 1), *nkx2.5* expression recovers after transient treatment in early somitogenesis (Fig. 4J,M). Continuous inhibitor treatment, however, prevents this recovery (Fig. 4K,N), suggesting that recovery is due to other Fgfs that act during later stages of heart development.

Table 1. Cardiac marker gene expression in *acerebellar* mutants

Marker gene expression	1 som	3 som	6 som	15 som	22 som	26 som
gata4	nd	–	–	+	+	+
gata6	nd	+	+	+	+	+
nkx2.5	nd	–	–	–	+	+
nkx2.7	–	+	+	+	+	+
bmp4	nd	nd	nd	+	+	+

som: somite-stage. + unaffected, – affected, nd, not detectable.

fgf8 itself is later expressed specifically in ventricular tissue (Fig. 2F), and *acerebellar* mutants show strongly impaired ventricle development (Fig. 1O,P). The ventricle defect could either be a consequence of abnormal formation of the primordium, or could represent an independent later function of Fgf8. To distinguish these possibilities, Fgf signaling was inhibited by SU5402 treatment after initial primordium formation, from late somitogenesis onwards. This treatment results in absence of ventricular tissue and apparent enlargement of atrial tissue, indicating that Fgf signaling continues to be required specifically for ventricular development (Fig. 4O,P).

DISCUSSION

Cardiovascular phenotype of *acerebellar*

Our analysis shows that *fgf8* is expressed in and required for the development of cardiogenic precursors of the zebrafish heart. Homozygous *acerebellar/fgf8* mutants fail to initiate proper gene expression of the cardiac transcription factors *nkx2.5* and *gata4*, resulting in a severely malformed heart. Protein bead implantations and receptor inhibition show that Fgf8 can act directly on the myocardial primordium during

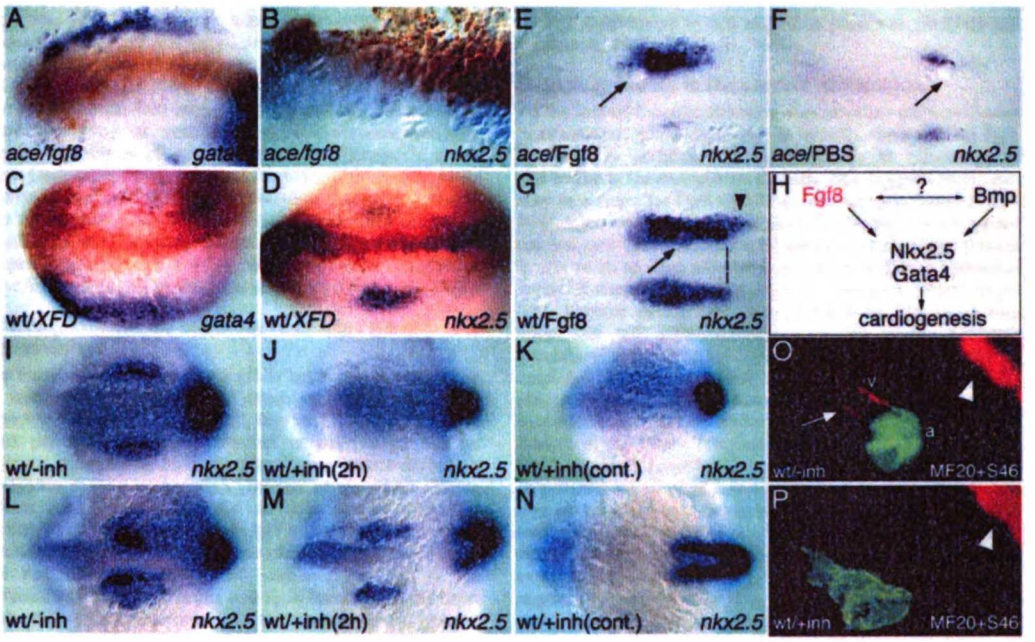

Fig. 4. Fgf8 functions in the heart primordium. (A,B) Misexpression of *fgf8* in *ace* embryos by RNA injection. Localization of *lacZ* co-injected cells with an antibody to β-gal (brown). *fgf8* RNA injection can restore *gata4* (A), but not *nkx2.5* (B) expression in mutant embryos. (C,D) Expression of *XFD* in wild-type embryos by RNA injection. Localization of *lacZ* co-injected cells with an antibody to β-gal. *XFD* RNA injection suppresses *gata4* (C) and *nkx2.5* (D) expression in wild-type embryos. (E,F) Implantation of a Fgf8-soaked bead (arrow) after gastrulation can rescue *nkx2.5* expression in *ace* embryos (E), while PBS bead gives no effect (F). (G) Implantation of a Fgf8-soaked bead (arrow) after gastrulation can caudally extend (dashed line) the endogenous *nkx2.5* expression domain in wild-type embryos. (H) Model of Fgf8 function in cardiogenesis. All embryos are oriented with anterior to the left; A,B,E-G are flat mounted; C,D are dorsal views of whole embryos. *nkx2.5* and *gata4* were detected by in situ hybridization. (I-P) Fgfr inhibitor treatments. (I-K) 10-somite stage, (L,M) 15-somite stage, (N) 18-somite stage, (O,P) 26 hpf. (I-N) *nkx2.5* and *myoD* expression detected by ISH; dorsal view of whole embryo, anterior to the left. (O,P) Double staining with MF20 and S46 antibodies, lateral view, anterior to the left. (I-N) Embryos have been treated with SU5402 from the 1-somite stage onwards for 2 hours (J,M) or continuously (K,N). (I,L) Non-treated control embryos. *nkx2.5* expression is absent after short exposure to the inhibitor at the 10-somite stage (J), but begins to recover at the 15-somite stage (M). Continuous treatment results in permanent loss of *nkx2.5* expression (K,N). (O,P) Embryos that have been continuously treated with SU5402 from the 18-somite stage onwards show no ventricular tissue (P); compare with the untreated control (O). Arrow marks the ventricle, arrowheads point to the MF20-positive somites. a, atrium; v, ventricle.

postgastrulation stages. We therefore propose that Fgf8 functions in induction of the earliest cardiac gene expression (Fig. 4H).

In addition to its role in cardiac precursor development (see below), *fgf8* is more specifically required in the ventricle of the zebrafish heart at later stages, since this is the most strongly affected structure in *acerebellar* embryos. This finding is consistent with the predominant expression of *fgf8* in the ventricle. In addition to *fgf8*, *fgf1*, *fgf7* and *fgf12* are reported to be expressed in a chamber-specific manner. Additional *fgfs* are expressed during heart development (*fgf2*, *4*, *13* and *16*) (Parlow et al., 1991; Spirito et al., 1991; Engelmann et al., 1993; Mason et al., 1994; Zhu et al., 1996; Hartung et al., 1997; Miyake et al., 1998). Although data concerning their function in heart development are lacking, the presence of these additional Fgfs may account for the variability of the *acerebellar* heart phenotype, since the other Fgfs might partially compensate for the lack of Fgf8. The stronger effect on *nkx2.5* expression in myocardial precursors of inhibitor-treated embryos compared to the expression in *acerebellar* mutants, and the loss of ventricular tissue after late inhibitor treatment are consistent with this possibility.

Our analysis of the vascular system in *acerebellar* mutants shows that the defect in circulation is largely, if not exclusively, due to the severely dysmorphic heart. This is consistent with the fact that *fgf8* is expressed during several stages of heart development. *fgf8* expression is closely associated with some or all heart precursor cells from blastula stage onwards and is later on expressed in the ventricle of the heart proper. Since Fgf8 is likely to be a secreted molecule (Baird, 1994; Fernig and Gallagher, 1994; Fürthauer et al., 1997; Reifers et al., 1998), it may very well function in signaling processes in the

heart mesoderm. Consistent with this possibility, the Fgf receptors *fgfr1*, *fgfr2* and *fgfr4* are expressed during vertebrate heart development (Orr-Urtreger et al., 1991; Peters et al., 1992; Sugi et al., 1995; Thisse et al., 1995). Functional inactivation of the four mouse Fgf receptors causes either no heart phenotype or results in early embryonic lethality preventing analysis of heart development (Yamaguchi et al., 1991; Deng et al., 1994; Arman et al., 1995; Colvin et al., 1996; Weinstein et al., 1998). Our study predicts that Fgfrs probably also function in heart development, possibly in a redundant fashion. In vitro binding studies of Fgf8 protein to Fgfrs suggest Fgfr3 and Fgfr4 as the most likely candidates (MacArthur et al., 1995; Ornitz et al., 1996; Blunt et al., 1997).

Fgf8 requirement for initiation of cardiac gene expression

Our results demonstrate that Fgf8 is necessary for initiation of cardiac gene expression, since the onset and early expression of *gata4*, *nkx2.5* and, less severely, *nkx2.7* in the heart precursor field are affected in *acerebellar* mutant embryos. *acerebellar* embryos also display minor defects in mesoderm during gastrulation (Reifers et al., 1998). These defects are however unlikely to account for the heart phenotype described here, since *fgf8* is expressed in and can function independently in the developing heart precursors. The results of our Fgf8 bead implantations and of the inhibitor treatment both argue that Fgf8 functions in the heart primordium independently of its expression in general endomesodermal precursors during gastrulation (Reifers et al., 1998). Fgf8 function is required for the expression of cardiac genes for different periods of time: from its onset at the tailbud/1 somite stage, *nkx2.7* is very transiently affected, whereas *gata4* and *nkx2.5* are strongly affected until mid- and late somitogenesis, respectively. After this early requirement, the expression recovers at least in the remaining heart cells of *acerebellar* mutants. This recovery most likely reflects functional redundancy with other Fgf family members at later stages in cardiac mesoderm. Recent studies in frog and mouse demonstrated that the *tinman*-related *Nkx* genes in vertebrates are essential for heart development (Grow and Krieg, 1998; Tanaka et al., 1999). In addition, it has been shown in vitro that GATA4 enhances cardiogenesis (Grepin et al., 1997). Since GATA4 may cooperate with Nkx2.5 in activating downstream cardiac genes, and since GATA4 can act as a transcriptional activator of cardiac *Nkx2.5* expression (Durocher et al., 1997; Durocher and Nemer, 1998; Searcy et al., 1998; Lien et al., 1999), it appears that these two transcription factors work within a transcriptional network to drive cardiac development. Since both factors are affected very early in *acerebellar* mutant embryos, we suggest that the failure of early myocardial *nkx2.5* and *gata4* expression may largely account for the severe malformation of the mutant hearts at later stages.

gata6, another cardiac transcription factor of the GATA family (Kelley et al., 1993; Heikinheimo et al., 1994; Laverriere et al., 1994; Jiang and Evans, 1996), is not affected in *acerebellar* mutants. *gata6* expression may therefore occur independently of Fgf signaling. The presence of *gata6*-positive cells also demonstrates that the failure to activate proper expression of *nkx2.7*, *nkx2.5* and *gata4* is not due to the absence of the cardiac precursors, a possibility that was raised by Fgf involvement in cell migration processes (Bodmer and Venkatesh, 1998; Sun et al., 1999).

Signaling events in the cardiac primordium

As the loss-of-function situation in *acerebellar* mutants clearly demonstrates, *gata4* expression is initially dependent on Fgf8 function. In addition, *fgf8* is sufficient to restore *gata4* expression in the endogenous domain. This suggests that Gata4 may be a target for Fgf8 signaling. Interestingly, however, *fgf8* RNA injections cannot restore *nkx2.5* expression, while a bead applied after gastrulation as a localized source for Fgf8 protein is able to do so. One possible explanation is that an additional factor is needed for proper *nkx2.5* expression, which might have become delocalized or suppressed by the dorsalizing effect that *fgf8* RNA overexpression has on the zebrafish gastrula (Fürthauer et al., 1997; Reifers et al., 1998). A candidate for this additional signal is BMP2, since BMP2-coated beads or BMP2-producing cells can induce *Nkx2.5* expression in chicken embryos (Schultheiss et al., 1997; Andrée et al., 1998). Previous exposure to BMP2 or another BMP signal in gastrulation could therefore be necessary for responsiveness of *nkx2.5* to Fgf8 induction. Our observation that *nkx2.5* expression is not restored by *fgf8* RNA injections into *acerebellar* mutants is consistent with this possibility, since *fgf8* overexpression during gastrulation suppresses *bmp2* expression (Fürthauer et al., 1997), thereby eliminating the required second signal at early stages. In Fgf8 bead implanted embryos, *bmp2* expression in gastrulation is not affected due to the later stage of implantation, hence allowing rescue of *nkx2.5* expression (Fig. 4E).

Several lines of evidence suggest a role for BMP2 in cardiogenesis. (i) *BMP2* is expressed close to precardiac mesoderm and later on in the heart (Lyons et al., 1989, 1990; Schultheiss et al., 1997; Nikaido et al., 1997; Andrée et al., 1998). *BMP2* mutant embryos show cardiac defects, and a subset of the *BMP2* mutant embryos does not express *Nkx2.5*. BMP2 may therefore be directly required for cardiogenesis, although the alternative possibility that the heart abnormalities are secondary to altered patterning of the gastrula cannot yet be ruled out (Hogan, 1996; Zhang and Bradley, 1996; Kishimoto et al., 1997). (ii) The *Nkx2.5* heart enhancer contains partial consensus sequences for the Smad transducers of BMP signaling. Although this element also contains GATA binding sites that are required for expression (Searcy et al., 1998; Lien et al., 1999), they cannot be sufficient since Fgf8-driven *gata4* expression does not restore *nkx2.5* expression in *acerebellar* embryos. (iii) The general idea that *Nkx2.5* expression is regulated by the BMP pathway is also suggested by *Drosophila* studies (Frasch, 1995). (iv) In vertebrates, Lough et al. (1996) demonstrated in vitro that the combined action of BMP2 and FGF4, but neither factor alone, promotes cardiogenesis in non-precardiac mesodermal explants. Taken together, these data and our observations suggest that Bmp2 may be the second signal needed and that Fgf8 cooperates with Bmp signals to initiate cardiogenesis (Fig. 4H). A similar, but antagonistic cooperation between FGF and BMP signals has been suggested to occur in tooth development (Neubüser et al., 1997).

Interestingly, Fgf8 may be differentially required for the expression of *nkx2.5*. The caudal part of the *nkx2.5* expression appears to be more dependent on functional Fgf8 than the

rostral part, since this caudal subdomain is always affected more strongly in *acerebellar* mutants. These cells contribute to the otic vesicle (Serbedzija et al., 1998), which also shows malformations in *acerebellar* mutants (Brand et al., 1996; S. Léger and M. B., unpublished). The anterior notochord has been shown to produce an inhibitory effect on the caudal-most *nkx2.5* expression (Goldstein and Fishman, 1998), and the possible differential requirement for Fgf8 in this domain suggests that Fgf8 may counteract this inhibitory signal from the notochord in wild-type embryos. This idea is further supported by our Fgf8 bead implantations into wild-type embryos, which result in a caudal extension of *nkx2.5* expression. The same expansion can also be observed in *ntl* mutants lacking a normal notochord, or after notochord ablation in wild-type embryos (Goldstein and Fishman, 1998). Thus, in this circumstance an Fgf signal, probably Fgf8, is even sufficient to activate *nkx2.5* expression in a longitudinal domain of the lateral plate mesoderm.

The involvement of Bmp and Fgf signals in cardiac induction may provide an explanation for the ability of the heart precursor field to regulate itself after laser ablation (Serbedzija et al., 1998), since non-ablated cells in the lateral plate mesoderm, which usually would not give rise to heart tissue, may now be driven into cardiac fate by the inductive signals they receive. Since *fgf8* continues to be expressed in the heart, it may well perform, apart from its role in induction of early gene expression in heart precursors, additional functions in development of the heart, e.g. in polarization or control of proliferation, as has been proposed for other tissues (Picker et al., 1999). Human *fgf8* mutations are not yet known, but given our findings it is conceivable that heart disease would be among the symptoms.

We thank members of the Brand and Stainier labs for discussion, Wieland B. Huttner, Jeremy Garwood and Deborah Yelon for comments on the manuscript, Heike Böhli for excellent technical assistance, Alexander Picker for help with confocal microscopy, Bernadette Fouquet for the microangiography protocol, Frank Stockdale for the gift of S46 antibody, and Shantha Shanmugalingam for help with the inhibitor protocol. This work was supported by grants from the Deutsche Forschungsgemeinschaft (SFB317) and the Förderprogramm Neurobiologie Baden-Württemberg (to M. B.), a HHMI predoctoral fellowship to E. C. W., and grants from the American Heart Association, the NIH and the Packard foundation (to D. Y. R. S.).

REFERENCES

Amaya, E., Musci, T. J. and Kirschner, M. W. (1991). Expression of a dominant negative mutant of the FGF receptor disrupts mesoderm formation in Xenopus embryos. *Cell* **66**, 257-270.

Andrée, B., Duprez, D., Vorbusch, B., Arnold, H.-H. and Brand, T. (1998). BMP-2 induces ectopic expression of cardiac lineage markers and interferes with somite formation in chicken embryos. *Mech. Dev.* **70**, 119-131.

Arman, E., Haffner-Krausz, R., Chen, Y., Heath, J. and Lonai, P. (1995). Targeted disruption of fibroblast growth factor (FGF) receptor 2 suggests a role for FGF signaling in pregastrulation mammalian development. *Proc. Natl. Acad. Sci. USA* **95**, 5082-5087.

Azpiazu, N. and Frasch, M. (1993). *tinman* and *bagpipe*: two homeobox genes that determine cell fates in the dorsal mesoderm of *Drosophila*. *Genes Dev.* **7**, 1325-1340.

Baird, A. (1994). Fibroblast growth factors: activities and significance of non-neurotrophin growth factors. *Curr. Opin. Neurobiol.* **4**, 78-86.

Beiman, M., Shilo, B.-Z. and Volk, T. (1996). Heartless, a *Drosophila* FGF receptor homolog, is essential for cell migration and establishment of several mesodermal lineages. *Genes Dev.* **10**, 2993-3002.

Blunt, A. G., Lawshé, A., Cunningham, M. L., Seto, M. L., Ornitz, D. M. and MacArthur, C. A. (1997). Overlapping expression and redundant activation of mesenchymal fibroblast growth factor (FGF) receptors by alternatively spliced FGF-8 ligands. *J. Biol. Chem.* **272**, 3733-3738.

Bodmer, R. (1993). The gene *tinman* is required for specification of the heart and visceral muscles in *Drosophila*. *Development* **118**, 719-729.

Bodmer, R. and Venkatesh, T. V. (1998). Heart development in *Drosophila* and Vertebrates: conservation of molecular mechanisms. *Dev. Genet.* **22**, 181-186.

Bour, B. A., O'Brien, M. A., Lockwood, W. L., Goldstein, E. S., Bodmer, R., Taghert, P. H., Abmayr, S. M. and Nguyen, H. T. (1995). *Drosophila* MEF2, a transcription factor that is essential for myogenesis. *Genes Dev.* **9**, 730-741.

Brand, M., Heisenberg, C.-P., Jiang, Y.-J., Beuchle, D., Lun, K., Furutani-Seiki, M., Granato, M., Haffter, P., Hammerschmidt, M., Kane, D. et al. (1996). Mutations in zebrafish genes affecting the formation of the boundary between midbrain and hindbrain. *Development* **123**, 179-190.

Brand, M. and Granato, M. (1999). Keeping and raising zebrafish. In *Zebrafish: a practical approach*. (ed. Nüsslein-Volhard, C. and Schulte-Merker, S.). IRL Press, Oxford.

Brand, T., Andrée, B., Schneider, A., Buchberger, A. and Arnold, H.-H. (1997). Chicken Nkx2-8, a novel homeobox gene expressed in early heart and foregut development. *Mech. Dev.* **64**, 53-59.

Chen, J.-N. and Fishman, M. C. (1996). Zebrafish *tinman* homolog demarcates the heart field and initiates myocardial differentiation. *Development* **122**, 3809-3816.

Cleaver, O. B., Patterson, K. D. and Krieg, P. A. (1996). Overexpression of the *tinman*-related genes *XNkx2.5* and *XNkx2.3* in *Xenopus* embryos results in myocardial hyperplasia. *Development* **122**, 3549-3556.

Colvin, J. S., Bohne, B. A., Harding, G. W., McEwen, D. G. and Ornitz, D. M. (1996). Skeletal overgrowth and deafness in mice lacking fibroblast growth factor receptor 3. *Nat. Genet.* **12**, 390-397.

Crossley, P. H. and Martin, G. R. (1995). The mouse Fgf8 gene encodes a family of polypeptides and is expressed in regions that direct outgrowth and patterning in the developing embryo. *Development* **121**, 439-451.

DeHaan, R. L. (1965). Morphogenesis of the Vertebrate Heart. New York: Holt, Rinehart and Winston.

Deng, C. X., Wynshaw-Boris, A., Shen, M. M., Daugherty, C., Ornitz, D. M. and Leder, P. (1994). Murine FGFR-1 is required for early postimplantation growth and axial organisation. *Genes Dev.* **8**, 3045-3057.

DeRuiter, M. C., Poelmann, R. E., VanderPlas-de Vries, I., Mentink, M. M. T. and Gittenberger-deGroot, A. C. (1992). The development of the myocardium and endocardium in mouse embryos. *Anat. Embryol.* **185**, 461-473.

Dono, R., Texido, G., Dussel, R., Ehmke, H. and Zeller, R. (1998). Impaired cerebral cortex development and blood pressure regulation in FGF-2-deficient mice. *EMBO J.* **17**, 4213-4225.

Dornseifer, P., Takke, C. and Campos-Ortega, J. A. (1997). Overexpresion of a zebrafish homologue of the *Drosophila* neurogenic gene *Delta* perturbs differentiation of primary neurons and somite development. *Mech. Dev.* **63**, 159-171.

Durocher, D., Charron, F., Warren, R., Schwartz, R. J. and Nemer, M. (1997). The cardiac transcription factors Nkx2-5 and GATA-4 are mutual cofactors. *EMBO J.* **16**, 5687- 5696.

Durocher, D. and Nemer, M. (1998). Combinatorial interactions regulating cardiac transcription. *Dev. Genet.* **22**, 250-262.

Edmondson, D. G., Lyons, G. E., Martin, J. F. and Olson, E. N. (1994). *Mef2* gene expression marks the cardiac and skeletal muscle lineages during mouse embryogenesis. *Development* **120**, 1251-1263.

Engelmann, G. L., Dionne, C. A. and Jaye, M. C. (1993). Acidic fibroblast growth factor and heart development. Role in myocyte proliferation and capillary angiogenesis. *Circ. Res.* **72**, 7-19.

Feldman, B., Poueymirou, W., Papaioannou, V. E., DeChiara, T. M. and Goldfarb, M. (1995). Requirement for FGF-4 for postimplantation mouse development. *Science* **267**, 246-249.

Fernig, D. G. and Gallagher, J. T. (1994). Fibroblast growth factors and their receptors: an information network controlling tissue growth, morphogenesis and repair. *Prog. Growth Factor Res.* **5**, 353-377.

Fishman, M. C. and Chien, K. R. (1997). Fashioning the vertebrate heart: earliest embryonic decisions. *Development* **124**, 2099-2117.

Fouquet, B., Weinstein, B. M., Serluca, F. C. and Fishman, M. C. (1997). Vessel patterning in the embryo of the zebrafish: guidance by notochord. *Dev. Biol.* **183**, 37-48.

Frasch, M. (1995). Induction of visceral and cardiac mesoderm by ectodermal DPP in the early *Drosophila* embryo. *Nature* **374**, 464-467.

Fürthauer, M., Thisse, C. and Thisse, B. (1997). A role for Fgf-8 in the dorsoventral patterning of the zebrafish gastrula. *Development* **124**, 4253-4264.

Gajewski, K., Kim, Y., Lee, Y. M., Olson, E. N. and Schulz, R. A. (1997). *D-mef2* is a target for Tinman activation during *Drosophila* heart development. *EMBO J.* **16**, 515-522.

Gisselbrecht, S., Skeath, J. B., Doe, C. Q. and Michelson, A. M. (1996). *heartless* encodes a fibroblast growth factor receptor (DFR1/DFGF-R2) involved in the directional migration of early mesodermal cells in the *Drosophila* embryo. *Genes Dev.* **10**, 3003-3017.

Goldstein, A. M. and Fishman, M. C. (1998). Notochord regulates cardiac lineage in zebrafish embryos. *Dev. Biol.* **201**, 247-252.

Grepin, C., Nemer, G. and Nemer, M. (1997). Enhanced cardiogenesis in embryonic stem cells overexpressing the GATA-4 transcription factor. *Development* **124**, 2387-2395.

Grow, M. W. and Krieg, P. A. (1998). Tinman function is essential for vertebrate heart development: elimination of cardiac differentiation by dominant inhibitory mutants of the *tinman*-related genes, *XNkx2.3* and *XNkx2.5*. *Dev. Biol.* **204**, 187-196.

Haffter, P., Granato, M., Brand, M., Mullins, M. C., Hammerschmidt, M., Kane, D. A., Odenthal, J., van Eeden, F. J. M., Jiang, Y.-J., Heisenberg, C.-P. et al. (1996). The identification of genes with unique and essential functions in the development of the zebrafish, *Danio rerio*. *Development* **123**, 1-36.

Hartung, H., Feldman, B., Lovec, H., Coulier, F., Birnbaum, D. and Goldfarb, M. (1997). Murine FGF-12 and FGF-13: expression in embryonic nervous system, connective tissue and heart. *Mech. Dev.* **64**, 31-39.

Harvey, R. P. (1996). NK-2 homeobox genes and heart development. *Dev. Biol.* **178**, 203-216.

Heikinheimo, M., Scandrett, J. M. and Wilson, D. B. (1994). Localisation of transcription factor GATA-4 to regions of the mouse embryo involved in cardiac development. *Dev. Biol.* **164**, 361-373.

Hogan, B. L. M. (1996). Bone morphogenetic proteins in development. *Curr. Opin. Genet. Dev.* **6**, 432-438.

Jiang, Y. and Evans, T. (1996). The *Xenopus GATA4/5/6* genes are associated with cardiac specification and can regulate cardiac-specific transcription during embryogenesis. *Dev. Biol.* **174**, 258-270.

Johnson, D. E. and Williams, L. T. (1993). Structural and functional diversity in the Fgf receptor multigene family. *Adv. Cancer Res.* **60**, 1-41.

Kelley, C., Blumberg, H., Zon, L. I. and Evans, T. (1993). GATA-4 is a novel transcription factor expressed in endocardium of the developing heart. *Development* **118**, 817-827.

Kimmel, C. B., Ballard, W. W., Kimmel, S. R., Ullmann, B. and Schilling, T. F. (1995). Stages of embryonic development of the zebrafish. *Dev. Dyn.* **203**, 253-310.

Kishimoto, Y., Lee, K.-H., Zon, L., Hammerschmidt, M. and Schulte-Merker, S. (1997). The molecular nature of zebrafish *swirl*: BMP2 function is essential during early dorsoventral patterning. *Development* **124**, 4457-4466.

Komuro, I. and Izumo, S. (1993). *Csx*: a murine homeobox-containing gene specifically expressed in the developing heart. *Proc. Natl. Acad. Sci. USA* **90**, 8145-8149.

Kuo, C. T., Morrisey, E. E., Anandappa, R., Sigrist, K., Lu, M. M., Parmacek, M. S., Soudais, C. and Leiden, J. M. (1997). GATA4 transcription factor is required for ventral morphogenesis and heart tube formation. *Genes Dev.* **11**, 1048-1060.

Kuwada, J. Y., Bernhardt, R. R. and Chitnis, A. B. (1990). Pathfinding by identified growth cones in the spinal cord of zebrafish embryos. *J. Neurosci.* **10**, 1299-1308.

Laverriere, A. C., MacNeill, C., Mueller, C., Poelmann, R. E., Burch, J. B. E. and Evans, T. (1994). GATA-4/5/6: a subfamily of three transcription factors transcribed in the developing heart and gut. *J. Biol. Chem.* **269**, 23177-23184.

Lee, K.-H., Xu, Q. and Breitbart, R. E. (1996). A new *tinman*-related gene, *nkx2.7*, anticipates the expression of *nkx2.5* and *nkx2.3* in zebrafish heart and pharyngeal endoderm. *Dev. Biol.* **180**, 722-731.

Liao, W., Bisgrove, B. W., Sawyer, H., Hug, B., Bell, B., Peters, K., Grunwald, D. J. and Stainier, D. Y. R. (1997). The zebrafish gene cloche acts upstream of a flk-1 homologue to regulate endothelial cell differentiation. *Development* **124**, 319-389.

Lien, C.-L., Wu, C., Mercer, B., Webb, R., Richardson, J. A. and Olson, E. N. (1999). Control of early cardiac-specific transcription of *Nkx2-5* by a GATA-dependent enhancer. *Development* **126**, 75-84.

Lilly, B., Galewsky, S., Firulli, A. B., Schulz, R. A. and Olsone, E. N. (1994). D-MEF2: a MADS box transcription factor expressed in differentiating mesoderm and muscle cell lineages during *Drosophila* embryogenesis. *Proc. Natl. Acad. Sci. USA* **91**, 5662-5666.

Lilly, B., Zhao, B., Ranganayakulu, G., Paterson, B. M., R.A., S. and Olson, E. N. (1995). Requirement of MADS domain transcription factor D-MEF2 for muscle formation in *Drosophila*. *Science* **267**, 688-693.

Lin, Q., Schwarz, J., Bucana, C. and Olson, E. N. (1997). Control of mouse cardiac morphogenesis and myogenesis by transcription factor MEF-2C. *Science* **276**, 1404-1407.

Lints, T. J., Parsons, L. M., Hartley, L., Lyons, I. and Harvey, R. P. (1993). *Nkx-2.5*: a novel murine homeobox gene expressed in early heart progenitor cells and their myogenic descendants. *Development* **119**, 419-431.

Lough, J., Barron, M., Brogley, M., Sugi, Y., Bolender, D. L. and Zhu, X. (1996). Combined BMP-2 and FGF-4, but neither factor alone, induces cardiogenesis in non-precardiac embryonic mesoderm. *Dev. Biol.* **178**, 198-202.

Lyons, G. E. (1996). Vertebrate heart development. *Curr. Opin. Genet. Dev.* **6**, 454-460.

Lyons, I., Parsons, L. M., Hartley, L., Li, R., Andrews, J. E., Robb, L. and Harvey, R. P. (1995). Myogenic and morphogenetic defects in the heart tubes of murine embryos lacking the homeobox gene *Nkx2.5*. *Genes Dev.* **9**, 1654-1666.

Lyons, K. M., Pelton, R. W. and Hogan, B. L. M. (1989). Patterns of expression of murine *Vgr-1* and BMP-2a RNA suggest that transforming growth factor-b-like genes coordinately regulate aspects of embryonic development. *Genes Dev.* **3**, 1657-1668.

Lyons, K. M., Pelton, R. W. and Hogan, B. L. M. (1990). Organogenesis and pattern formation in the mouse: RNA distribution patterns suggest a role for Bone Morphogenetic Protein-2A (BMP-2A). *Development* **109**, 833-844.

MacArthur, C. A., Lawshe, A., Xu, L., Santos-Ocampo, S., Heikinheimo, M., Chellaiah, A. T. and Ornitz, D. M. (1995). FGF-8 isoforms activate receptor splice forms that are expressed in mesenchymal regions of mouse development. *Development* **121**, 3603-3613.

Mason, I. J., Fuller-Pace, F., Smith, R. and Dickson, C. (1994). FGF-7 (keratinocyte growth factor) expression during mouse development suggests roles in myogenesis, forebrain regionalisation and epithelial-mesenchymal interactions. *Mech. Dev.* **45**, 15-30.

Meyers, E. N., Lewandowski, M. and Martin, G. R. (1998). An Fgf8 mutant allelic series generated by Cre- and Flp-mediated recombination. *Nat. Genet.* **18**, 136-142.

Michelson, A. M., Gisselbrecht, S., Buck, K.-H. and Buff, E. M. (1998). Dual functions of the heartless fibroblast growth factor receptor in the development of *Drosophila* embryonic mesoderm. *Dev. Genet.* **22**, 212-229.

Miyake, A., Konishi, M., Martin, F. H., Hernday, N. A., Ozaki, K., Yamamoto, S., Mikami, T., Arakawa, T. and Itoh, N. (1998). Structure and expression of a novel member, FGF-16, of the fibroblast growth factor family. *Biochem. Biophys. Res. Commun.* **243**, 148-152.

Mohammadi, M., McMahon, G., Sun, L., Tang, C., Hirth, P., Yeh, B. K., Hubbard, S. R. and Schlessinger, J. (1997). Structures of the tyrosine kinase domain of fibroblast growth factor receptor in complex with inhibitors. *Science* **276**, 955-960.

Mohun, T. and Sparrow, D. (1997). Early steps in vertebrate cardiogenesis. *Curr. Opin. Genet. Dev.* **7**, 628-633.

Molkentin, J. D., Firulli, A. B., Black, B. L., Martin, J. F., Hustad, C. M., Copeland, N., Jenkins, N., Lyons, G. and Olson, E. N. (1996). *MEF2B* is a potent *trans*activator expressed in early myogenic lineages. *Mol. Cell Biol.* **16**, 3814-3824.

Molkentin, J. D., Lin, Q., Duncan, S. A. and Olson, E. N. (1997). Requirement of the transcription factor GATA4 for heart tube formation and ventral morphogenesis. *Genes Dev.* **11**, 1061-1072.

Narita, N., Bielinska, M. and Wilson, D. B. (1997a). Cardiomyocyte differentiation by GATA-4-deficient embryonic stem cells. *Development* **124**, 3755-3764.

Narita, N., Bielinska, M. and Wilson, D. B. (1997b). Wild-type endoderm abrogates the ventral developmental defects associated with GATA-4 deficiency in the mouse. *Dev. Biol.* **189**, 270-274.

Neubüser, A., Peters, H., Balling, R. and Martin, G. R. (1997). Antagonistic

interactions between FGF and BMP signaling pathways: a mechanism for positioning the sites of tooth formation. *Cell* **90**, 247-255.

Nikaido, M., Tada, M., Saji, T. and Ueno, N. (1997). Conservation of BMP signaling in zebrafish mesoderm patterning. *Mech. Dev.* **61**, 75-88.

Olson, E. L., Perry, M. and Shultz, R. A. (1995). Regulation of muscle differentiation by the MEF2 family of MADS box transcription factors. *Dev. Biol.* **172**, 2-14.

Olson, E. N. and Srivastava, D. (1996). Molecular pathways controlling heart development. *Science* **272**, 671-676.

Ornitz, D. M., Xu, J., Colvin, J. S., McEwen, D. G., MacArthur, C. A., Coulier, F., Gao, G. and Goldfarb, M. (1996). Receptor specificity of the fibroblast growth factor family. *J. Biol. Chem.* **271**, 15292-15297.

Orr-Urtreger, A., Givol, D., Yayon, A., Yarden, Y. and Lonai, P. (1991). Developmental expression of two murine fibroblast growth factor receptors, *flg* and *bek*. *Development* **113**, 1419-1434.

Parlow, M. H., Bolender, D. L., Kokan-Moore, N. P. and Lough, J. (1991). Localization of bFGF-like proteins as punctate inclusions in the preseptation myocardium of the chicken embryo. *Dev. Biol.* **146**, 139-147.

Peters, K. G., Werner, S., Chen, G. and Williams, L. T. (1992). Two FGF receptor genes are differentially expressed in epithelial and mesenchymal tissues during limb formation and organogenesis in the mouse. *Development* **114**, 233-243.

Picker, A., Brennan, C., Reifers, F., Clarke, J., Holder, N. and Brand, M. (1999). Requirement for the zebrafish mid-hindbrain boundary in midbrain polarisation, mapping and confinement of the retinotectal projection. *Development* **126**, 2967-2978.

Reifers, F., Böhli, H., Walsh, E. C., Crossley, P. H., Stainier, D. Y. R. and Brand, M. (1998). *Fgf8* is mutated in zebrafish *acerebellar(ace)* mutants and is required for maintenance of midbrain-hindbrain boundary development and somitogenesis. *Development* **125**, 2381-2395.

Rupp, R. A. W., Snider, L. and Weintraub, H. (1994). Xenopus embryos regulate the nuclear localization of XMyoD. *Genes Dev.* **8**, 1311-1323.

Schultheiss, T. M., Burch, J. B. E. and Lassar, A. B. (1997). A role for bone morphogenetic proteins in the induction of cardiac myogenesis. *Genes Dev.* **11**, 451-462.

Searcy, R. D., Vincent, E. B., Liberatore, C. M. and Yutzey, K. E. (1998). A GATA-dependent *nkx-2.5* regulatory element activates early cardiac gene expression in transgenic mice. *Development* **125**, 4461-4470.

Serbedzija, G. N., Chen, J.-N. and Fishman, M. C. (1998). Regulation in the heart field of zebrafish. *Development* **125**, 1095-1101.

Spirito, P., Fu, Y. M., Yu, Z. X., Epstein, S. E. and Casscells, W. (1991). Immunohistochemical localization of basic and acidic fobroblast growth factors in the developing rat heart. *Circulation* **84**, 322-332.

Srivastava, D., Cserjesi, P. and Olson, E. N. (1995). A subclass of bHLH proteins required for cardiac morphogenesis. *Science* **270**, 1995-1999.

Stainier, D. Y. R. and Gilbert, W. (1990). Pioneer neurons in the mouse trigeminal sensory system. *Proc. Natl. Acad. Sci. USA* **87**, 923-927.

Stainier, D. Y. R. and Fishman, M. C. (1992). Patterning the zebrafish heart tube: Acquisition of anteroposterior polarity. *Dev. Biol.* **153**, 91-101.

Stainier, D. Y. R., Lee, R. K. and Fishman, M. C. (1993). Cardiovascular development in the zebrafish. *Development* **119**, 31-40.

Sugi, Y. and Lough, J. (1995). Activin-A and FGF-2 mimic the inductive effects of anterior endoderm on terminal cardiac myogenesis *in vitro*. *Dev. Biol.* **168**, 567-574.

Sugi, Y., Sasse, J., Barron, M. and Lough, J. (1995). Developmental expression of fibroblast growth factor receptor-1 (*cek: flg*) during heart development. *Dev. Dyn.* **202**, 115-125.

Sun, X., Meyers, E. N., Lewandowski, M. and Martin, G. R. (1999). Targetede disruption of *Fgf8* causes failure of cell migration in the gastrulating mouse embryo. *Genes Dev.* **13**, 1834-1846.

Tanaka, M., Chen, Z., Bartunkova, S., Yamasaki, N. and Izumo, S. (1999). The cardiac homeobox gene *Csx/Nkx2.5* lies genetically upstream of multiple genes essential for heart development. *Development* **126**, 1269-1280.

Thisse, B., Thisse, C. and Weston, J. A. (1995). Novel FGF receptor (Z-FGFR4) is dynamically expressed in mesoderm and neurectoderm during early zebrafish embryogenesis. *Dev. Dyn.* **203**, 377-391.

Ticho, B. S., Stainier, D. Y. R., Fishman, M. C. and Breitbart, R. E. (1996). Three zebrafish MEF2 genes delineate somitic and cardiac muscle development in wild-type and mutant embryos. *Mech. Dev.* **59**, 205-218.

Warga, R. M. and Kimmel, C. B. (1990). Cell movements during epiboly and gastrulation in zebrafish. *Development* **108**, 569-580.

Weinstein, B. M., Stemple, D. L., Driever, W. and Fishman, M. C. (1995). *gridlock*, a localized heritable vascular patterning defect in the zebrafish. *Nat. Med.* **1**, 1143-1147.

Weinstein, M., Xu, X., Ohyama, K. and Deng, C.-X. (1998). FGFR-3 and FGFR-4 function cooperatively to direct alveogenesis in the murine lung. *Development* **125**, 3615-3623.

Westerfield, M. (1994). *The Zebrafish Book*. Oregon: University of Oregon Press.

Yamaguchi, T. P., Harpal, K., Henkemeyer, M. and Rossant, J. (1991). fgfr-1 is required for embryonic growth and mesodermal patterning during mouse gastrulation. *Genes Dev.* **8**, 3032-3044.

Zhang, H. and Bradley, A. (1996). Mice deficient for BMP2 are nonviable and have defects in amnion/chorion and cardiac development. *Development* **122**, 2977-2986.

Zhu, X., Sasse, J., McAllister, D. and Lough, J. (1996). Evidence that fibroblast growth factors 1 and 4 participate in regulation of cardiogenesis. *Dev. Dyn.* **207**, 429-438.

Appendix 5: Analysis of BMP pathway mutant heart phenotypes: *lost-a-fin* and *snailhouse* mutations

lost-a-fin (*laf*) is a mutation in the zebrafish homologue of the *alk8* gene which encodes a Bmp receptor.[67,68] Mutants display heart fusion defects as seen by *cmlc in situ* hybridization analysis at 22 hpf (Fig. 27 A, D). *bmp4* expression at 36 hpf reveals pharyngeal endoderm dysmorphology in this mutant as the field of *bmp4* positive cells does not extend anteriorly (B, E) or posteriorly (C, F) to the normal extent. MF20 S46 immunofluorescence at 48 hpf reveals grossly dysmorphic hearts, likely results from the earlier fusion delays. As mutant hearts exhibit defects at early steps in heart development, the role of *laf* in AV boundary formation could not be properly assessed.

snailhouse (*snh*) is a variably expressive mutation in the zebrafish *bmp7* gene.[69,70] AV boundary formation appears normal in mildly affected mutant embryos (Fig. 28, compare wildtype (A) to mutant (B-E), arrows indicate boundary). However, in class IV *snh* mutants (F) the boundary appears less well-formed. This may suggest a role for Bmp7 in AV boundary induction or simply reflect earlier defects in general heart induction in these severely affected embryos. I favor the latter hypothesis as the mutant heart (F) does appear to be much smaller than normal. However recent work on *bmp5*/*bmp7* double knockouts implicates these genes in both trabeculation and AV cushion formation.[71]

Figure 27

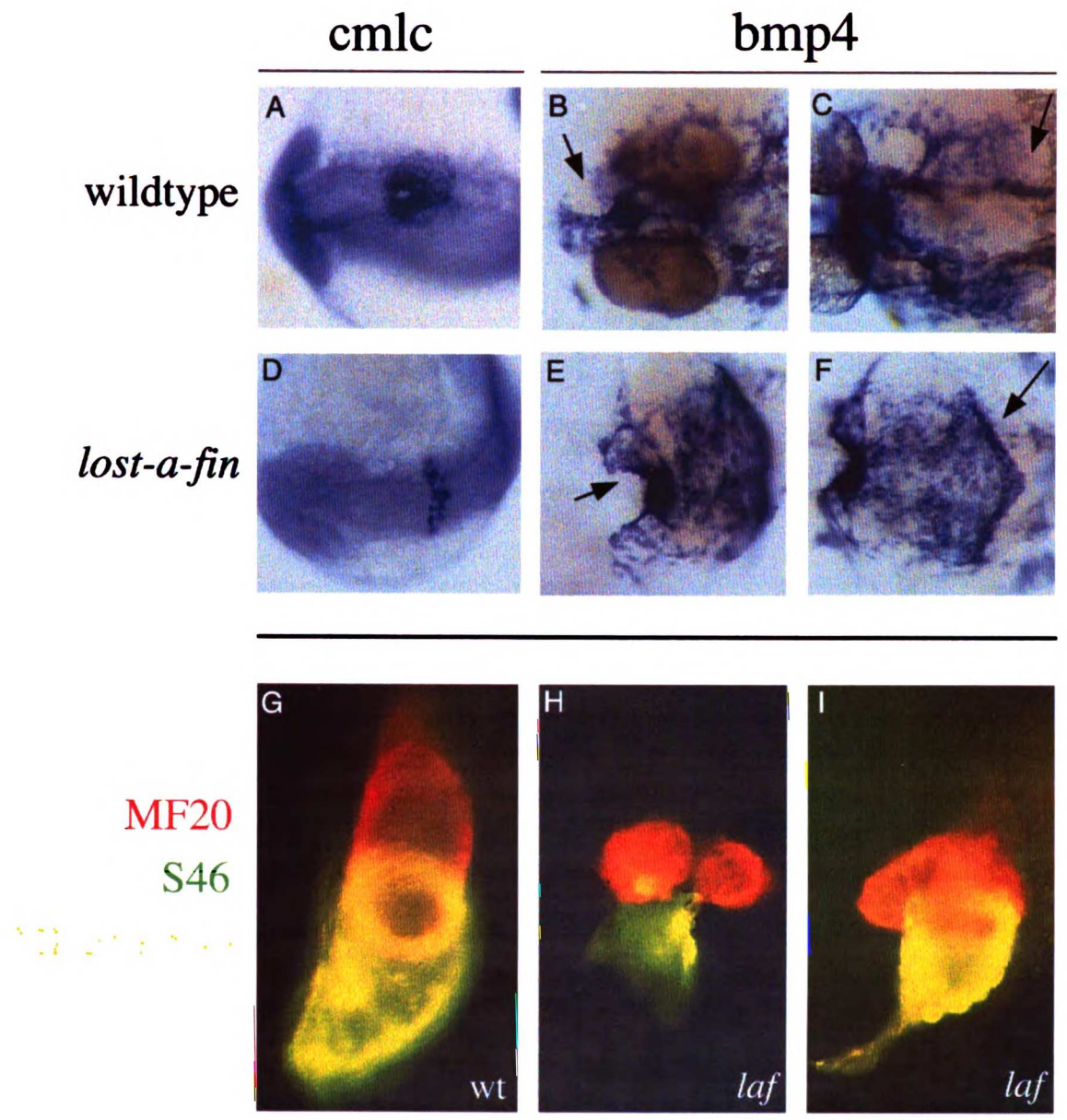

Figure 28

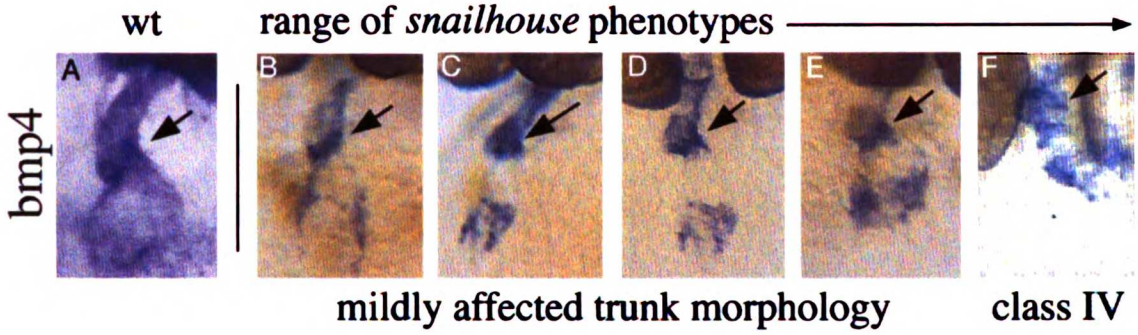
wt
range of *snailhouse* phenotypes
bmp4
A
B
C
D
E
F
mildly affected trunk morphology
class IV

Appendix 6: RNA *in situ* analysis of zebrafish heart differentiation.

Figure 29. Analysis of potential AV boundary markers in zebrafish. (A-D) ***msxB***, ***msxC***, ***msxD***, and ***msxE*** all encode members of the Msx class of homeodomain proteins. Members of this class are reportedly expressed at the AV boundary in chick and mouse. ***msxB*** (A, lateral view) shows no apparent AV expression. ***msxC*** and ***msxD*** (B, C, ventral view) seem to have some expression in the heart although neither is strongly expressed. ***msxE*** (D, lateral view) may also be expressed, although again very lightly. (E, F) As first seen by J. Reiter (Reiter and Stainier, unpublished observations), ***serrateB*** is expressed in the AV boundary (lateral views). This expression is missing in ***jekyll*** mutant embryos. (G) ***bmpRIb*** is expressed myocardially throughout the anteroposterior extent of the heart as shown in this ***clo*** mutant embryo (ventral view). (H) ***notch5*** is reportedly expressed in the endocardium and myocardium at the valve however, this probe has never worked well (lateral view). (I) ***snail2*** (an orthologue of the chicken gene ***slug***) may be expressed at the boundary at 72 hpf, albeit lightly (ventral view). (J, K) ***br146***, a ***versican*** orthologue, is expressed throughout the heart at 24 hpf and then becomes restricted to the boundary by 48 hpf. At 48 hpf, it is also expressed in the distal fin bud and in the semicircular canals of the otic vesicle (lateral views). (L, M) ***fibulin-1*** is also expressed in the myocardial AV boundary, becoming restricted after 38 hpf and before 48 hpf. This restriction occurs after the ***bmp4*** myocardial expression becomes restricted at 36 hpf (ventral views). (N-P) ***h15*** is expressed throughout the anteroposterior extent of the heart at all stages examined (ventral views). (Q) Frank Reifers first noted that ***nkx2.5*** is restricted to the AV boundary at 48 hpf, this is an example of his ***in situ*** hybridization experiment (lateral view). (R, S) My efforts to repeat this result have not shown the

expression as cleanly however there may be some heightened expression at the boundary that is missing in *cloche* mutants (ventral views). (T-V) Frank also noted *gata6* restriction (data not shown) however I could never repeat that result (ventral views). In all cases arrows indicate the AV boundary.

Figure 30. (A-H) A time course of *notch1b* expression in wt and *jekyll* mutants. notch1b restriction occurs sometime between 42 hpf (C, D) and 45 hpf (G) in wildtype and fails to occur in the *jekyll* mutant (H).

Figure 29

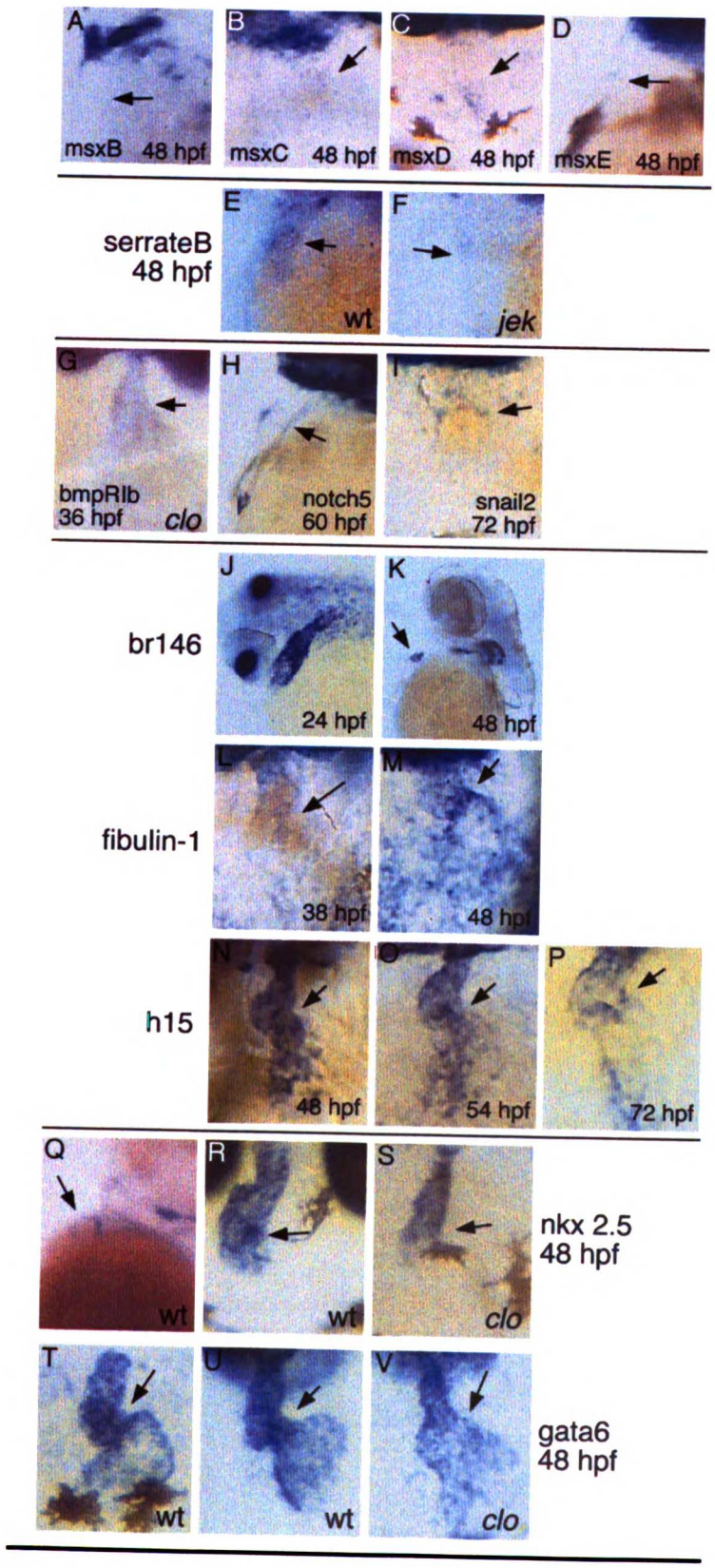
A
msxB 48 hpf
B
msxC 48 hpf
C
msxD 48 hpf
D
msxE 48 hpf
serrateB
48 hpf
E
wt
F
jek
G
bmpRIb
36 hpf
clo
H
notch5
60 hpf
I
snail2
72 hpf
br146
J
24 hpf
K
48 hpf
fibulin-1
L
38 hpf
M
48 hpf
h15
N
48 hpf
O
54 hpf
P
72 hpf
Q
wt
R
wt
S
clo
nkx 2.5
48 hpf
T
wt
U
wt
V
clo
gata6
48 hpf

Figure 30

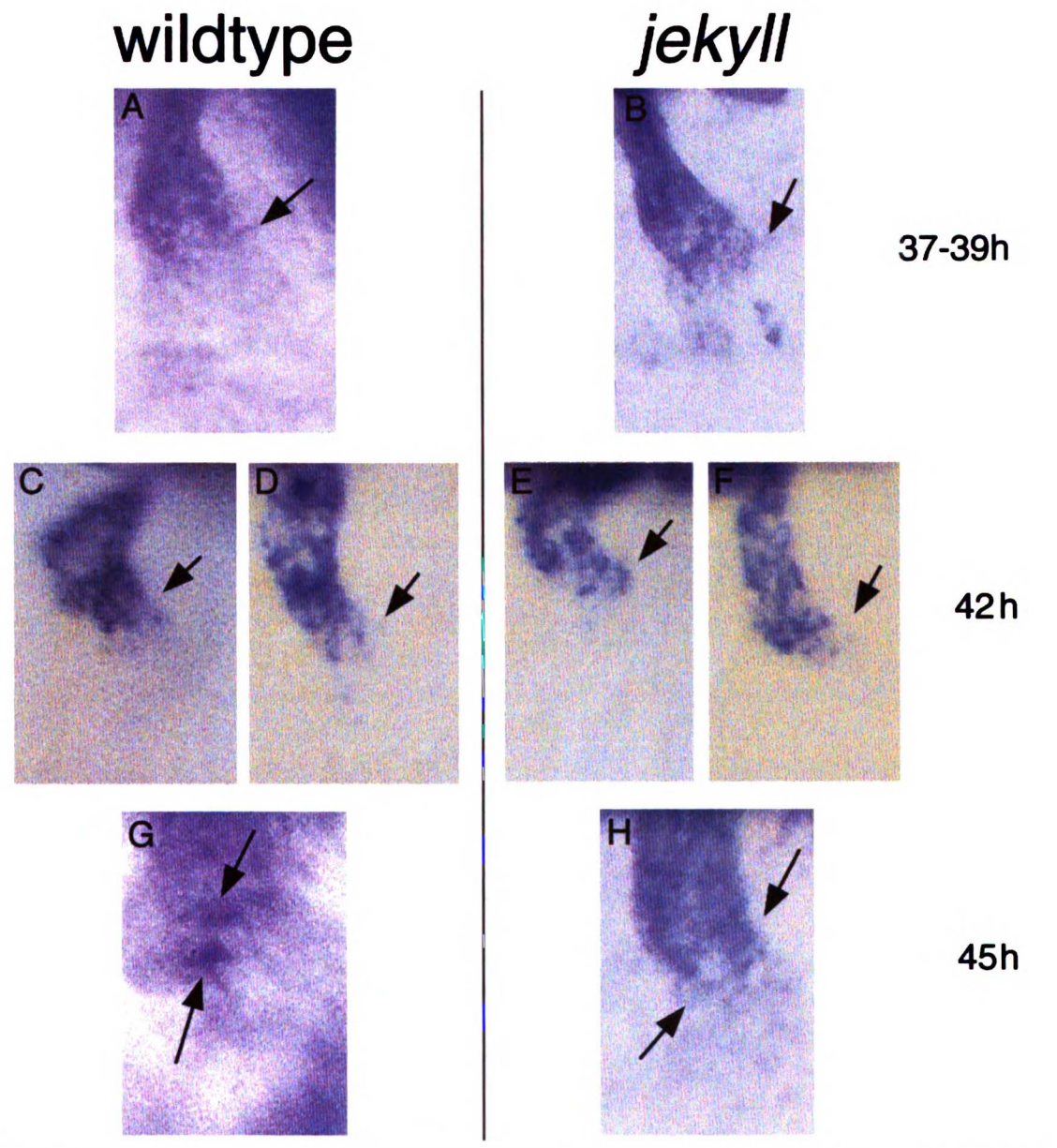

Appendix 7: Analysis of TC2 antibody staining of *jekyll* and *cardiofunk* mutant embryos

TC2 antibody detects a glycosaminoglycan attachment site on some proteoglycans.[72] The colocalization of TC2 staining and anti-Versican antibodies in early chick development suggests that the chondroitin sulfate proteoglycan is at least one of the targets of the TC2 antibody. The general absence of TC2 staining in *hdf* mice which are homozygous for insertions in *versican*, is further evidence that TC2 recognizes Versican.

Here I show that TC2 antibody does crossreact with fish proteins and that consistent with its role in chondroitin glycosaminoglycan production, *jekyll* mutant embryos fail to stain with TC2 (Fig. 31). Wildtype (A) and *jekyll* mutant (B) hearts at 48 hpf, note the absence of staining in the mutant ventricle compared to wildtype (arrows indicate ventricle). At this stage TC2 epitope is present throughout the heart however ventricular levels appears higher.

Later, staining is observed in the branchial arches (C, high magnification of wildtype arches at 4 dpf, arrow indicates first arch). This staining is absent in the *jekyll* mutant (compare E with wildtype embryo in D) but unaffected in cardiofunk mutants (F) consistent with the observation that alcian staining is unaffected in this mutant (Walsh, data not shown).

Figure 31

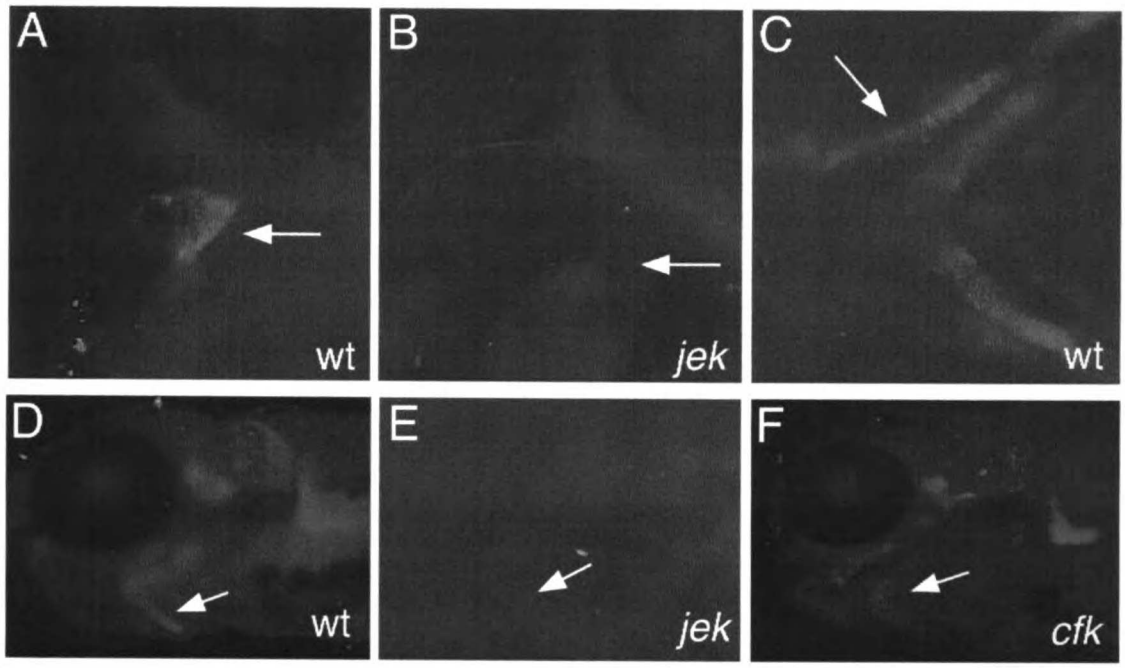

Appendix 8: Attempts to establish a binary system in zebrafish.

My initial project in the Stainier lab was the creation of a transgenic binary system for tissue specific misexpression in order to assess the role of Bmp4 in heart development. I began this by testing for transient transactivation through coinjections of RNAs encoding either Lac repressor or Gal4 based transactivator proteins and their appropriate reporter constructs. These experiments pointed toward a LacVP16 based misexpression system as the Gal4 construct tried never elicited reporter expression (this was later shown to be a problem with the transactivator construct I had been working with).

After completing these first experiments, I set out to create a myocardially expressing *lac-vp16* construct using the Xenopus alpha cardiac actin promoter[73] (a kind gift of Dan Weeks, University of Iowa). Injection of a linearized version of this DNA construct into single cell embryos was performed. About 100 F_0 founders were raised to adulthood and intercrossed to PCR identify those with germline transmission. Sixteen founders had transgenic germlines and of those four expressed the *lacvp16* gene as assessed by RNA in situ hybridization. One of the expressing transgenics had low levels of heart restricted expression of *lacvp16*. The remaining three had much more ubiquitous expression patterns.

A dual-specifity reporter (UL1- for UAS/Lac Binding site-1) was created for the system so that it might be used in concert with LacVP16 and Gal4 expressing lines. Embryos were injected, raised to adulthood, and identified by PCR. However no intercross of the *lacvp16* transgenics with the reporter transgenics ever yielded reporter gene expression. It was later shown by N. Osborne that a CA expansion had occurred in

the minimal promoter (the mouse *wnt1* minimal) of the reporter construct (Osborne and Stainier, unpublished observations). This is likely why no transactivation was ever observed in the transgenics.

As most laboratories are now employing Gal-based systems, the *lacvp16* and *ul1* transgenics have been sacrificed. Currently, as detailed in chapter 3, work in the Stainier lab focused on constructing a Gal4VP16 based system for misexpression experiments in the endocardial and myocardial cell layers.

Appendix 9: Comparison of wildtype and *jekyll notch1b* neural expression at 36 and 48 hpf. Figure 32. *notch1b* appears to be expressed more broadly in the developing rhombomeres of *jekyll* (B, D) mutant embryos than wildtype (A, C). While these data required further confirmation and genotyping analysis, they suggest that *jekyll* may be required for neural development.

Figure 32

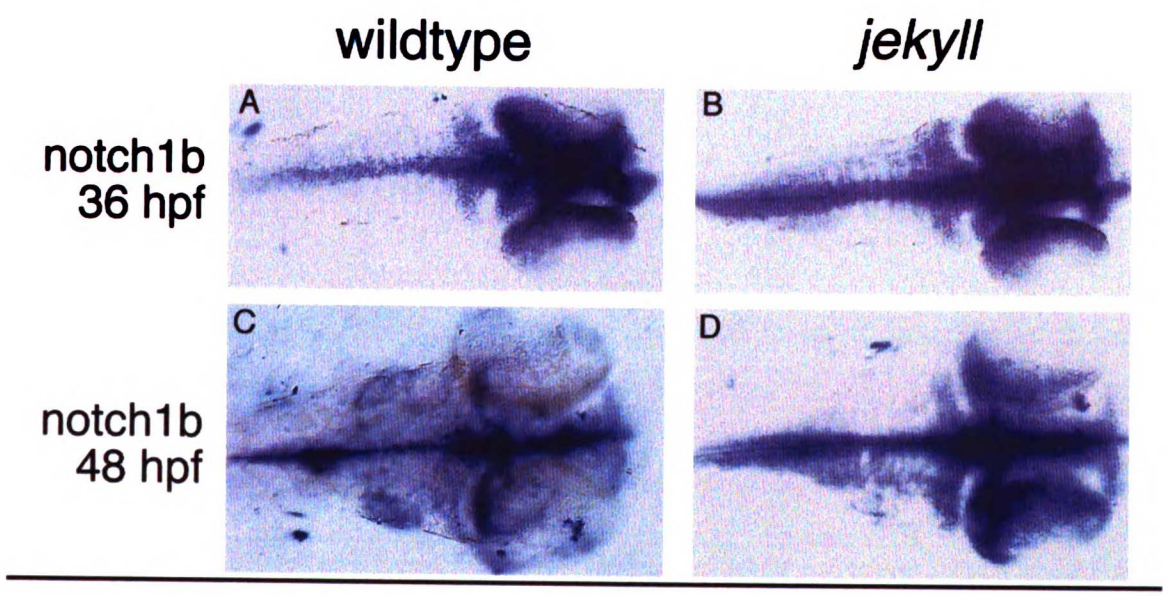

Appendix 10. Future Directions.

There are three main veins of experimentation that arise as a result of the work presented in this thesis:

1) exploration of the role of Neuregulin in the process of valve formation (chapter 3--pgs. 47-51, Fig. 20)
2) determination of the cell autonomy of the *jekyll* mutation and relative contribution of HA and proteoglycans in the process (chapter 3--pg 51 and appendix3 respectively)
3) further analysis of the role of *snailhouse* in AV boundary formation (chapter 3--pg. 47, appendix 5)

These are discussed at length in the text and will not be revisited here. There are, however, a number of interesting subquestions not considered thus far in this text which will be explored here.

The first and perhaps most interesting subquestion is the nature of the *cardiofunk/jekyll* genetic interaction. If, as *bmp4* expression analysis of single mutants suggests, *cardiofunk* acts downstream or in parallel to the *jekyll* mutation, why do these two mutations fail to complement? This question can be answered simply by examining the expression of valve restricted genes (*bmp4*, *notch1b*, *fibulin*) in double heterozygous embryos. There are multiple possible outcomes. If the double heterozygous embryo has the same *bmp4* expression as a *cardiofunk* mutant, this may suggest that *jekyll* has multiple sequential roles in valve formation, one of which involves the pathway in which cardiofunk acts. This would be the most exciting result as it would mean that sensitized screening using the *jekyll* background might be able to isolate mutations in multiple pathways functioning sequentially at the AV boundary to establish valve formation. If,

however, the double heterozygous embryo has the same *bmp4* expression as a *jekyll* mutant, interpretation of this result might be much more difficult. This finding would suggest that cardiofunk might act at multiple steps but is only absolutely required at a post *bmp4*-restriction step. In either case, this simple experiment will certainly shed more light on the process of AV boundary formation.

This approach can also be applied to another, as yet unnamed, second site interactor I recovered from the *jekyll* map cross. This mutation was determined to be second site as affected embryos show no apparent alcian staining defects. While it is still possible that this mutation lies in the *cardiofunk* gene, if it does not, analysis of double heterozygotes will add yet more depth to our understanding of valve formation. Tom Bartman is now performing complementation testing of this mutation with *cardiofunk*.

It will also be interesting to analyze the roles of Bmp and Notch signalling in AV valve formation. Simple approaches to this will be injection of embryos with morpholinos targeting *bmp4*, *notch1b*, and *serrateB*. Gain-of-function and dominant loss-of-function experiments examining the roles of these signalling pathways will be easily executed with the creation of the GalVP16 misexpression system detailed in chapter 3. For instance, endocardial expression of the activated *notch*-intra domain will help to determine if the AV boundary endocardial clustering that correlates with upregulation of *notch1b* expression is a result of increased *notch* signalling. Also comparison of dominant negative Bmp receptor expression in endocardium versus myocardium will help to determing whether Bmp4 signals in an autocrine or paracrine fashion.

Lastly, much attention needs to be directed toward determining the role of *jekyll* in muscularization/trabeculation of the ventricle. It will be interesting to determine if the late (3 dpf) toggling phenotypes that develop in some *has2*-morpholino injected embryos (appendix 3), as well as some of the novel mutations being isolated by Benno Jungblut and Suk-won Jin as part of the Baier screen, represent a trabeculation defect phenotype occuring in the absence of defects in atrioventricular valve development. If so, it is possible that *jekyll* may be playing separable roles in the ventricle and valve. Currently I favor a single role for *jekyll* in a ventricular differentiation step that is required for both trabeculation and AV boundary establishment. However, it is still formally possible that there are two separate functions: a potentially HA-dependent trabeculation role, and a separate role in differentiation of the AV boundary. Transient rescue experiments with myocardial and endocardially expressed GalVP16; UAS-*ugdh* constructs may help to tease this apart. Transient experiments would provide expression of *ugdh* in discrete domains of the heart which may reveal sublocalized requirement of Ugdh function for specific aspects of the *jekyll* phenotype. If Ugdh function in the valve is spatially distinct from its function in the ventricle, it would be consistent with the possibility that Ugdh is required in two separate signalling events in the heart. However this evidence would only be correlative, more definitive experiments would include analysis of genetic interaction between *jekyll* and mutations that result in trabeculation defects.

As is apparent in many of the remaining questions listed here and in the text, there are three approaches that will be invaluable in future study: further screening to isolate additional mutations affecting these processes, molecular epistasis and characterization of those mutant phenotypes, and perhaps most importantly, the establishment of a GalVP16

misexpression system to detail the cell autonomy and signaling direction of implicated signaling pathways between the endocardial and myocardial layers of the heart. These combined techniques are what sets analysis of the zebrafish heart apart from analysis of more embryologically manipulable hearts like those in mouse and chick. These approaches allow zebrafish researchers to answer, in a more molecularly definitive fashion, the various and plentiful remaining questions regarding late heart morphogenesis.

Reagents and Methods

Zebrafish strains and studies

Zebrafish were maintained and staged as described [74]. One allele of jekyll (m151) was obtained from Mark Fishman (MGH) and used for these studies. Strains bearing *tie2*-GFP[46] were created by crossing of a *tie2*-GFP hemizygote with a *jekyll* heterozygote. Phenylthiourea (Sigma) was used to inhibit pigmentation in some cases (0.003% w/v).

Sequencing

All sequencing was performed by the Genome Core Facility at UCSF.

Sequence, Mapping and Synteny Analysis

Analysis of all DNA sequence was performed using DNA Strider, BCM Search Launcher, NCBI Blast, Contig Analysis Program (CAP), Primer3 program, Webcutter 2.0, REBASE and Sequencing Analysis 3.3. Protein analysis used the above programs as well as SWISS-MODEL, and Rasmol.

Mapping was done with Map Manager 2.6.5 and Excel.

Synteny analysis between zebrafish and human was done using the Genome Database (GDB), OMIM, Stanford Zebrafish Genome Project database, Tubingen RH Map of the Zebrafish Genome, WashU-Zebrafish Genome Resourses, MGH Zebrafish WWW Server, ZFIN, and the Children's Hospital Zebrafish RH Map. Particularly helpful were GDB, Tubingen and Children's Hospital maps.

Linkage analysis, mapping, and cloning

Haploid wild-types and diploid mutants from AB/SJD hybrids were genotyped for agarose polymorphisms in z1154, z20950, and z6974 (using the MGH Zebrafish WWW Server published primers), as well as an SSCP polymorphism in the 3'UTR of *ldb3* (using the primers: F-GAGAGAAGGTGTGTGCGTG, R-CCTTTTCAGAATTTGGGTTG). The coding sequence mutation in *ugdh* was determined by sequencing wild-type and mutant cDNA clones isolated with primers designed from zebrafish EST sequence information (zebrafish *ugdh*, accession: AF361478; fc15f10 *ugdh* EST, accession: AI657608). The mutations were confirmed by dCAP-based[39] restriction-fragment length polymorphism generated by the T to A substitution at base pair 992 using the primers, 5'-GACATGAATGAATATCAGAGAAAGAG-3' and 5'-AGGAGAAACCCAACAACGC-3', and digesting with MluI.

Injection and morpholino experiments

All injections were performed on a Drummond Nanoject II microinjector with a Narshige micromanipulator. Embryos were aligned in rows on1.3% agarose/Embryo medium plates containing methylene blue as an antifungal agent. Morpholinos for *ugdh*, *has2*, and *ig-neu* were injected at 4 and 8 ng. Morpholinos were dissolved in 300 µl ddH2O or 1mM Hepes to create 1mM stocks. Those stocks were then diluted 1:10 for injection at either 2.3 or 4.6 nl per embryo. Injections were targeted either for the single cell of for the yolk directly underneath it. PACs180A23, 142J10, and 97M23 were injected for rescue as 2.3 nl of a 0.006 ug/ul solution.

Sequences:

ugdh-biotin	5'-TCTTTTTAATCTGAAACATCGTGTC-3'
has2-biotin	5'-GCTGACCGCTTTATCACATCTCATC-3'
ig-neu	5'-CCATGATGCAGTTTAGATGTGGGAT-3'

Transplantation experiments

All transplantations were performed on sphere stage embryos. Embryos were aligned in rows on1.3% agarose/Embryo medium plates containing methylene blue as an antifungal agent. Donors were labelled by injection with 5% rhodamine dextran. Dechorionation was performed by hand. Approximately 30 cells were transplanted into two locations in the germ ring to increase probability of heart anlage contribution.

Alcian Green staining

Embryos were fixed for 8-24 hours at 3-6 days post fertilization in 1ml 4% PFA, Fix was removed and 1ml of the Alcian solution was added (embryos were incubated 8-24 hours at room temp with shaking). Alcian was removed and embryos washed 4 times in acid/alcohol solution. Acid/alcohol was slowly replaced with ddH2O and then embryos were washed gently in PBST. For bleaching purposes, embryos were incubated for 20 minutes in 3% H2O2 in 0.5M KOH and washed gently again in PBST before clearing in 0.5% KOH/glycerol.

Alcian reagents:

acid/alcohol: final concentration 0.37% HCl, 70% EtOH

alcian green: 0.1% alcian green powder in acid/alcohol

0.5% KOH/glycerol: final concentration 0.25% KOH, 50% glycerol

In Situ Hybridization

Embryos were dechorionated before fixing in 4% paraformaldehyde (PFA) at 4 degrees C overnight. Embryos were washed twice in PBST, and dehydrated by 5 washes in MeOH over 10 minutes. Embryos were rehydrated in graded washes of MeOH and PBST (5 minutes each). After 4 washes in PBST embryos were digested in 10ug/ml proteinase K at room temperature (24 hpf for 5 minutes, 36 hpf for 25 minutes, 48 hpf for 35 minutes and 72

hpf for 45 minutes). Embryos were then washed twice in PBST, post-fixed in 4% PFA for 20 minutes at room temperature, and washed again 5 times in PBST. 65% Hyb was added to the tubes, and they were incubated at 70 degrees C for 4-6 hours before prewarmed probe diluted in 65% Hyb was added for incubation overnight. Embryos were then washed in graded Hyb/2X SSC washes at 70 degrees C (15 minutes each). Then they were washed twice in 0.2X SSC at 70 degrees C (30-45 minutes each). Embryos were then washed through graded 0.2X SSC/PBST washes into PBST at room temperature (5 minutes each). Embryos were blocked in 10% sheep serum, 2mg/ml bovine serum albumin (BSA) in PBST for 90 minutes at room temperature, incubated in 1:5000 diluted AP conjugated anti-digoxigenin antibodies in 2mg/ml BSA in PBST, and washed 8 times overnight in 2 mg/ml BSA in PBST. Embryos were rinsed 3 times in fresh NTMT and then incubated with substrate as necessary. Reaction was stopped in PBST, and embryos dehydrated in MeOH before clearing in 2:1 benzyl benzoate:benzyl alcohol.

Reagents for In Situs:

In all cases millipure water was considered RNAse free and vials/bottles were rinsed with RNAse ZAP and ddH2O before use.

1 x PBST--Add 1ml of 100% tween to 1 L of PBS to get a final concentration of 0.1%tween..

10 x PBS stock--Prepare RNAse Free; 40g NaCl, 1g KCl, 7.2g Na2HPO4, 1.2g KH2PO4

Add 450ml of dH2O and dissolve above reagents. pH to 7.3 and then top off to 500mls. Autoclave for 20 min at 15lb/sq in on liquid cycle. Store at RT

20 x SSC--Prepare RNAse Free; 175.3g NaCl, 88.2g Na citrate. Add 800mls of dH2O. pH to 7.0. Add remaining water to 1 L and autoclave.

65% HYB solution--Prepare RNAse Free

For 100mls of 65% HYB add the following: 65ml of formamide deionized, 25ml of 20x SSC (RT), 100ul of 50mg/ml stock Heparin (4°C), 1ml 10% Tween, 1ml of 0.9M Citric Acid (pH 6.0) stock, 7.9ml ddH20. Add stir bar and 0.1g of tRNA. Aliquot into sterile 15ml Falcon tubes and store at -80°C.

Staining buffer-NTMT--make fresh every time

For 10mls: 1ml of 1.0M Tris pH 9.5, 0.5ml of 1.0M MgCl2, 0.2ml of 5.0M NaCl, 0.1ml 10% tween20, and 8.2ml ddH20

Substrate Solution per 1ml of the above Staining buffer NTMT.

4.5ul NBT (75mg/ml NBT in 70% dimethylformamide)

3.5ul X-phosphate (50 mg/ml X-phosphate in dimethylformamide)

Probe-specific restriction enzymes and RNA polymerases:

bmp4	EcoRI	T7
col2a	HindIII	T3
fgf8	XhoI	T7
msxB	BamHI	T3
nkx2.5	EcoRI	T7

ntl	NotI	T3
snail2	XbaI	T7
notch1b	BamHI	T3
irx4	NotI	T7
notch5	BamHI	T3
ugdh(10.1.1)	ApaI	SP6
fc73b01	PvuII	T7
br146	NotI	T7
fibulin	XhoI	SP6
neuregulin	SpeI	T7
bmpR1b	BamHI	T3
sox9a	EcoRV	T7
sox9b	StuI	T7

MF20 S46 Antibody staining

As previously published by Alexander et al.[3]

TC2 Antibody staining

Embryos were fixed in 4:1 MeOH:DMSO at -20 degrees C overnight to a few days, then washed through graded EtOH's into water. Next, embryos were washed 2x 10' each in PBS, blocked overnight in 3% BSA/1% normal goat serum in PBS + 0.5% DMSO. Embryos were then incubated over day and night in undiluted TC2, washed 4x 30' each in PBS + 0.5% DMSO, and incubated in FITC-goat anti-mouse IgM 1:100 in block overnight. After final washes (5x 30' each in PBS) embryos were mounted and viewed.

Methylene Blue staining

Embryos were fixed and sectioned in JB4 plastic medium from Polyscience, Inc. as per kit instructions. Mounted sections are immersed into warm (60 degree C) 0.005% Methylene blue in ddH2O for 60-90 seconds, then rinsed in ddH2O until water is clear.

Microscopy

All microscopy, fluorescence and DIC, was performed on an Zeiss Axioplan compound microscope. Images were either saved as files using an Zeiss Axiocam or taken as slides using E-6 Kodak film and scanned with a Sprintscan 35 slide scanner. Mounting of hearts was performed at times by dissection of embryos in benzyl benzoate:benzyl alcohol with small curved scissors from fine science tools. Analysis of images was performed using Canvas 5.0 and Adobe Photoshop 4.0.

Whole RNA preparation, cDNA preparation, 3' RACE and general subcloning

For whole RNA preparation Trizol reagent was used as directed. For 3' RACE cDNA preparation, Gibco BRL's 3'RACE Superscript II kit was used. Amplification was performed using Promega taq in buffer B and the lab PCR mix buffer using the universal adapter primer (UAP) provided in the kit as well as a gene-specific primer.

PCR was electrophoresed on a1% Nusieve GTG gel or Seaplaque GTG gel from BMA, depending on fragment size. DNA containing fragments are cut from the gel, melted at 68 degrees, and used in a ligation reaction using the Promega TA cloning kit. 50ul reaction was prepared with 20ul gel, 25ul 2x buffer, 2ul ligase and 1ul pGEM vector and incubated at 15 degrees overnight. Transformation reactions was prepared with 20ul of ligation reaction added to 20ul of 5x KCM buffer and 60ul of sterile dH2O. 5x KCM buffer consists of 0.5M KCl, 0.15M CaCl2, and 0.25M MgCl2. This mix was added to 75-100ul of commercial chemically competent cells. Incubate on ice for 20 minutes, 42 degree C heat shock for 45 seconds, and returned to ice before a 30-60 minute rescue at 37 degrees C and plating on agarose media appropriate antibiotics.

Sense RNA production

In all cases a mMessage machine kit from Ambion was used.

PAC DNA Preparation

5 ml cultures were grown overnight at 37C in TB ("terrific broth", recipe in Sambrook et al. 1989, A2) containing 25 ug/ml kanamycin. 250 ml TB (25 ug/ml kanamycin) was innoculatde in 2.8 L culture flask w/ the 10 ml overnight culture and shake at 37 C overnight. Qiagen "Qiafilter Maxiprep" kit was used to prepare DNA. PACs 77C7, 78P16, and 95F2 were isolated by PCR using primers for z20950 on PAC library pools and oriented using nearby markers and markers derived from end-sequencing of the PAC clones. PACs 142J10, 97M23, and 180A23 were isolated by PCR using zUGDH F1 and R1 primers for *ugdh* (see figure 9). Sizing of PACs was performed by pulse field gel electrophoresis of NotI digests in a 1% agarose gel made with 0.5X TBE.

Genomic DNA Preparation

Dechorionated embryos or clipped fins were placed in single tubes of an 8-tube microstrip. Egg water was removed and 50-100 µl Embryo Lysis buffer added. Embryos were boiled at 98 degrees C for 10 minutes, then 5-10 µl of 10 mg/ml proteinase K (in dH2O) was added. Embryos were incubated at 55 degrees C for 6 hours

and then boiled again. Detritus was centrifuged to the bottom of the tube and supernatent was removed and diluted 1:50 for use at 5 µl per PCR reaction

PCR Amplification

Typically, 18 ml of lab PCR mix, 0.325 ml of each 20 mMolar primer, 0.6 ml Taq and appropriate amounts of DNA template/ddH2O were used with the following PCR program:

94 degrees 1-5 minutes

cycle 25-35X

94 degrees 45 seconds

T_m-5 degrees 45 seconds

72 degrees 1-2 minutes

---

72 degrees 10 minutes

β-xyloside treatment

β-xylosides (Sigma) were dissolved in egg water at 1, 5, and 20 mM concentrations and added to embryos (dechorionated and undechorionated) at a number of timepoints.

Curriculum Vitae

Emily Cecile Walsh
date of birth March 13, 1973
ewalsh@itsa.ucsf.edu;
emilycwalsh@yahoo.com

Education

August 2001 Ph.D. Genetics, University of California, San Francisco

May 1995 B.S. Biology with highest honors, University of North Carolina, Chapel Hill

Research Experience

1995-present Thesis research at UC-San Francisco with Dr. Didier Y.R. Stainier "Jekyll/UDP-glucose dehydrogenase is required for cardiac valve, semicircular canal, and cartilage development in zebrafish.

1994-1995 Undergraduate honors thesis research at UNC-Chapel Hill with Dr. John Pringle "The role of CDC3 in bud site selection in the yeast, *S. cerevisiae*."

Fellowships and Scholarships

1996 Howard Hughes Medical Institute Predoctoral Fellowship (5 year award)

1995 NIH Developmental Biology Training Grant Fellowship (1 year award)

1991 James M. Johnston Scholar at UNC-Chapel Hill (4 year award)

Publications

Walsh E.C., and D.Y.R. Stainier. (2001) *UDP-glucose dehydrogenase* Required for Cardiac Valve Formation in Zebrafish, *Science*, August 31, 2001.

Walsh E.C., and D.Y.R. Stainier. (2000) Cardiac development in vertebrates. In *Genetic Models in Cardiorespiratory Biology* (eds. Haddad, G.G. and Xu, T.; ex. ed. Lenfant, C.).

Reifers F., **Walsh E.C.**, Leger S., Stainier D.Y.R., and M. Brand. (2000) Induction and differentiation of the zebrafish heart requires fibroblast growth factor 8 (fgf8/acerebellar). *Development* 127.

Reifers F., Bohli H., **Walsh E.C.**, Crossley P.H., Stainier D.Y.R., and M. Brand. (1998) *Fgf8* is mutated in zebrafish *acerebellar* (*ace*) mutants and is required for maintenance of midbrain-hindbrain boundary development and somitogenesis. *Development* 125.

Invited Talks

"UDP-Glucose Dehydrogenase is required for cardiac valve, semicircular canal, and cartilage development in zebrafish." Weinstein Cardiovascular Development Conference, Dallas, TX, 2001 (talk).

"UDP-Glucose Dehydrogenase is required for cardiac valve, semicircular canal, and cartilage development in zebrafish." Zebrafish Genetics and Development Conference, London, England, 2001 (talk).

Zebrafish heart valve formation: misexpression and mutant analyses. Zebrafish Genetics and Development Conference, Tubingen, Germany, 1999 (talk).

Zebrafish heart valve formation: the *jekyll* mutation. California Polytechnic State University, San Luis Obispo, CA, 1999 (talk).

Teaching Experience

Teaching assistant for the zebrafish module of the embryology course at the Marine Biological Laboratory, Woods Hole, MA (Summer 1998-2001)

Triad Girls' Science Club scientist-teacher and curriculum developer, Horace Mann Middle School, San Francisco (1996-1999)

Organizer and developer, hands-on science activity for UCSF Take Our Daughters To Work Day, elementary and middle school ages (1996-1999).

Teaching Assistant, Human Metabolism for Pharmacy Students, UCSF (Fall 1996)

Honors and Awards

American Heart Association Council Travel Award winner for the Weinstein Cardiovascular Development Conference; Tucson, AZ 1999.

Travel Award winner for the First European Meeting on Zebrafish Genetics and Development; Tubingen, Germany 1999.

Tuition Scholarship to attend the Embryology course at Marine Biological Laboratory, Woods Hole, Massachusetts, 1997.

Phi Beta Kappa, UNC-Chapel Hill 1994.

Works Cited:

1. Chen, J. N. *et al.* Mutations affecting the cardiovascular system and other internal organs in zebrafish. *Development* **123**, 293-302 (1996).

2. Stainier, D. Y. *et al.* Mutations affecting the formation and function of the cardiovascular system in the zebrafish embryo. *Development* **123**, 285-292 (1996).

3. Alexander, J., Stainier, D. Y. & Yelon, D. Screening mosaic F1 females for mutations affecting zebrafish heart induction and patterning. *Developmental Genetics* **22**, 288-299 (1998).

4. Lee, K. H., Xu, Q. & Breitbart, R. E. A new tinman-related gene, nkx2.7, anticipates the expression of nkx2.5 and nkx2.3 in zebrafish heart and pharyngeal endoderm. *Developmental Biology* **180**, 722-731 (1996).

5. Reiter, J. F. *et al.* Gata 5 is required for the development of the heart and endoderm in zebrafish. *Genes and Development* **in press** (1999).

6. Tam, P. P., Parameswaran, M., Kinder, S. J. & Weinberger, R. P. The allocation of epiblast cells to the embryonic heart and other mesodermal lineages: the role of ingression and tissue movement during gastrulation. *Development* **124**, 1631-1642 (1997).

7. Lints, T. J., Parsons, L. M., Hartley, L., Lyons, I. & Harvey, R. P. Nkx-2.5: a novel murine homeobox gene expressed in early heart progenitor cells and their myogenic descendants [published erratum appears in Development 1993 Nov;119(3):969]. *Development* **119**, 419-431 (1993).

8. Heikinheimo, M., Scandrett, J. M. & Wilson, D. B. Localization of transcription factor GATA-4 to regions of the mouse embryo involved in cardiac development. *Developmental Biology* **164**, 361-373 (1994).

9. Morrisey, E. E., Ip, H. S., Tang, Z., Lu, M. M. & Parmacek, M. S. GATA-5: a transcriptional activator expressed in a novel temporally and spatially-restricted pattern during embryonic development. *Developmental Biology* **183**, 21-36 (1997).

10. Yelon, D., Horne, S. A. & Stainier, D. Y. Restricted expression of cardiac myosin genes reveals regulated aspects of heart tube assembly in zebrafish. *Developmental Biology* **214**, 23-37 (1999).

11. Perens, E. & Stainier, D. Y. (unpublished data).

12. Stainier, D. Y., Weinstein, B. M., Detrich, H. W., 3rd, Zon, L. I. & Fishman, M. C. Cloche, an early acting zebrafish gene, is required by both the endothelial and hematopoietic lineages. *Development* **121**, 3141-3150 (1995).

13. Kuo, C. T. *et al.* GATA4 transcription factor is required for ventral morphogenesis and heart tube formation. *Genes and Development* **11**, 1048-1060 (1997).

14. Vir gh, S., Szab , E. & Challice, C. E. Formation of the primitive myo- and endocardial tubes in the chicken embryo. *Journal of Molecular and Cellular Cardiology* **21**, 123-137 (1989).

15. DeRuiter, M. C., Poelmann, R. E., VanderPlas-de Vries, I., Mentink, M. M. & Gittenberger-de Groot, A. C. The development of the myocardium and endocardium in mouse embryos. Fusion of two heart tubes? *Anatomy and Embryology* **185**, 461-473 (1992).

16. Shalaby, F. *et al.* Failure of blood-island formation and vasculogenesis in Flk-1-deficient mice. *Nature* **376**, 62-66 (1995).

17. Olson, E. N. & Srivastava, D. Molecular pathways controlling heart development. *Science* **272**, 671-676 (1996).

18. Walsh, E. C. & Stainier, D. Y. R. UDP-glucose dehydrogenase Required for Cardiac Valve Formation in Zebrafish. *Science* **in press** (2001).

19. Westin, J. & Lardelli, M. Three novel Notch genes in zebrafish: implications for vertebrate Notch gene evolution and function. *Development Genes and Evolution* **207**, 51-63 (1997).

20. Zhang, H.-Y., Lardelli, M. & Ekblom, P. Sequence of the zebrafish fibulin-1 and its expressionin developing heart and other embryonic organs. *Development Genes and Evolution* **207**, 340-351 (1997).

21. Dickson, M. *et al.* Defective haematopoiesis and vasculogenesis in transforming growth factor-beta 1 knock out mice. *Development* **121**, 1845 (1995).

22. Kaartinen, V. *et al.* Abnormal lung development and cleft palate in mice lacking TGF-beta 3 indicatesdefects of epithelial-mesenchymal interaction. *Nature Genetics* **11**, 415 (1995).

23. Sanford, L. P. *et al.* TGFbeta2 knockout mice have multiple developmental defects that are non-overlapping with other TGFbeta knockout phenotypes. *Development* **124**, 2659-2670 (1997).

24. Ramsdell, A. F. & Markwald, R. R. Induction of endocardial cushion tissue in the avian heart is regulated, in part, by TGFbeta-3-mediated autocrine signaling. *Developmental Biology* **188**, 64-74 (1997).

25. Brown, C. B., Boyer, A. S., Runyan, R. B. & Barnett, J. V. Antibodies to the Type II TGFbeta receptor block cell activation and migration during atrioventricular cushion transformation in the heart. *Developmental Biology* **174**, 248-257 (1996).

26. Brown, C. B., Boyer, A. S., Runyan, R. B. & Barnett, J. V. Requirement of type III TGF-beta receptor for endocardial cell transformation in the heart. *Science* **283**, 2080-2082 (1999).

27. Nakajima, Y., Yamagishi, T., Hokari, S. & Nakamura, H. Mechanisms involved in valvuloseptal endocardial cushion formation in early cardiogenesis: roles of transforming growth factor (TGF)-beta and bone morphogenetic protein (BMP). *Anatomical Record* **258**, 119-127 (2000).

28. Boyer, A. S. *et al.* TGFbeta2 and TGFbeta3 have separate and sequential activities during epithelial-mesenchymal cell transformation in the embryonic heart. *Developmental Biology* **208**, 530-545 (1999).

29. Creazzo, T. L., Godt, R. E., Leatherbury, L., Conway, S. J. & Kirby, M. L. Role of cardiac neural crest cells in cardiovascular development. *Annual reviews of Physiology* **60**, 267 (1998).

30. Yamamura, H., Zhang, M., Markwald, R. R. & Mjaatvedt, C. H. A heart segmental defect in the anterior-posterior axis of a transgenic mutant mouse. *Developmental Biology* **186**, 58-72 (1997).

31. Mjaatvedt, C. H., Yamamura, H., Capehart, A. A., Turner, D. & Markwald, R. R. The Cspg2 gene, disrupted in the hdf mutant, is required for right cardiac chamber and endocardial cushion formation. *Developmental Biology* **202**, 56-66 (1998).

32. Camenisch, T. D. *et al.* An essential role for hyaluronan in mammalian development and cardiac morphogenesis. *submitted* (1999).

33. Walsh, E. C. & Stainier, D. Y. (unpublished data).

34. Jones, C. M., Lyons, K. M. & Hogan, B. L. Involvement of Bone Morphogenetic Protein-4 (BMP-4) and Vgr-1 in morphogenesis and neurogenesis in the mouse. *Development* **111**, 531-542 (1991).

35. Winnier, G., Blessing, M., Labosky, P. A. & Hogan, B. L. Bone morphogenetic protein-4 is required for mesoderm formation and patterning in the mouse. *Genes and Development* **9**, 2105-2116 (1995).

36. Neuhauss, S. C. *et al.* Mutations affecting craniofacial development in zebrafish. *Development* **123**, 357-367 (1996).

37. Haddon, C. & Lewis, J. Hyaluronan as a propellant for epithelial movement: the development of semicircular canals in the inner ear of Xenopus. *Development* **112**, 541 (1991).

38. Postlethwait, J. H. & Talbot, W. S. Zebrafish genomics: from mutants to genes. *Trends in Genetics* **13**, 183-190 (1997).

39. Neff, M. M., Neff, J. D., Chory, J. & Pepper, A. E. dCAPS, a simple technique for the genetic analysis of single nucleotide polymorphisms: experimental applications in Arabidopsis thaliana genetics. *Plant Journal* **14**, 387-392 (1998).

40. Campbell, R. E., Mosimann, S. C., van De Rijn, I., Tanner, M. E. & Strynadka, N. C. The first structure of UDP-glucose dehydrogenase reveals the catalytic residues necessary for the two-fold oxidation. *Biochemistry* **39**, 7012-7023 (2000).

41. Lander, A. D. & Selleck, S. B. The elusive functions of proteoglycans: in vivo veritas. *Journal of Cell Biology* **148**, 227-232 (2000).

42. Lin, X. *et al.* Disruption of gastrulation and heparan sulfate biosynthesis in EXT1-deficient mice. *Developmental Biology* **224**, 299-311 (2000).

43. Topczewski, J. *et al.* The zebrafish glypican Knypek controls cell polarity during gastrulation movements of convergent extension. *Developmental Cell* **In press** (2001).

44. Nasevicius, A., Hyatt, T. M., Hermanson, S. B. & Ekker, S. C. Sequence, expression, and location of zebrafish frizzled 10. *Mechanisms of Development* **92**, 311-314 (2000).

45. The Human Genome Consortium. Initial sequencing and analysis of the human genome. *Nature* **409**, 860-921 (2001).

46. Motoike T, L. S., Perens E, Roman BL, Liao W, Chau TC, Richardson CD, Kawate T, Kuno J, Weinstein BM, Stainier DY, Sato TN. Universal GFP reporter for the study of vascular development. *Genesis* **28**, 75-81 (2000).

47. Eisenberg, L. M. & Markwald, R. R. Molecular regulation of atrioventricular valvuloseptal morphogenesis. *Circulation Research* **77**, 1-6 (1995).

48. Thisse, C. & Thisse, B. Antivin, a novel and divergent member of the TGFbeta superfamily, negatively regulates mesoderm induction. *Development* **126**, 229-240 (1999).

49. Data not shown.

50. Zecca, M., Basler, K. & Struhl, G. Direct and long-range action of a wingless morphogen gradient. *Cell* **87**, 833-844 (1996).

51. Rodriguez-Esteban, C. *et al.* Radical fringe positions the apical ectodermal ridge at the dorsoventral boundary of the vertebrate limb [see comments] [published erratum appears in Nature 1997 Aug 28;388(6645):906]. *Nature* **386**, 360-366 (1997).

52. Laufer, E. *et al.* Expression of Radical fringe in limb-bud ectoderm regulates apical ectodermal ridge formation [see comments] [published erratum appears in Nature 1997 Jul 24;388(6640):400]. *Nature* **386**, 366-373 (1997).

53. H cker, U., Lin, X. & Perrimon, N. The Drosophila sugarless gene modulates Wingless signaling and encodes an enzyme involved in polysaccharide biosynthesis. *Development* **124**, 3565-3573 (1997).

54. Haerry, T. E., Heslip, T. R., Marsh, J. L. & O'Connor, M. B. Defects in glucuronate biosynthesis disrupt Wingless signaling in Drosophila. *Development* **124**, 3055-3064 (1997).

55. Lin, X., Buff, E. M., Perrimon, N. & Michelson, A. M. Heparan sulfate proteoglycans are essential for FGF receptor signaling during Drosophila embryonic development. *Development* **126**, 3715-3723 (1999).

56. Binari, R. C. *et al.* Genetic evidence that heparin-like glycosaminoglycans are involved in wingless signaling. *Development* **124**, 2623-2632 (1997).

57. Perrimon, N. & Bernfield, M. Specificities of heparan sulphate proteoglycans in developmental processes. *Nature* **404**, 725 (2000).

58. Meyer, D. & Birchmeier, C. Multiple essential functions of neuregulin in development [see comments] [published erratum appears in Nature 1995 Dec 14;378(6558):753]. *Nature* **378**, 386-390 (1995).

59. Lee, K. F. *et al.* Requirement for neuregulin receptor erbB2 in neural and cardiac development [see comments]. *Nature* **378**, 394-398 (1995).

60. Gassmann, M. *et al.* Aberrant neural and cardiac development in mice lacking the ErbB4 neuregulin receptor [see comments]. *Nature* **378**, 390-394 (1995).

61. Liu, X. *et al.* Domain-specific gene disruption reveals critical regulation of neuregulin signaling byits cytoplasmic tail. *PNAS* **95**, 13024 (1998).

62. Erickson, S. L. *et al.* ErbB3 is required for normal cerebellar and cardiac development: a comparison with ErbB2-and heregulin-deficient mice. *Development* **124**, 4999-5011 (1997).

63. Meyer, D. *et al.* Isoform-specific expression and function of neuregulin. *Developmental Biology* **124**, 3575 (1997).

64. Koster, R. & Fraser, S. Tracing transgene expression in living zebrafish embryos. *Developmental Biology* **233**, 329 (2001).

65. Reifers, F., Walsh, E., Leger, S., Stainier, D. & Brand, M. Induction and differentiation of the zebrafish heart requires fibroblast growth factor 8 (fgf8/acerebellar). *Development* **127**, 225 (2000).

66. Reifers, F. *et al.* Fgf8 is mutated in zebrafish acerebellar (ace) mutants and is required for maintenance of midbrain-hindbrain boundary development and somitogenesis. *Development* **125**, 2381 (1998).

67. Bauer, H., Lele, Z., Rauch, G., Geisler, R. & Hammerschmidt, M. The type I serine/threonine kinase receptor Alk8/Lost-a-fin is required for Bmp2b/7 signal transduction during dorsoventral patterning of the zebrafish embryo. *Development* **128**, 849 (2001).

68. Mintzer, K. *et al.* Lost-a-fin encodes a type I BMP receptor, Alk8, acting maternally and zygotically in dorsoventral pattern formation. *Development* **128**, 859 (2001).

69. Dick, A. *et al.* Essential role of Bmp7 (snailhouse) and its prodomain in dorsoventral patterning of the zebrafish embryo. *Development* **127**, 343 (2000).

70. Schmid, B. *et al.* Equivalent genetic roles for bmp7/snailhouse and bmp2b/swirl in dorsoventral pattern formation. *Development* **127**, 957 (2000).

71. Solloway, M. & Robertson, E. Early embryonic lethality in Bmp5;Bmp7 double mutant mice suggests functional redundancy within the 60A subgroup. *Development* **126**, 1753 (1999).

72. Capehart, A., Mjaatvedt, C., Hoffman, S. & Krug, E. Dynamic expression of a native chondroitin sulfate epitope reveals microheterogeneity of extracellular matrix organization in the embryonic chick heart. *Anatomical Record* **254**, 181 (1999).

73. Kroll, K. & Amaya, E. Transgenic Xenopus embryos from sperm nuclear transplantations reveal FGF signaling requirements during gastrulation. *Development* **122**, 3173 (1996).

74. Westerfield, M. *The Zebrafish Book* (University of Oregon Press, Eugene, 1993).

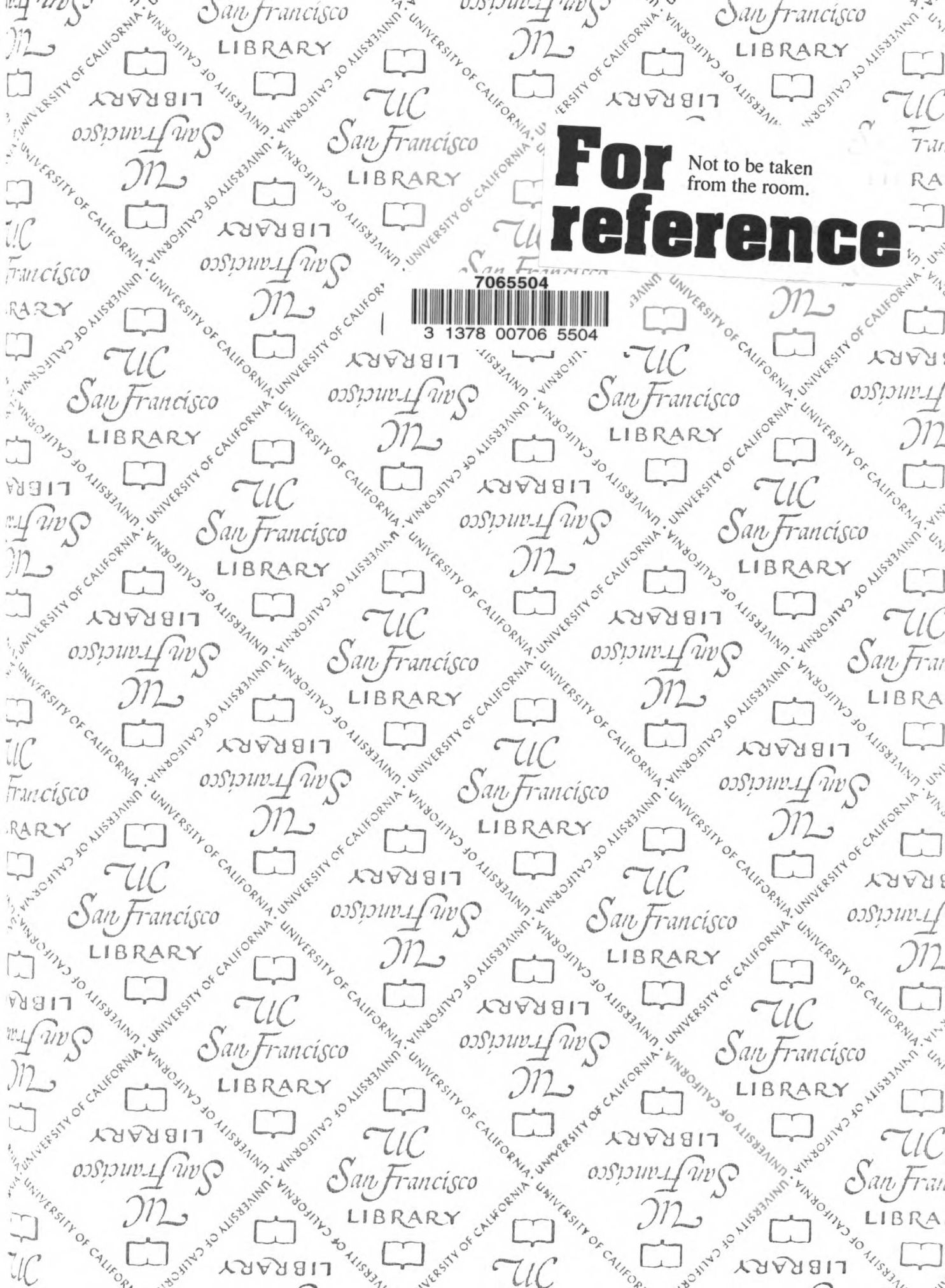
For reference
Not to be taken from the room.
7065504
3 1378 00706 5504
UC San Francisco LIBRARY
UNIVERSITY OF CALIFORNIA · UNIVERSITY OF CALIFORNIA